Dipartimento di Scienze della Terra
Università di Pisa

Atlas of Meteorites in Thin Section

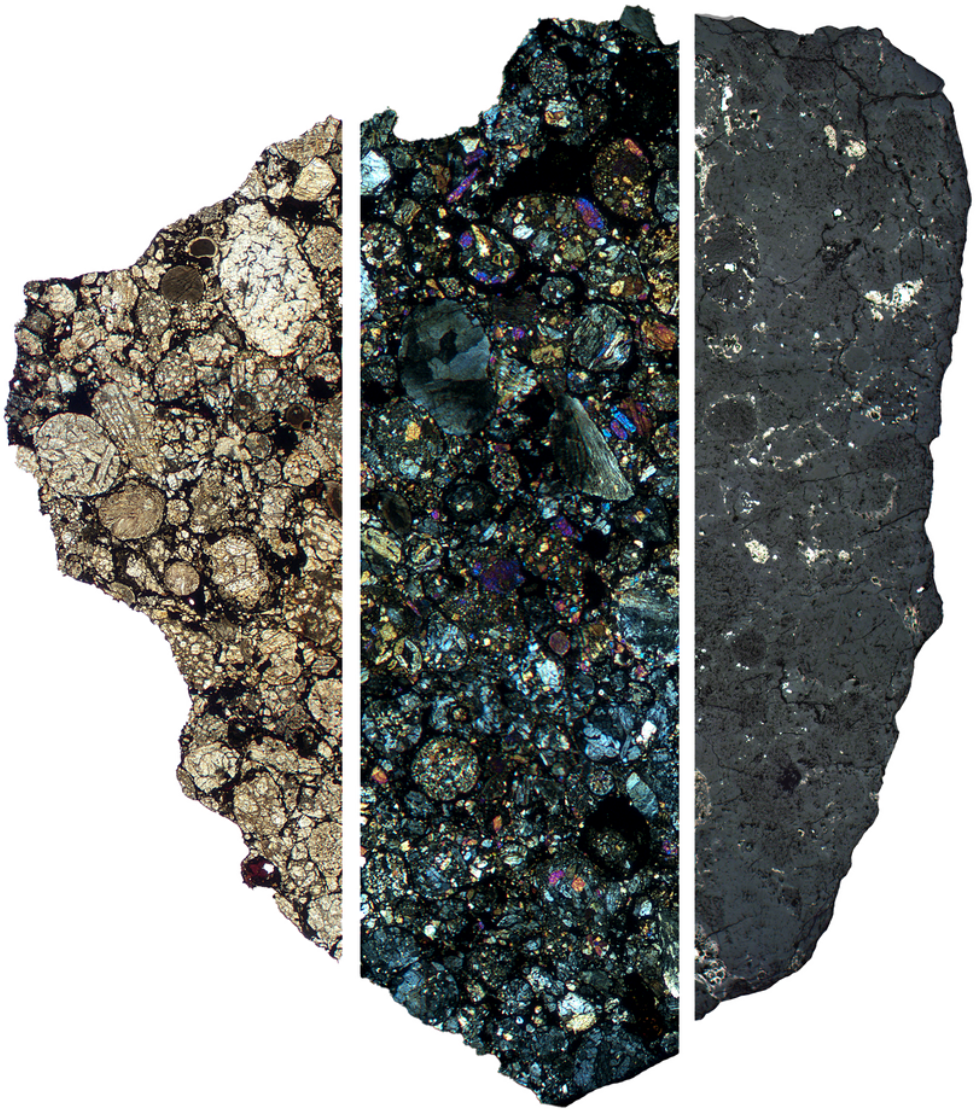

Anna Musolino Luigi Folco

Contents

Preface

The Atlas of Meteorites in Thin Section is an on-line educational resource of the Dipartimento di Scienze della Terra of the Università di Pisa, Italy. It is a collection of optical microscopic images of 45 polished thin sections from 45 meteorites representative of a variety of different types of stony meteorites, including chondrites, primitive and differentiated achondrites, and planetary meteorites from primitive and evolved bodies in the solar system.

The catalogue is an educational tool for students interested in the petrography and petrology of planetary materials, particularly those attending the courses of Planetary Geology and Cosmochemistry. The polished thin sections featured in the catalogue constitute the set of thin sections used for the practicals of the Cosmochemistry course and are an educational loan belonging to the Museo Nazionale dell'Antartide in Siena, Italy.

The micrographs in the catalogue include both whole section images with additional textural–mineralogical details taken with the petrographic microscope under both transmitted and reflected light and provide an introductory guide to the petrographic analyses and classification of meteorites.
Images were acquired using a polarizing microscope ZEISS Axioplan equipped with an Axiocam 105 color camera at the Dipartimento di Scienze della Terra of the Università di Pisa, and processed with the Axioscope image software. All the images can be downloaded in high resolution through the links present above each section.

The atlas is organized in three chapters and an appendix: chapter 1 is a brief general introduction to meteorites; chapters 2 and 3 provide petrographic images in thin section of chondrites and non-chondritic meteorites, like achondrites and planetary meteorites; the appendix includes the meteorite classifications schemes used in this work.

Details of the meteorites featured in this book are synoptically reported in Table 1. The majority are finds recovered from hot and cold deserts by researchers and students of the Dipartimento di Scienze della Terra (Università di Pisa) and are curated by the Museo Nazionale dell'Antartide. Additional details on the circumstances of the recovery, classification and repository can be found through the Meteoritical Bulletin Database of the Meteoritical Society (www.lpi.usra.edu/meteor). Work continues in this collection to better document the variety of petrographic features of meteorites.

Table 1: Meteorites featured in the present atlas. For classification, please refer to the classification scheme in Tab. 2.1.

Name	**Locality**	**Date**	**Find/Fall**	**Classification**[1]	**SS**[2]	**WG**[3]
FRO 03011	Frontier Mountain, Antarctica	2003	Find	LL3	S2	W1
FRO 10083	Frontier Mountain, Antarctica	2011	Find	LL3	S3	W1
FRO 10097	Frontier Mountain, Antarctica	2011	Find	LL3	S1	W1
RKP 17105	Reckling Peak, Antarctica	2017	Find	LL3	S4	W0
FRO 10081*	Frontier Mountain, Antarctica	2010	Find	LL3	S2	W1
ALH 14005*	Allan Hills, Antarctica	2014	Find	LL6	S2	W0
ALH 99101	Allan Hills, Antarctica	2000	Find	L(LL)3	S4	W1
DaG 313	Dar al Gani, Lybia	1997	Find	L(LL)3	S3	W2
RKP 17043*	Reckling Peak, Antarctica	2017	Find	L3	S3	W1
MCY 14008	MacKay Glacier, Antarctica	2015	Find	L4	S3	W1
SAID 01*	Sahara Desert	-	-	L4-6	S1	W1
Beni M'Hira	Beni M'Hira, Tunisia	2001	Fall	L6	S5	W0
DaG 528	Dar al Gani, Lybia	1997	Find	L6	S6	W4
DaG 546	Dar al Gani, Lybia	1997	Find	L6	S6	W5
FRO 03050	Frontier Mountain, Antarctica	2003	Find	L6	S4	W0
FRO 90225*	Frontier Mountain, Antarctica	1990	Find	H3-4	S2	W2
FRO 90171*	Frontier Mountain, Antarctica	1990	Find	H4-5	S2	W2
ALH 14007*	Allan Hills, Antarctica	2014	Find	H5	S2	W1
JOH 01001	Johannessen Nunataks, Antarctica	2001	Find	H5	S1	W1
FRO 03019	Frontier Mountain, Antarctica	2003	Find	H6	S3	W1
FRO 03073	Frontier Mountain, Antarctica	2004	Find	H6	S1	W0
DaG 896	Dar al Gani, Lybia	2000	Find	H	melted	W1
DEW 12005*	Mount DeWitt, Antarctica	2013	Find	CM	S2	W1
DaG 667	Dar al Gani, Lybia	1999	Find	CO3	S1	W1
DaG 668	Dar al Gani, Lybia	1999	Find	CO3	S1	W1
FRO 97002	Frontier Mountain, Antarctica	1997	Find	CV3	S1	W0
ALH 12034*	Allan Hills, Antarctica	2012	Find	CC	S2	W0
EET 14079*	Elephant Moraine, Antarctica	2014	Find	CC	S2	W2
FRO 03005	Frontier Mountain, Antarctica	2004	Find	EL4	S1	W1
EAGLE 01	Cass County, Nebraska	1946/47	Fall	EL6	S2	W0
ALHAGGOUNIA 001	Saguia el Hamra, Morocco	2006	Find	EL	melted	W1
FRO 95029	Frontier Mountain, Antarctica	1995	Find	ACA	S1	W1
FRO 03001	Frontier Mountain, Antarctica	2003	Find	LOD	S1	W0
BAB 179*	Dar al Gani, Lybia	-	Find	URE	S4	L
DaG 660	Dar al Gani, Lybia	1990	Find	URE	S3	M
FRO 97013	Frontier Mountain, Antarctica	1997	Find	URE	S3	L
AIT 04*	Morocco	-	-	BRA	S4	H
DaG 684	Dar al Gani, Lybia	1999	Find	EUC	moderately	L
DaG 669	Dar al Gani, Lybia	1999	Find	EUC	moderately	L
DaG 671	Dar al Gani, Lybia	1999	Find	EUC	weakly	L
RKP 17029*	Reckling Peak, Antarctica	2019	Find	HOW	moderately	L
ALH 12073	Allan Hills, Antarctica	2012	Find	MSF	-	M
DEW 12007	Mount DeWitt, Antarctica	2013	Find	LUN	moderately	L
RKP 17064*	Reckling Peak, Antarctica	2017	Find	LUN	weakly	L
DaG 670	Dar al Gani, Lybia	1999	Find	SHE	S5	H

[1]Classification symbols refer to Tab. 2.1. Other abbreviations: ACA=Acapulcoite; LOD=Lodranite; URE=Ureilite; BRA=Brachinite; EUC=Eucrite; HOW=Howardite; MSF=Mesosiderite silicate fraction; LUN=Lunar; SHE=Shergottite.

[2]Shock Stages are only qualitative (as in "Description" in Tab. 3.2) whenever diagnostic features needed for shock classification are absent.

[3]Weathering Grades for differentiated achondrites are only qualitative: L=little or none weathered, M=moderately weathered, H=highly weathered.

*Provisional name and classification.

Meet The Authors

Anna Musolino is an MSc student in Geological Sciences and Technologies at the Dipartimento di Scienze della Terra of the Università di Pisa, with a Bachelor degree in Environmental and Natural Sciences. She is currently working on her master's thesis on the petrographic characterization and classification of six new carbonaceous chondrites recovered from Antarctica by the Italian Programma Nazionale delle Ricerche in Antartide (PNRA). She is also currently involved in the Space Tweezers project for the contactless nanophotonic manipulation of planetary materials funded by the Agenzia Spaziale Italiana (ASI). This Atlas is the product of her internship in Cosmochemistry at the Dipartimento di Scienze della Terra.

Luigi Folco is associate professor at the Dipartimento di Scienze della Terra of the Università di Pisa where he holds the courses of Planetary Geology, Cosmochemistry and Geowriting. His research focuses on the cosmochemistry of planetary materials to understand the origin and evolution of the solar system and the geochemistry of impactites to investigate the collisional history of our planet. He is also active in the systematic search for meteorites from hot and cold deserts, and has led several search expeditions in the Sahara and Antarctica. Folco 7006 is an asteroid within the main asteroid belt named after LF by the International Astronomical Union in recognition of his cosmochemical studies of meteorites.

Acknowledgements

The Museo Nazionale dell'Antartide, Sezione di Scienze della Terra, Siena is acknowledged for the loan of the polished thin sections featured in the present catalogue. Dr Antonio Ciccolella, a former MSc student at the Dipartimento di Scienze della Terra, took part in the early development of the present work and is kindly acknowledged. Laura Albertelli is acknowledged for her technical support during the photo editing. This work benefited of the detailed review of Profs Massimo D'Orazio and Matteo Masotta. This is an on-line educational resource of the Dipartimento di Scienze della Terra of the Università di Pisa, Italy.

Chapter 1

Meteorites: An Introduction

Meteorites are interplanetary rock debris captured by Earth's gravity and recovered at the Earth's surface (e.g., Rubin and Grossman, 2010 [17]). Their size ranges from millimeters to a few meters. Their pre-atmospheric sizes are large enough to survive ablation during atmospheric entry heating and small enough to survive impact against Earth's surface being decelerated from their cosmic velocities (greater than Earth's escape velocity of 11.2 km s^{-1}) through Earth's atmosphere. Their hypervelocity passage through the upper Earth's atmosphere gives rise to fireballs, explosions and detonations. This has made them known since early human history (e.g., D'Orazio, 2007 [6]). Object of veneration, popular superstition and recurring element in myths up until the 18th century CE, meteorites are for modern science a natural laboratory to explore how the solar system formed and evolved. Meteorites are in fact rock samples of a wide range of rocky bodies of the solar system, with a large variety of geological histories: from primitive minor bodies, like asteroids and comets, to more evolved planetary bodies, like Mars and the Moon (e.g., Chambers, 2006 [4]). The cosmochemical study of their physical-chemical properties thus allows investigation of the nearly 4.6 billion year-long sequence of astrophysical and geologic events through which an interstellar molecular cloud of gas and dust evolved in a system of planets and other minor bodies orbiting around the Sun (e.g., McSween et al., 2006 [13]; Russell et al., 2006 [18]). In other words, the great petrologic diversity of meteorites carries a nearly continuous record of planetary evolution. This spans from the early formation of primordial accretional aggregates (chondrites) in the protoplanetary disk to the differentiation of asteroids and terrestrial planets into metallic cores (iron meteorites) and silicate mantles (achondrites and planetary meteorites), including the proto-Earth.

Traditionally, meteorites have been distinguished into three broad categories: stones, irons, and stony-irons. This distinction is based on the relative proportions of silicate minerals and metallic iron-nickel. Modern classification schemes group meteorites into homogeneous classes according to their structure, mineralogy and chemical and isotopic compositions (e.g., Krot et al., 2014 [8]; Tab. 2.1). The most abundant meteorites in our collection ($> 99\%$ of the total) are impact debris from the collisions between asteroids orbiting between Mars and Jupiter in the so-called Main Asteroid Belt. Asteroids are "fossil bodies" of the planet-building era. Unlike geologically more evolved rocks from Earth, Mars and the Moon, asteroidal meteorites uniquely contain minerals that formed before the solar system, and during the growth and differentiation of planetesimals and planets in the "solar nebula"– the disk of dust and gas around the proto-Sun, within the first few tens of million years of solar system evolution. Amongst asteroidal meteorites, about 85% of the total that fall to Earth are chondrites. These are primitive rocks with elemental compositions similar to that of the Sun (e.g., Scott and Krot, 2014 [20]). They sample asteroids that did not undergo melting, although evidence of aqueous alteration and thermal metamorphism in some chondrite classes attests to some heating in bodies that accreted or did not accrete nebular ices, respectively. About 14% of meteorites falling to Earth consist of differentiated (or partly so) materials (McCoy et al., 2006 [10]). These are meteorites known under the names of

achondrites, irons, and stony-irons. They derive from asteroids that underwent various degrees of melting and differentiation into metallic iron cores and silicate mantles. The ∼500-km-diameter asteroid 4 Vesta, associated with one group of achondrites denominated HED (the howardite-eucrite-diogenite group) and target of the recent NASA space mission Dawn, is a spectacular example of a differentiated asteroid. Rare stony meteorites blasted off the surfaces of the Moon and Mars by cosmic impacts comprise less than about 1% of the total. The 428 lunar meteorites, or lunaites, to date present in our collections (December 2020 update) represent a valuable extension to the Apollo and Luna missions sampling of the Moon's surface debris, thereby providing additional clues into the geological evolution of the lunar crust, the formation of the Earth-Moon system, and the intense cosmic bombardment that affected the inner solar system bodies during the first few hundred million years of its evolution (e.g., Warren and Taylor, 2014 [22]). The 287 Martian meteorites are the only rock samples from planet Mars available in our laboratories (e.g., McSween and McLennan, 2014 [12]). They include basalts and cumulates formed from basaltic magmas. They have revealed that planetary differentiation on Mars occurred 4.5 billion years ago, probably during accretion, and that magmatism extended through the period from about 1.3 Ga to about 180 Ma. These meteorites have also provided insights into the geological history of the planet, including the composition of its Fe-rich mantle and its atmosphere, along with information about subsurface water circulation in response to changes in the global climatic evolution (e.g., Bridges et al., 2001 [3]; Chennaoui Aoudjehane et al., 2012 [5]).

Over 73,000 meteorites, of up to 60 t in mass, with many in the 10 to 100 g mass range, are listed in The Meteoritical Bulletin Database (https://www.lpi.usra.edu/meteor/metbull.php). This is the authoritative source of information on approved meteorites, which is provided by the Meteoritical Society. Of these, 1350 meteorites were seen to fall (and are known as "falls") to date. The oldest meteorite falls, for which material is still available for research, are the meteorite of Nōgata (Japan, fallen in 861) and Ensisheim (Alsace, France, fallen in 1492). Since the late 1950s, the fall of a few meteorites have been detected through camera networks (e.g. the European Camera Network in central Europe, Oberst et al., 1998 [16]; Prairie Meteorite Network in the Midwestern United States, McCrosky et al., 1971 [11]; The Meteorite Observation and Recovery Project in Western Canada, Halliday et al., 1978 [7]; the Australian Desert Fireball Network in Western Australia; Bland, 2004 [1]) designed to track meteoroids entering the atmosphere, determine pre-entry orbits, and recover meteorites unaffected (or nearly so) by terrestrial weathering and contamination. By far, most of the other meteorites are the thousands of 'finds' recovered from hot and cold deserts over the last 50 years. Hamada (nearly bare bedrock-desert) and serir (gravel/pebble-desert) type hot desert surfaces in the Sahara, Atacama, and Nullarbor Plain, and the many blue ice fields on the East Antarctic Ice Sheet are the most productive terrains for the collection of meteorites on Earth – truly a treasure-trove for planetary science.

Chapter 2

Chondrites

Chondrites are undifferentiated meteorites, considered the most primitive rocks of the solar system. They take their name from the abundant small spheroids they contain called "chondrules". Chondrules have dimensions of hundreds to thousands of micrometers, and are mainly made of olivine and pyroxene, Fe-Ni metal, and glass. Chondrules, FeNi-metal, refractory inclusions (Calcium Aluminium Inclusions or CAIs, and Ameboid Olivine Aggregates or AOAs), and fine-grained matrix are the four main components of chondrites (Brearley and Jones, 1998 [2]).

There are three classes of chondrite meteorites: (1) Carbonaceous Chondrites (CCs), (2) Ordinary Chondrites (OCs), Enstatite Chondrites (ECs) (Tab. 2.1). Based on chemistry, oxygen isotopes, mineralogy, and petrography, for these classes it is possible to define thirteen different groups. The OC class comprises the H, L, and LL groups; the CC class comprises the CI, CM, CO, CV, CK, CR, CB, CH groups; and the EC class comprises the EH and EL groups. Two groups, Rumuruti-like (R) and Kakangari-like (K) chondrites comprise a smaller number of meteorites. Different proportions between the chondritic components (chondrules, matrix, refractory inclusions, and metal) and variable chondrule mean diameter, allow identifying different groups of chondrites from a petrographic analysis (as shown in Tab. 2.2). Furthermore, each group is characterized by a specific O-isotopic composition.
Each chondrite meteorite is identified by a "petrologic type", namely a number from 1 to 6, that indicates the intensity of the alteration due to thermal or aqueous processes. Type 3 is used for unaltered chondrites, types 2 and 1 are indicative of an increasing aqueous alteration, and types 4 to 6 of increasing thermal metamorphism. When extreme thermal alteration conditions that cause complete melting and recrystallization of the rock occur, the chondrite could be identified with a petrologic type 7. Ordinary, enstatite, and also Rumuruti and Kakangari-like, chondrites usually have petrologic types from 3 to 6; instead carbonaceous chondrites from 3 to 1.

Ordinary chondrites are the most abundant class that fall to Earth, hence the name "ordinary". There are three groups of OCs, that are identified by different total Fe contents: (1) H-types contain high total Fe; (2) L-types contain low total Fe; (3) LL-types contain low metallic Fe compared to total Fe and low total Fe content.
In OCs, chondrules are the main component with abundances usually between 60 and 80 vol%. There seems to be a correlation between chondrule mean diameter and Fe-metal content, indeed H chondrites have smaller chondrules (0.3 mm) than L (0.7 mm) and LL (0.9 mm) chondrites. Metals and sulfides can be present in small grains around (or inside) chondrules or forming coarser grained assemblages (in low and high petrologic types respectively). Matrix is present but less abundant than in CCs.

Carbonaceous chondrites comprise eight groups: CI, CM, CO, CR, CB, CH, CV, and CK. Each group refers to a typical chondrite fall: Ivuna meteorite for the CIs, Mighei for CMs, Ornans for COs, Renazzo for CRs, Bencubbin for CBs, ALH 85085 for CHs, Vigarano for CVs, and

Karoonda for CKs.
These chondrites are named "carbonaceous" because of the presence of C-rich compounds, such as organic molecules. The preservation in their composition of extraterrestrial organic molecules and presolar grains (particles originated before the Sun was formed) makes the CCs important to better understand the processes linked to origin of life, nucleosynthesis and stellar evolution.
Petrographic characteristics useful to recognise different CC groups are shown in Tab. 2.2. Chondrule abundance and mean diameter are distinct in CC groups. Matrix is usually much more abundant than in the OCs (except for CBs and CHs); it is more than 90 vol% in CIs, where chondrules are basically absent. The metal content is variable, and in general proportions between the four components vary considerably between the groups. This collection includes members of CM, CO and CV groups, but some carbonaceous chondrites have not been classified yet and are only defined as "CC".

Enstatite chondrites include a smaller number of meteorites. These meteorites are characterized by reduced mineralogy and are made of enstatite, metals, and sulfides.
The oxygen isotopic composition of enstatites lies on the terrestrial fractionation line (or TFL, defined by the bulk oxygen isotopic composition of Earth). For this reason, enstatite chondrites are thought to have been formed on an asteroid similar to the proto-Earth. Enstatite chondrite groups are identified by different contents of metallic Fe: EH- and EL-groups have high and low metallic Fe contents, respectively.

Table 2.1: Meteorite classification scheme (modified after Krot et al., 2014 [8]).

Meteorite classification

Chondrites

Class	Carbonaceous								Ordinary			Enstatite			
Group	CI	CM	CO	CR	CB	CH	CV	CK	H	L	LL	EH	EL	R	K
Petrologic type	1	1-2	3-4	1-2	3	3	3-4	3-6	3-6			3-6		3-6	3

Non-chondritic meteorites

Primitive achondrites	Differentiated achondrites	Irons and stony irons	Planetary
Winonaites	Angrites	Mesosiderites	Martian
Acapodranites	Aubrites	Pallasites	Shergottites
Acapulcoites	Brachinites	Main group	Nakhlites
Lodranites	Ureilites	Eagle Station	Chassignites
	HED	IAB irons	Orthopyroxenites
	Howardites	IC irons	Lunar
	Eucrites	IIAB irons	
	Diogenites	IIC irons	
	Mesosiderite silicate fraction	IID irons	
		IIE irons	
		IIG irons	
		IIIAB irons	
		IIICD irons	
		IIIE irons	
		IIIF irons	
		IVA irons	
		IVB irons	

Table 2.2: Petrographic characteristics of the chondrite groups (after Brearley and Jones, 1998 [2]).

	Chondrule abundance[1] (vol%)	**Matrix abundance[2] (vol%)**	**Refractory inclusion abundance[3] (vol%)**	**Metal abundance[4] (vol%)**	**Chondrule mean diameter (mm)**
CI	<<1	>99	<<1	0	-
CM	20	70	5	0.1	0.3
CR	50-60	30-50	0.5	5-8	0.7
CO	48	34	13	1-5	0.15
CV	45	40	10	0-5	1.0
CK	15	75	4	<0.01	0.7
CH	∼70	5	0.1	20	0.02
H	60-80	10-15	0.1-1?	10	0.3
L	60-80	10-15	0.1-1?	5	0.7
LL	60-80	10-15	0.1-1?	2	0.9
EH	60-80	<2-15?	0.1-1?	8	0.2
EL	60-80	<2-15?	0.1-1?	15	0.6
R	>40	36	0	0.1	0.4
K	27	73	<0.1	0	0.6

[1]Chondrule abundance includes mineral fragments.

[2]Matrix abundance includes metal.

[3]Refractory inclusion abundance includes CAI + AOA.

[4]Metal abundance is for metal outside chondrules.

2.1 Ordinary Chondrites

2.1.1 LL3 Ordinary Chondrite: Frontier Mountain 03011

Find: Antarctica, 2003
Shock Stage: S2 Weathering Grade: W1
Section Label: FRO 03011,01
Type Specimen: Museo Nazionale dell'Antartide (Siena), PNRA
HD Images: TL-PPL / TL-CPL / RL

Figure 2.1: Photomicrograph of the polished thin section FRO 03011,01 (transmitted light, plane-polarized light, TL-PPL).

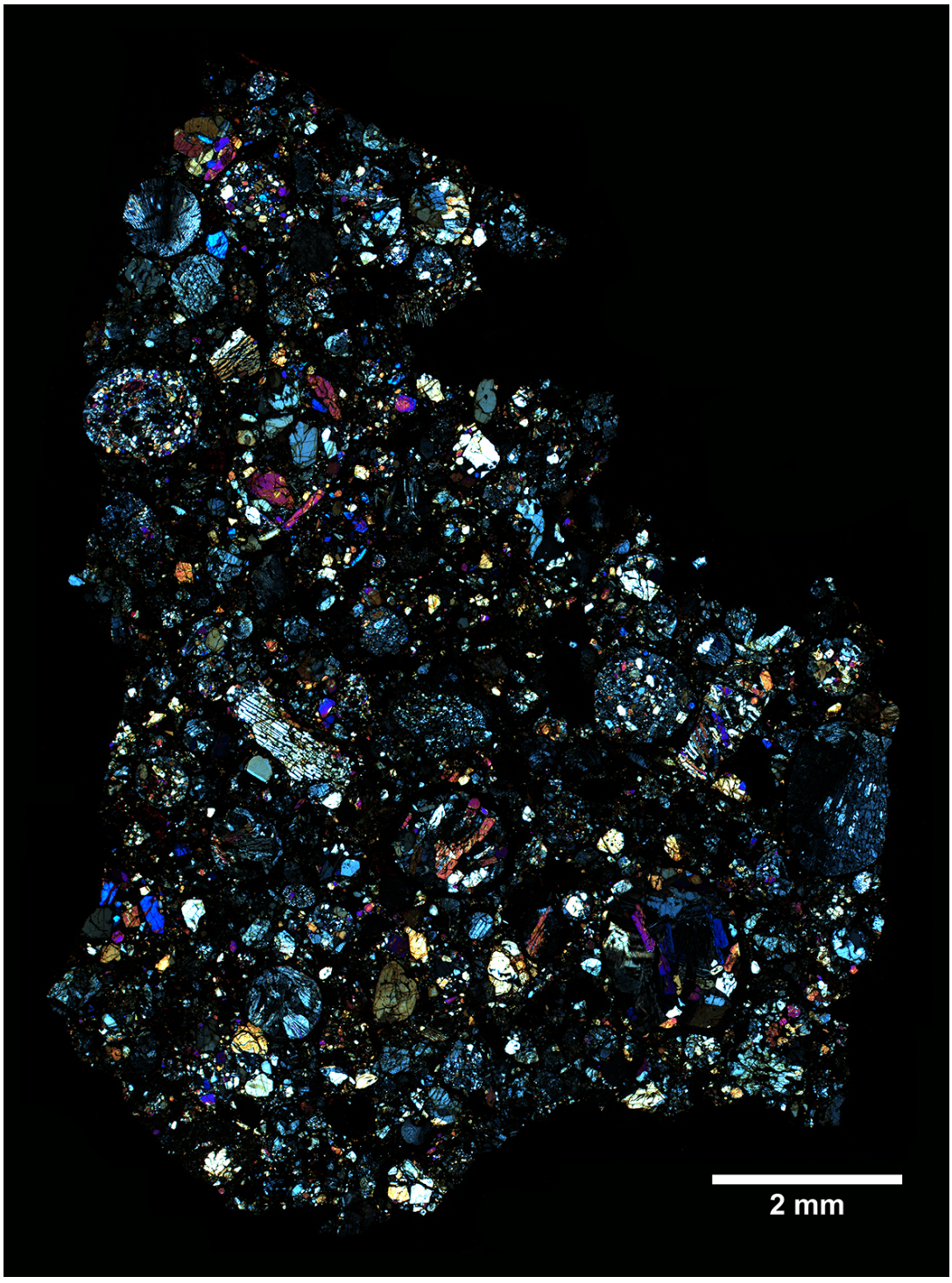

Figure 2.2: Photomicrograph of the polished thin section FRO 03011,01 (transmitted light, crossed-polarized light, TL-CPL).

Figure 2.3: Photomicrograph of the polished thin section FRO 03011,01 (reflected light, RL).

2.1.2 LL3 Ordinary Chondrite: Frontier Mountain 10083

Find: Antarctica, 2011
Shock Stage: S3 Weathering Grade: W1
Section Label: FRO 10083,01
Type Specimen: Museo Nazionale dell'Antartide (Siena), PNRA
HD Images: TL-PPL / TL-CPL / RL

Figure 2.4: Photomicrograph of the polished thin section FRO 10083,01 (transmitted light, plane-polarized light, TL-PPL).

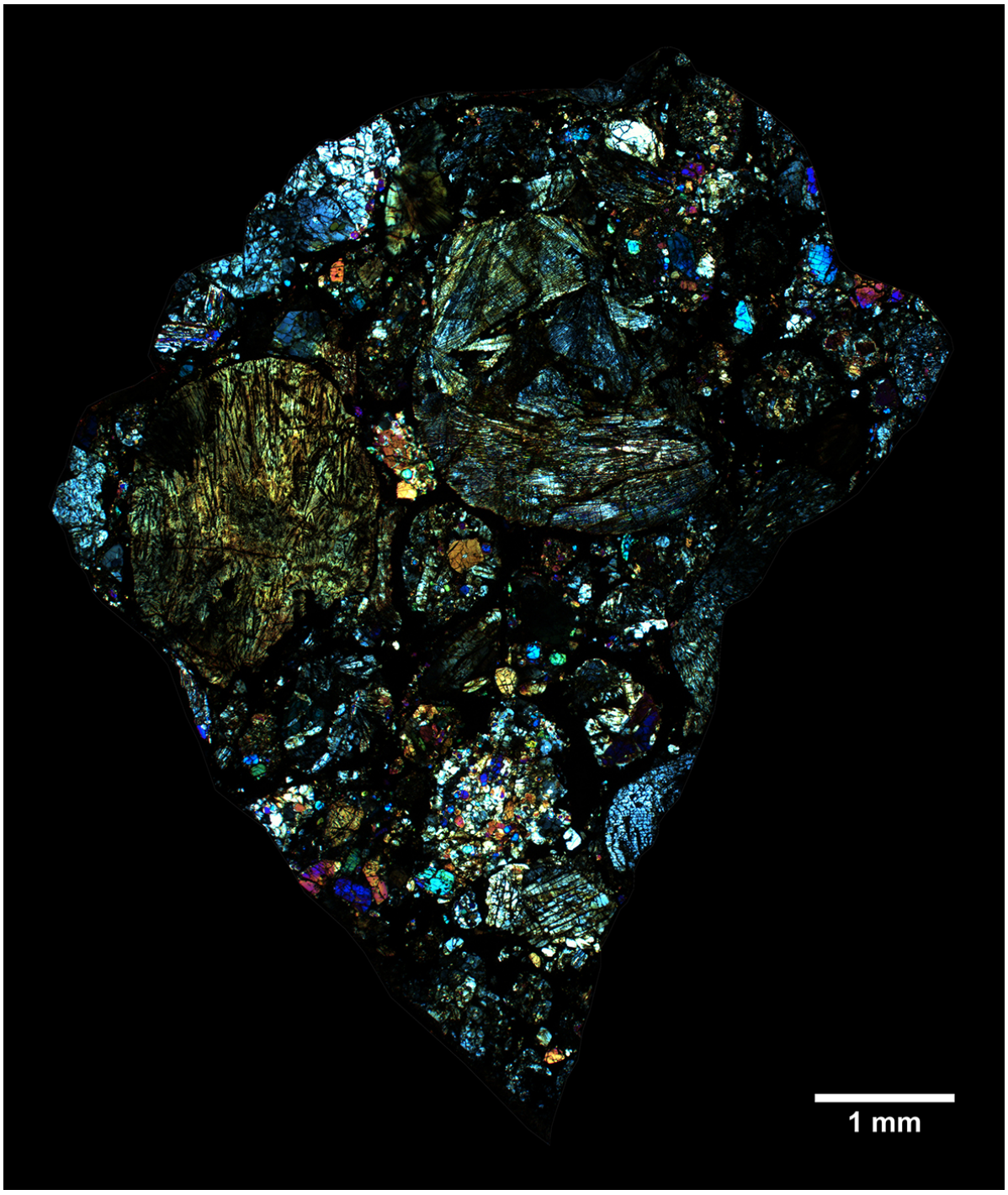

Figure 2.5: Photomicrograph of the polished thin section FRO 10083,01 (transmitted light, crossed-polarized light, TL-CPL).

Figure 2.6: Photomicrograph of the polished thin section FRO 10083,01 (reflected light, RL).

2.1.3 LL3 Ordinary Chondrite: Frontier Mountain 10097

Find: Antarctica, 2011
Shock Stage: S1 Weathering Grade: W1
Section Label: FRO 10097,01
Type Specimen: Museo Nazionale dell'Antartide (Siena), PNRA
HD Images: TL-PPL / TL-CPL / RL

Figure 2.7: Photomicrograph of the polished thin section FRO 10097,01 (transmitted light, plane-polarized light, TL-PPL).

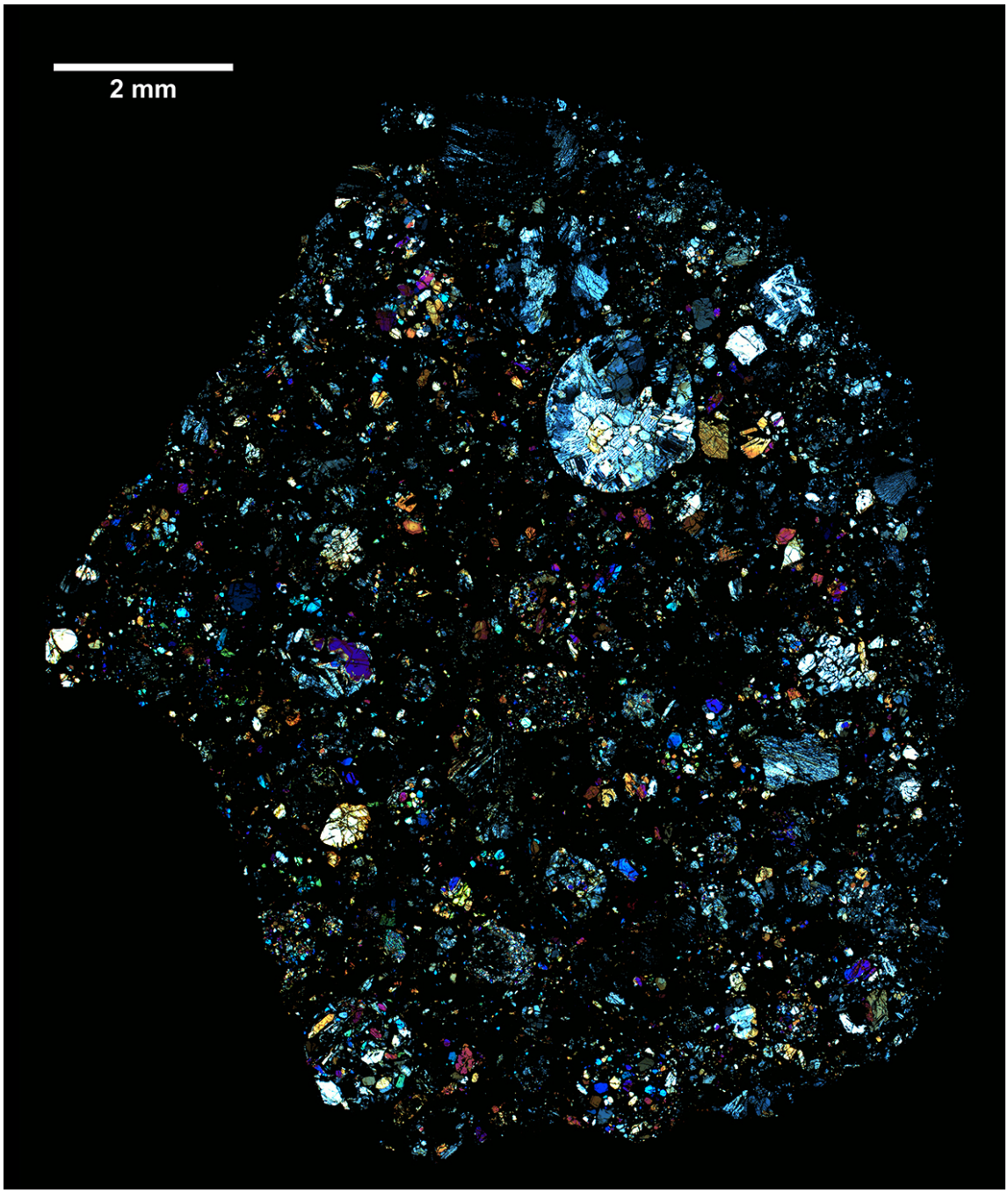

Figure 2.8: Photomicrograph of the polished thin section FRO 10097,01 (transmitted light, crossed-polarized light, TL-CPL).

Figure 2.9: Photomicrograph of the polished thin section FRO 10097,01 (reflected light, RL).

2.1.4 LL3 Ordinary Chondrite: Reckling Peak 17105

Find: Antarctica, 2018
Shock Stage: S4 Weathering Grade: W0
Section Label: RKP 17105,01
Type Specimen: Museo Nazionale dell'Antartide (Siena), PNRA
HD Images: TL-PPL / TL-CPL / RL

Figure 2.10: Photomicrograph of the polished thin section RKP 17105,01 (transmitted light, plane-polarized light, TL-PPL).

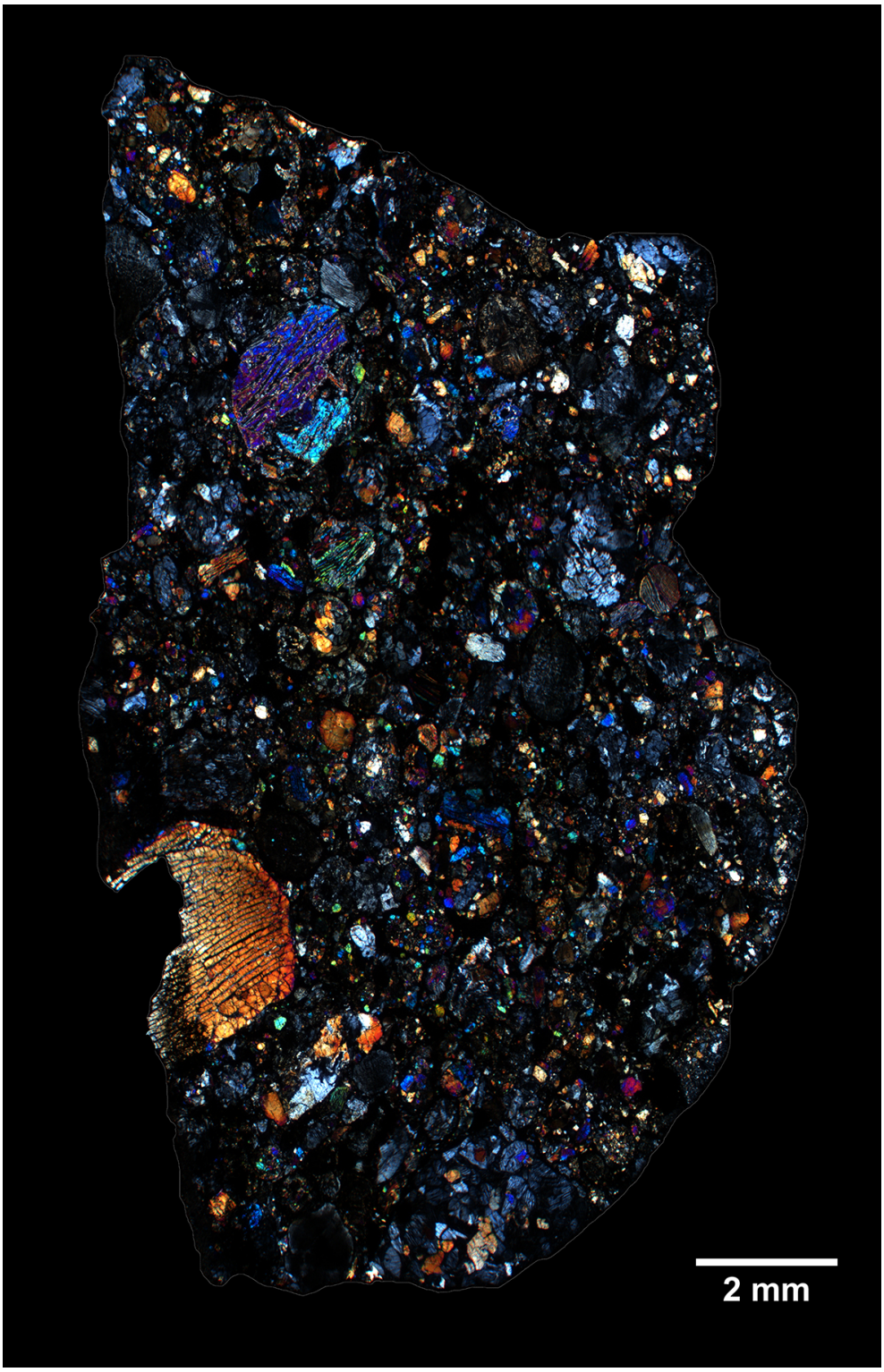

Figure 2.11: Photomicrograph of the polished thin section RKP 17105,01 (transmitted light, crossed-polarized light, TL-CPL).

Figure 2.12: Photomicrograph of the polished thin section RKP 17105,01 (reflected light, RL).

2.1.5 LL3 Ordinary Chondrite: Frontier Mountain 10081

Find: Antarctica, 2010
Shock Stage: S2 Weathering Grade: W1
Section Label: FRO 10081,01
Type Specimen: Museo Nazionale dell'Antartide (Siena), PNRA
HD Images: TL-PPL / TL-CPL / RL

Figure 2.13: Photomicrograph of the polished thin section FRO 10081,01 (transmitted light, plane-polarized light, TL-PPL).

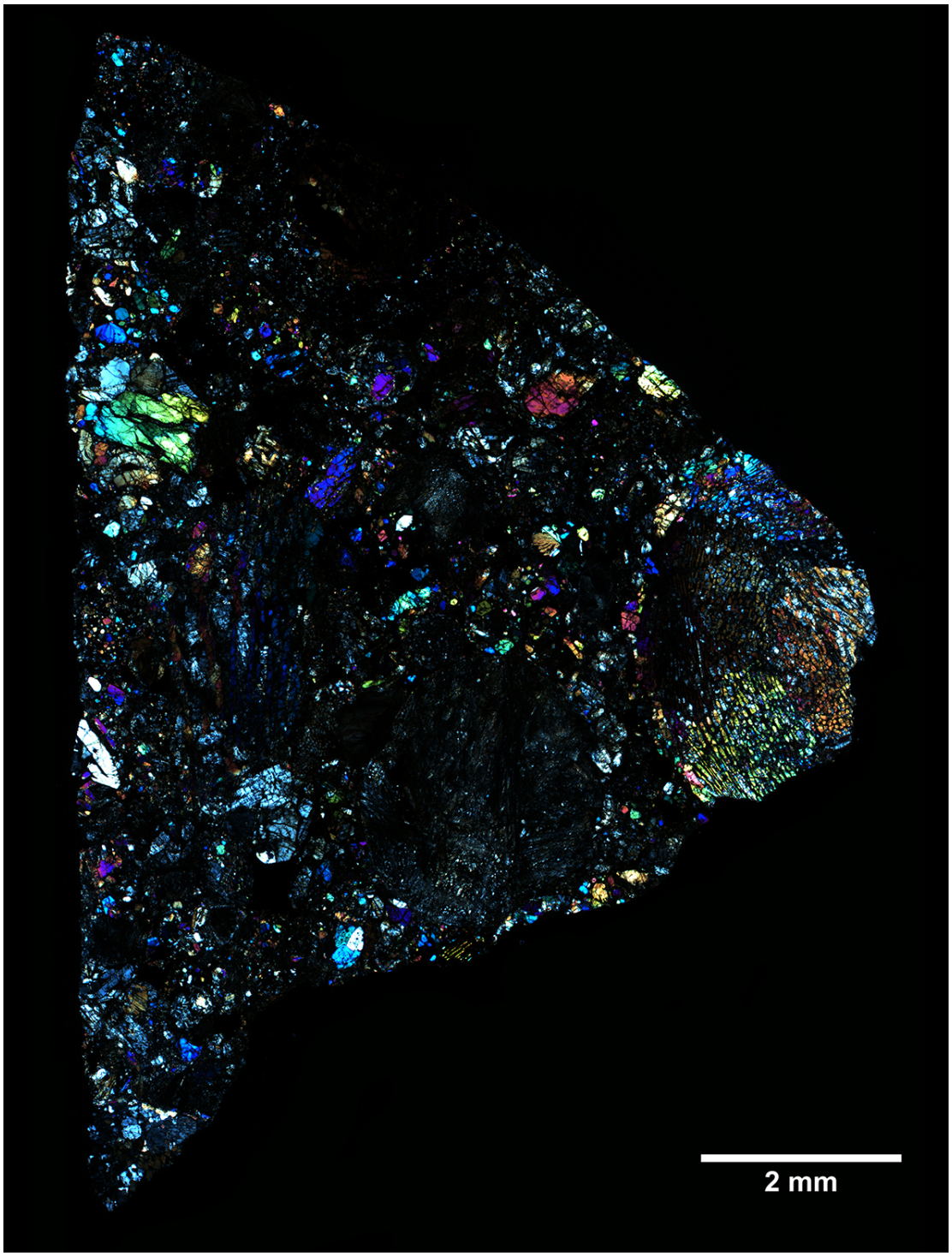

Figure 2.14: Photomicrograph of the polished thin section FRO 10081,01 (transmitted light, crossed-polarized light, TL-CPL).

Figure 2.15: Photomicrograph of the polished thin section FRO 10081,01 (reflected light, RL).

2.1.6 LL6 Ordinary Chondrite: Allan Hills 14005

Find: Antarctica, 2014
Shock Stage S2 Weathering Grade W0
Section Label: ALH 14005,01
Type Specimen: Museo Nazionale dell'Antartide (Siena), PNRA
HD Images: TL-PPL / TL-CPL / RL

Figure 2.16: Photomicrograph of the polished thin section ALH 14005,01. The section cuts across a complete individual with fusion crust (black rim) (transmitted light, plane-polarized light, TL–PPL).

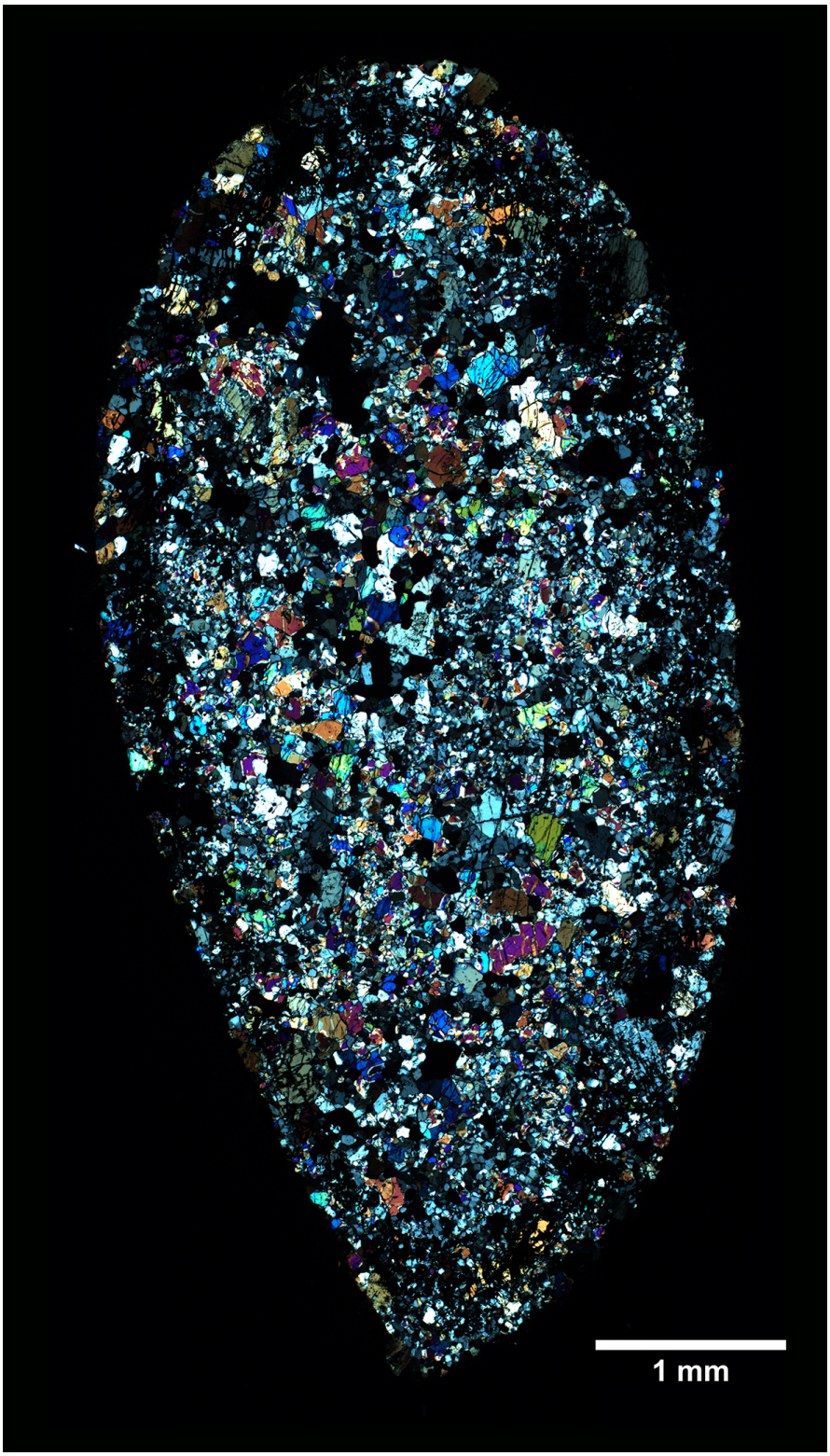

Figure 2.17: Photomicrograph of the polished thin section ALH 14005,01 (transmitted light, crossed-polarized light, TL-CPL).

Figure 2.18: Photomicrograph of the polished thin section ALH 14005,01 (reflected light, RL).

2.1.7 L(LL)3 Ordinary Chondrite: Allan Hills 99101

Find: Antarctica, 2000
Shock Stage: S4 Weathering Grade: W1
Section Label: ALH 99101,01
Type Specimen: Museo Nazionale dell'Antartide (Siena), PNRA
HD Images: TL-PPL / TL-CPL / RL

Figure 2.19: Photomicrograph of the polished thin section ALH 99101,01 (transmitted light, plane-polarized light, TL-PPL).

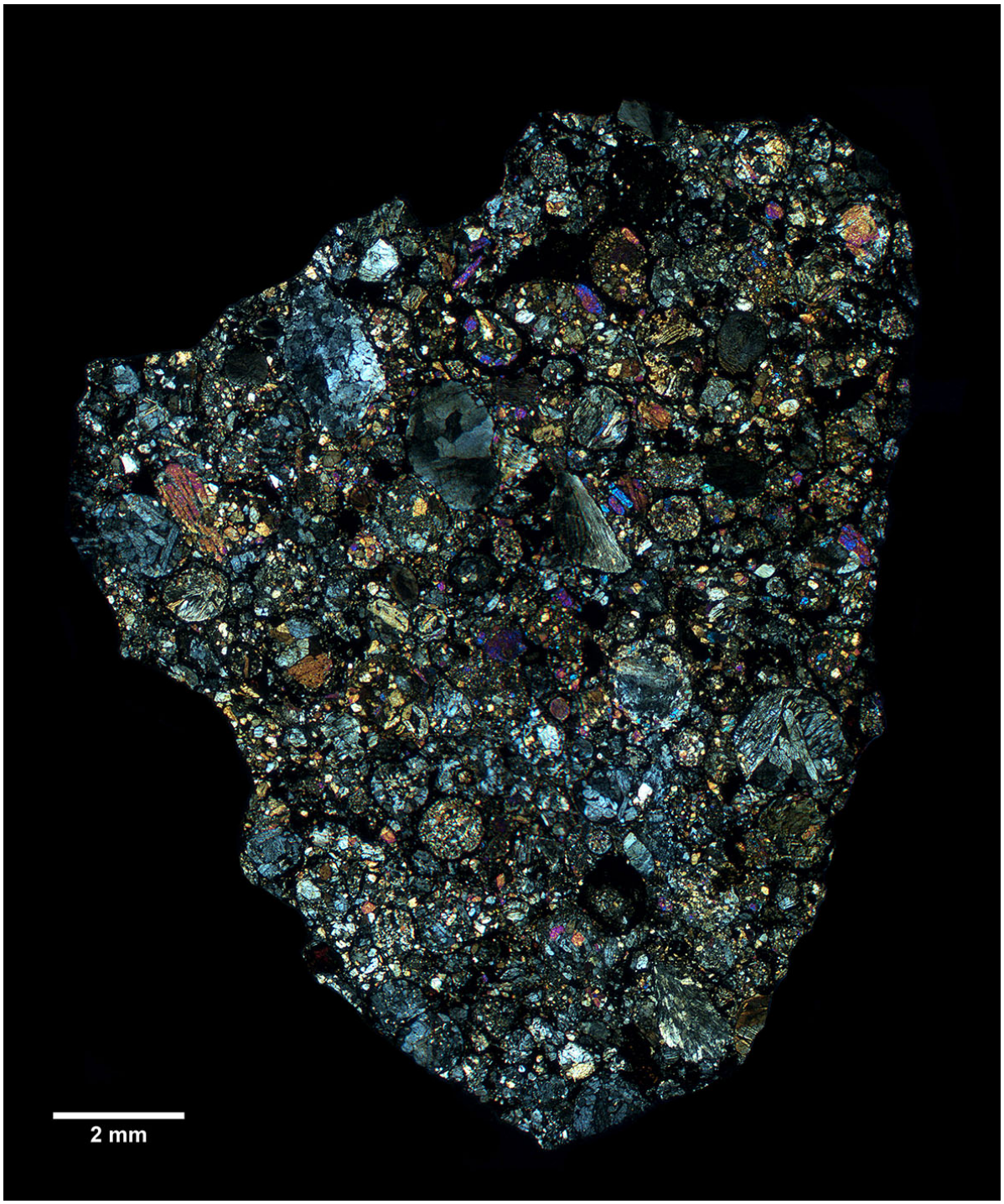

Figure 2.20: Photomicrograph of the polished thin section ALH 99101,01 (transmitted light, crossed-polarized light, TL-CPL).

Figure 2.21: Photomicrograph of the polished thin section ALH 99101,01 (reflected light, RL).

2.1.8 L(LL)3 Ordinary Chondrite: Dar al Gani 313

Find: Libya, 1997
Shock Stage: S3 Weathering Grade: W2
Section Label: DaG 313,01
Type Specimen: Museo Nazionale dell'Antartide (Siena)
HD Images: TL-PPL / TL-CPL / RL

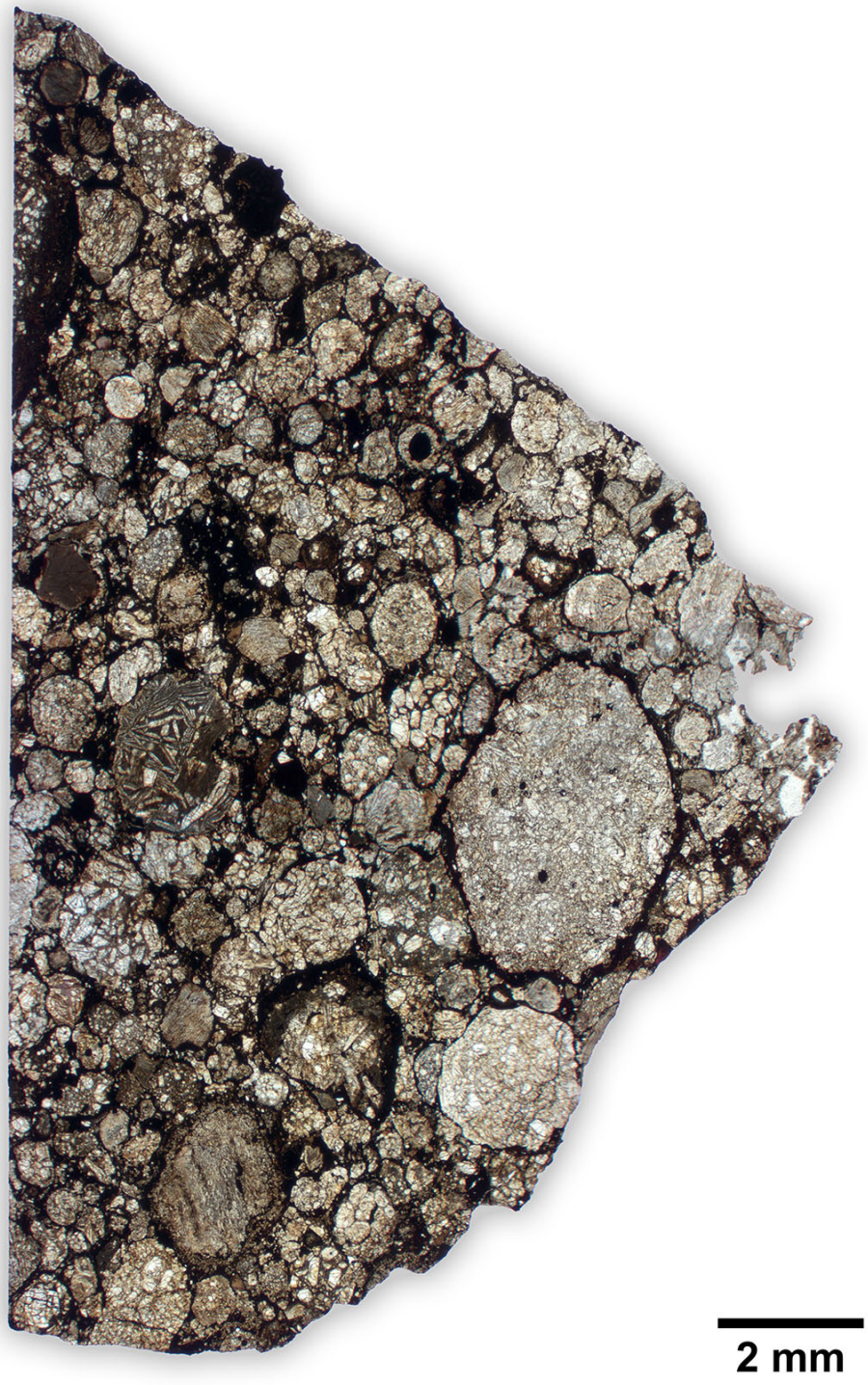

Figure 2.22: Photomicrograph of the polished thin section DaG 313,01 (transmitted light, plane-polarized light, TL-PPL).

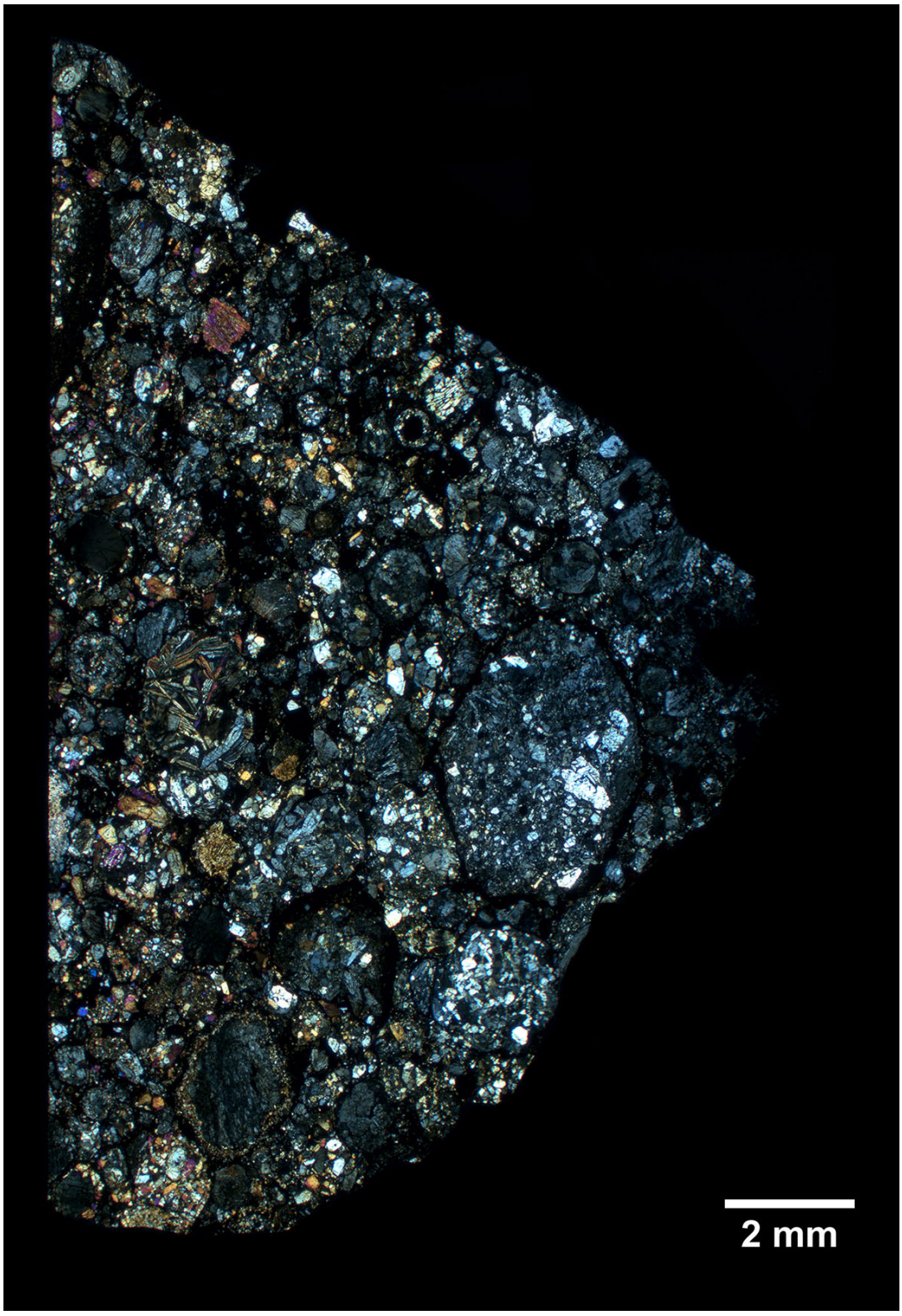

Figure 2.23: Photomicrograph of the polished thin section DaG 313,01 (transmitted light, crossed-polarized light, TL-CPL).

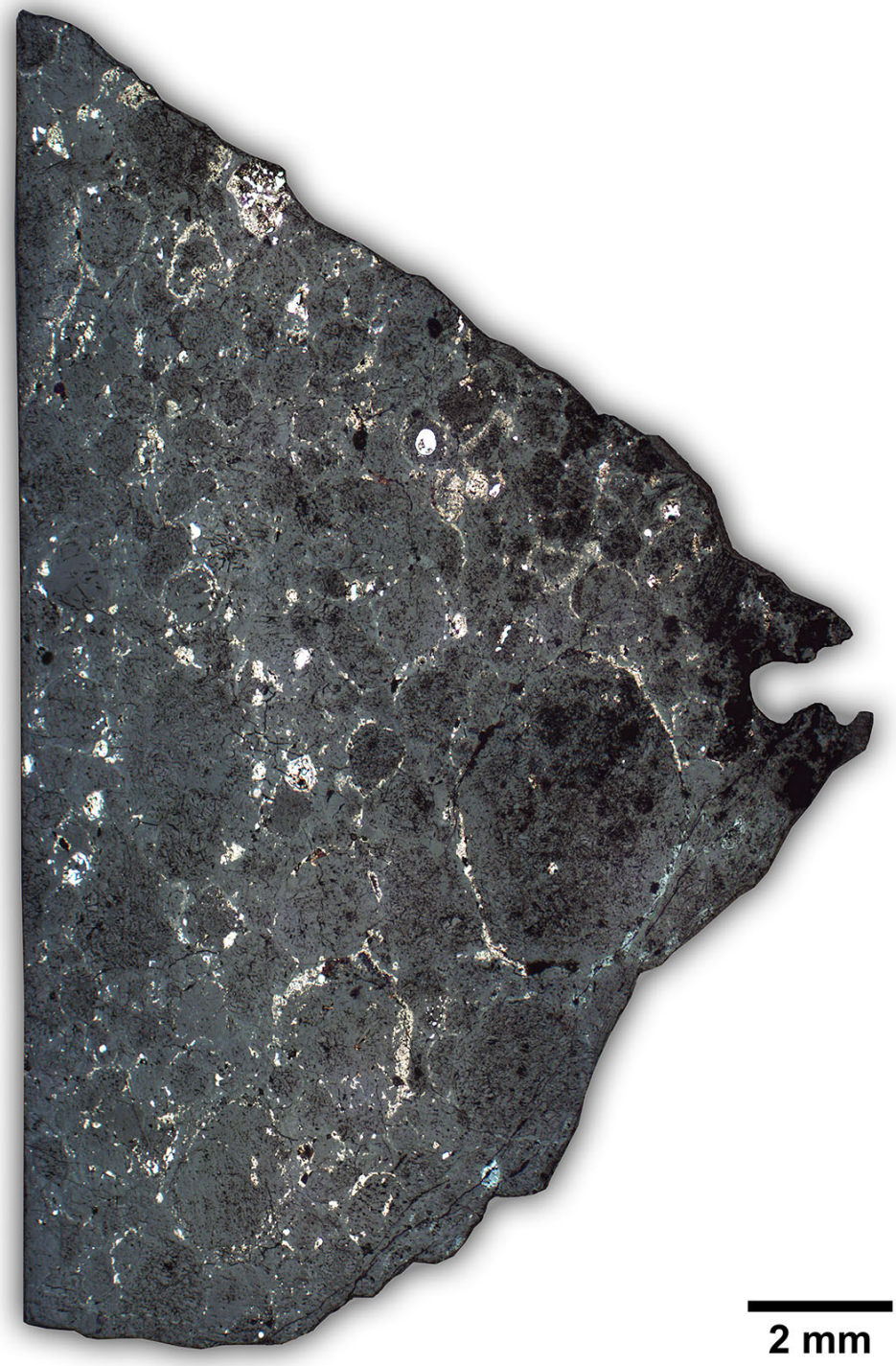

Figure 2.24: Photomicrograph of the polished thin section DaG 313,01 (reflected light, RL).

2.1.9 L3 Ordinary Chondrite: Reckling Peak 17043

Find: Antarctica, 2017
Shock Stage: S3 Weathering Grade: W1
Section Label: RKP 17043,01
Type Specimen: Museo Nazionale dell'Antartide (Siena), PNRA
HD Images: TL-PPL / TL-CPL / RL

Figure 2.25: Photomicrograph of the polished thin section RKP 17043,01 (transmitted light, plane-polarized light, TL-PPL).

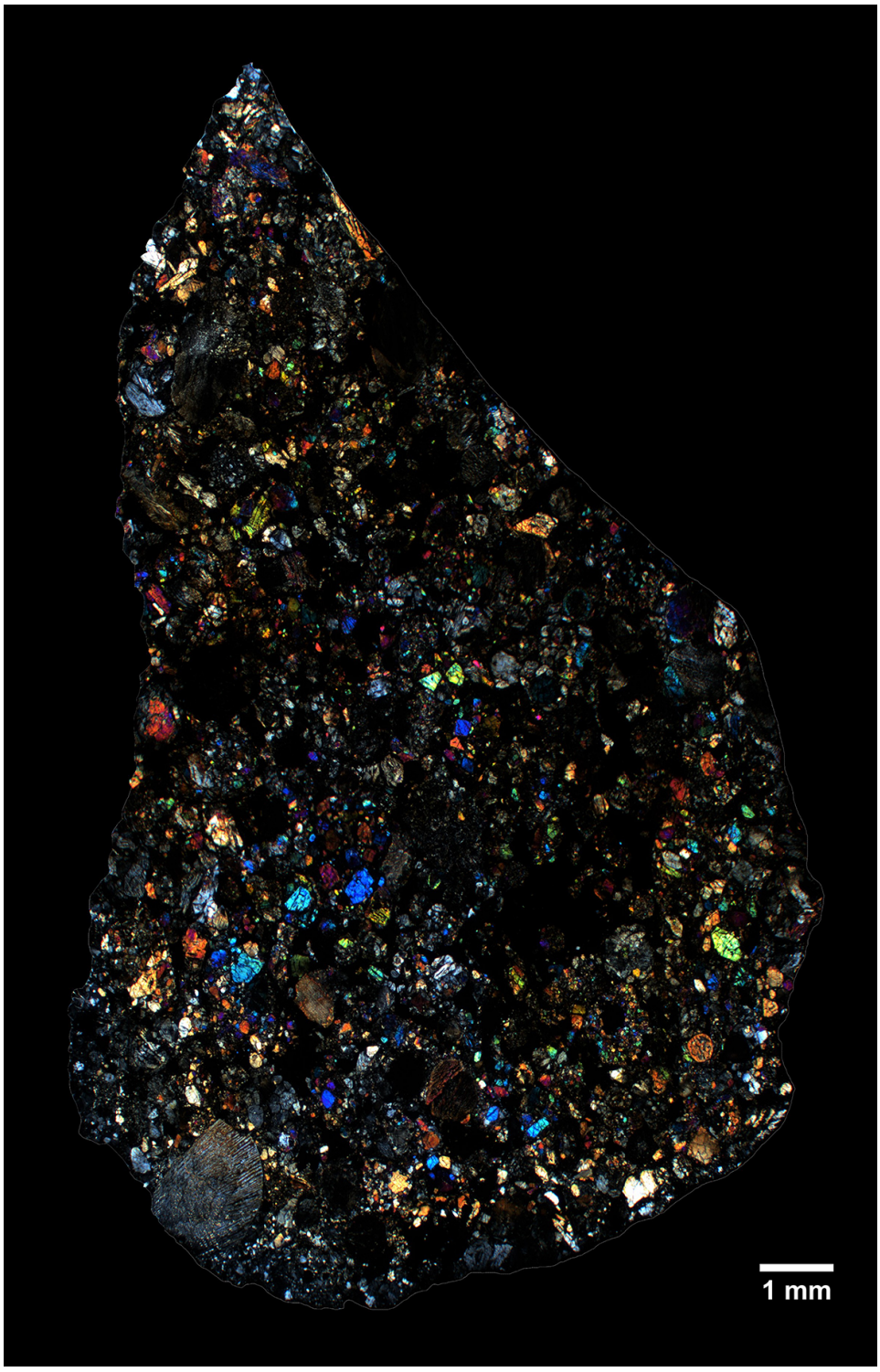

Figure 2.26: Photomicrograph of the polished thin section RKP 17043,01 (transmitted light, crossed-polarized light, TL-CPL).

Figure 2.27: Photomicrograph of the polished thin section RKP 17043,01 (reflected light, RL).

2.1.10 L4 Ordinary Chondrite: MacKay Glacier 14008

Find: Antarctica, 2015
Shock Stage: S3 Weathering Grade: W1
Section Label: MCY 14008,01
Type Specimen: Museo Nazionale dell'Antartide (Siena), PNRA
HD Images: TL-PPL / TL-CPL / RL

Figure 2.28: Photomicrograph of the polished thin section MCY 14008,01 (transmitted light, plane-polarized light, TL-PPL).

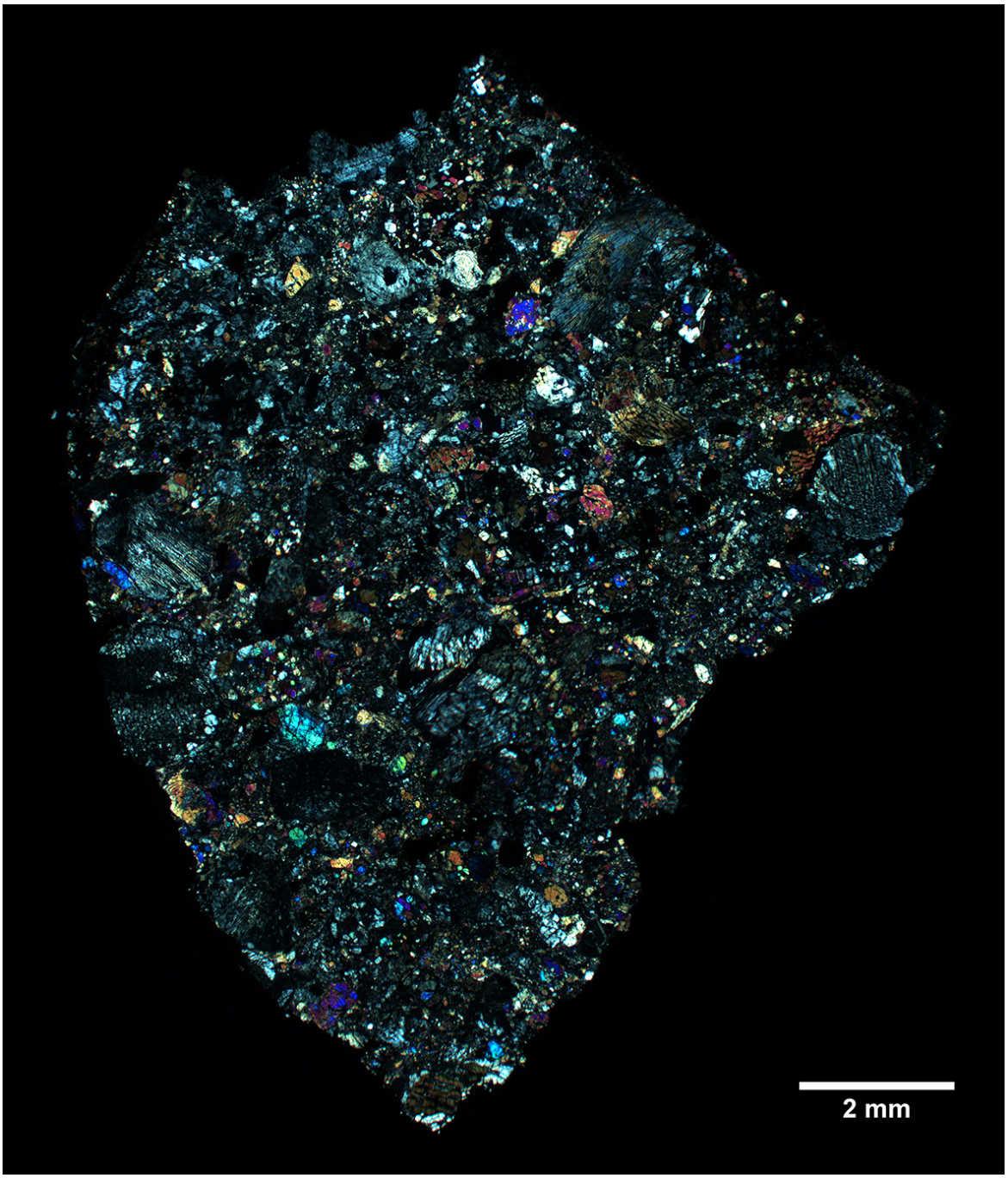

Figure 2.29: Photomicrograph of the polished thin section MCY 14008,01 (transmitted light, crossed-polarized light, TL-CPL).

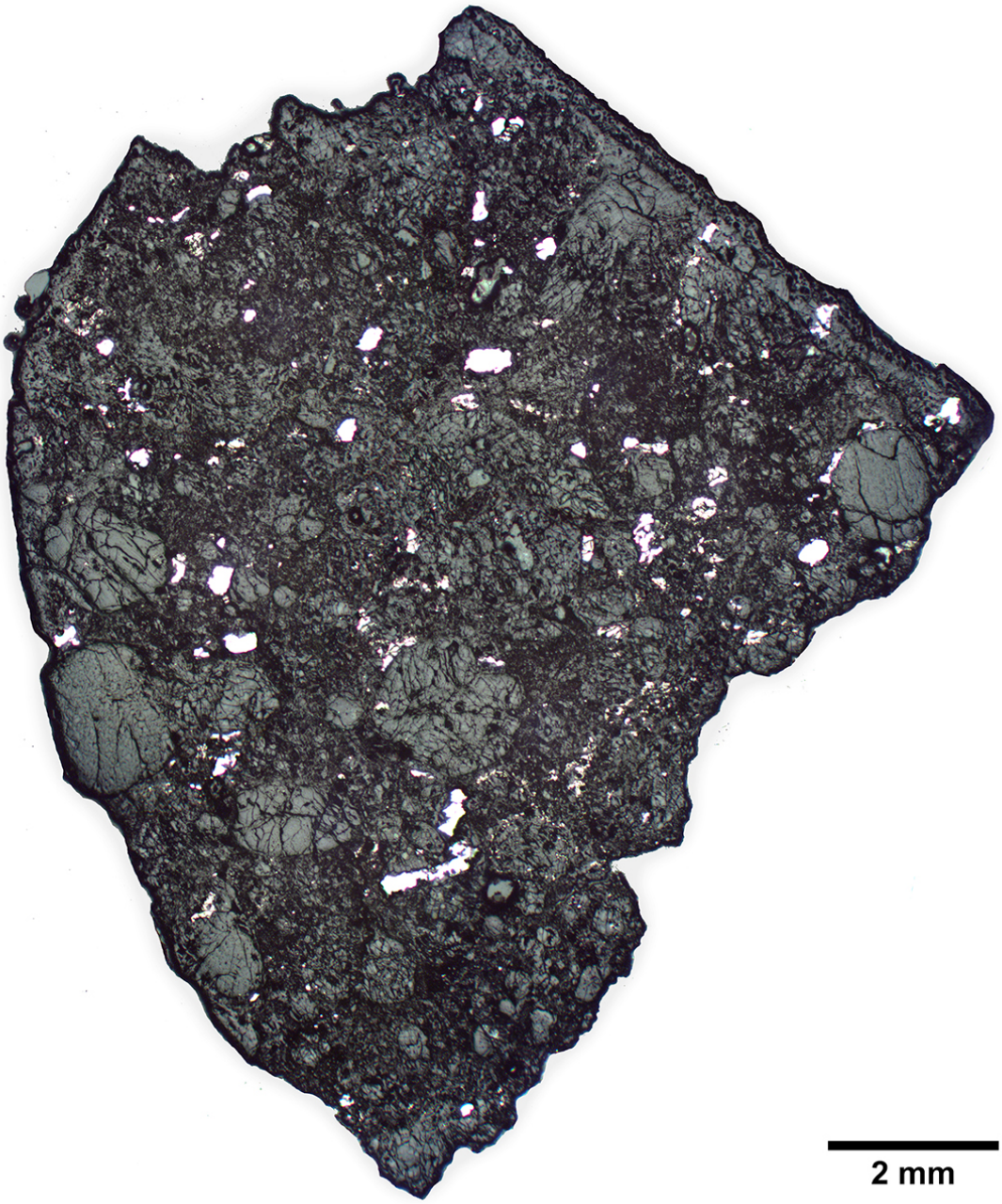

Figure 2.30: Photomicrograph of the polished thin section MCY 14008,01 (reflected light, RL).

2.1.11 L4-6 Ordinary Chondrite Breccia: SAID 01

Find/Fall: Sahara Desert, -
Shock Stage: S1 Weathering Grade: W1
Section Label: SAID 01,01
Type Specimen: Museo Nazionale dell'Antartide (Siena)
HD Images: TL-PPL / TL-CPL / RL

Figure 2.31: Photomicrograph of the polished thin section SAID 01,01 (transmitted light, plane-polarized light, TL-PPL).

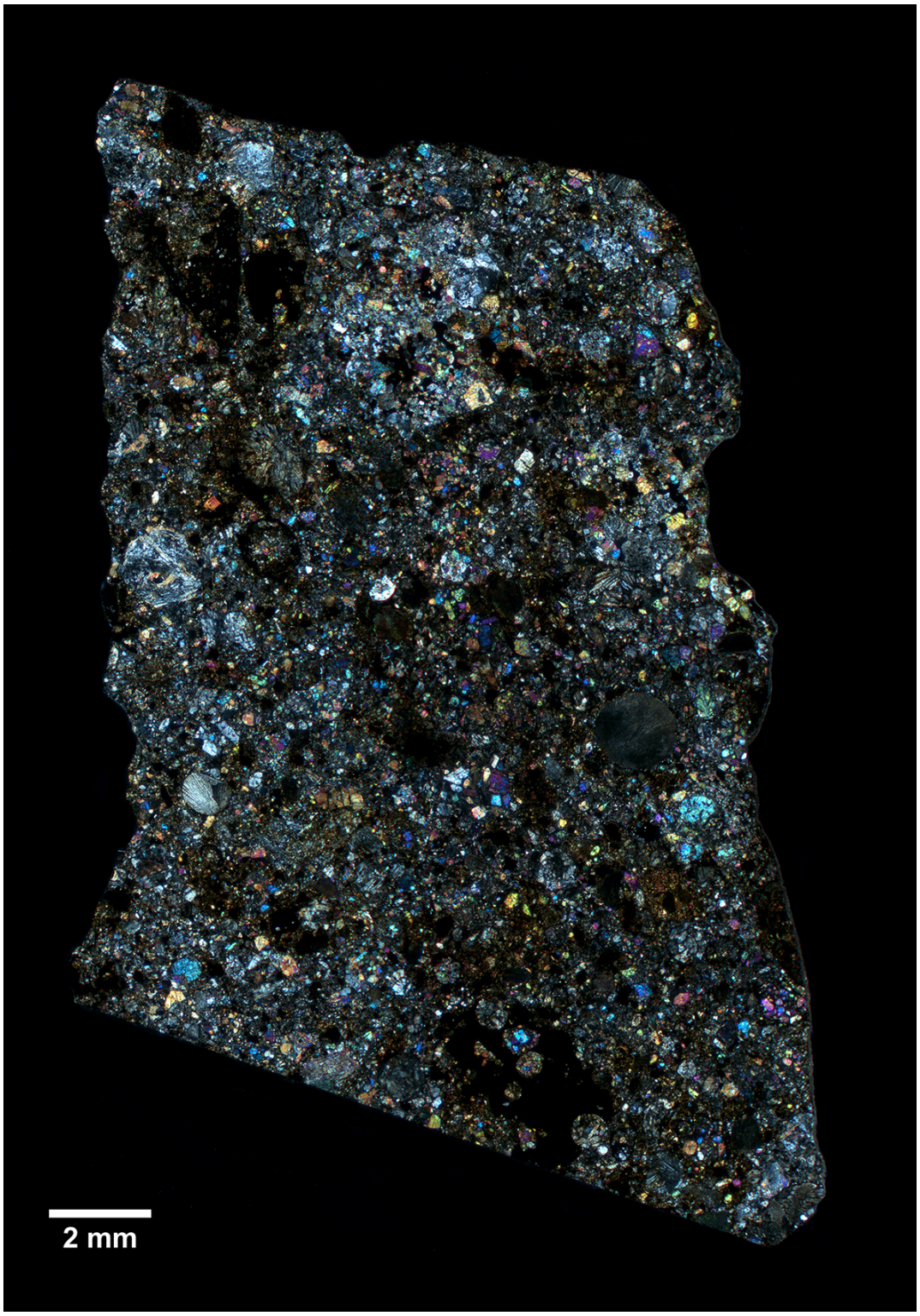

Figure 2.32: Photomicrograph of the polished thin section SAID 01,01 (transmitted light, crossed-polarized light, TL-CPL).

Figure 2.33: Photomicrograph of the polished thin section SAID 01,01 (reflected light, RL).

2.1.12 L6 Ordinary Chondrite: Beni M'Hira 01

Fall: Tunisia, 2001
Shock Stage: S5 Weathering Grade: W0
Section Label: Beni M'Hira,01
Type Specimen: Museo Nazionale dell'Antartide (Siena)
HD Images: TL-PPL / TL-CPL / RL

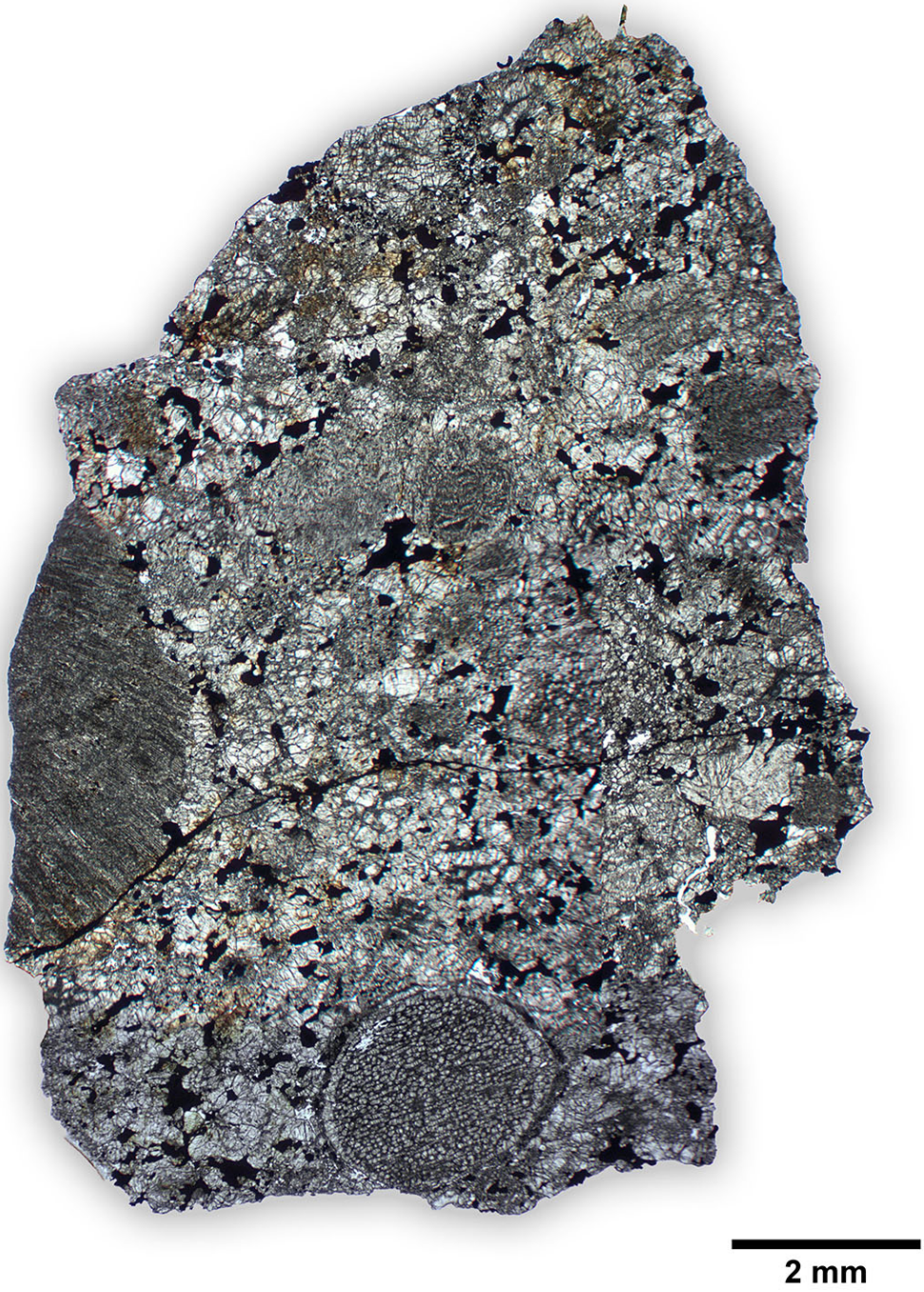

Figure 2.34: Photomicrograph of the polished thin section Beni M'Hira,01. Note the mm-sized macrochondrules and the thin black shock vein (transmitted light, plane-polarized light, TL-PPL).

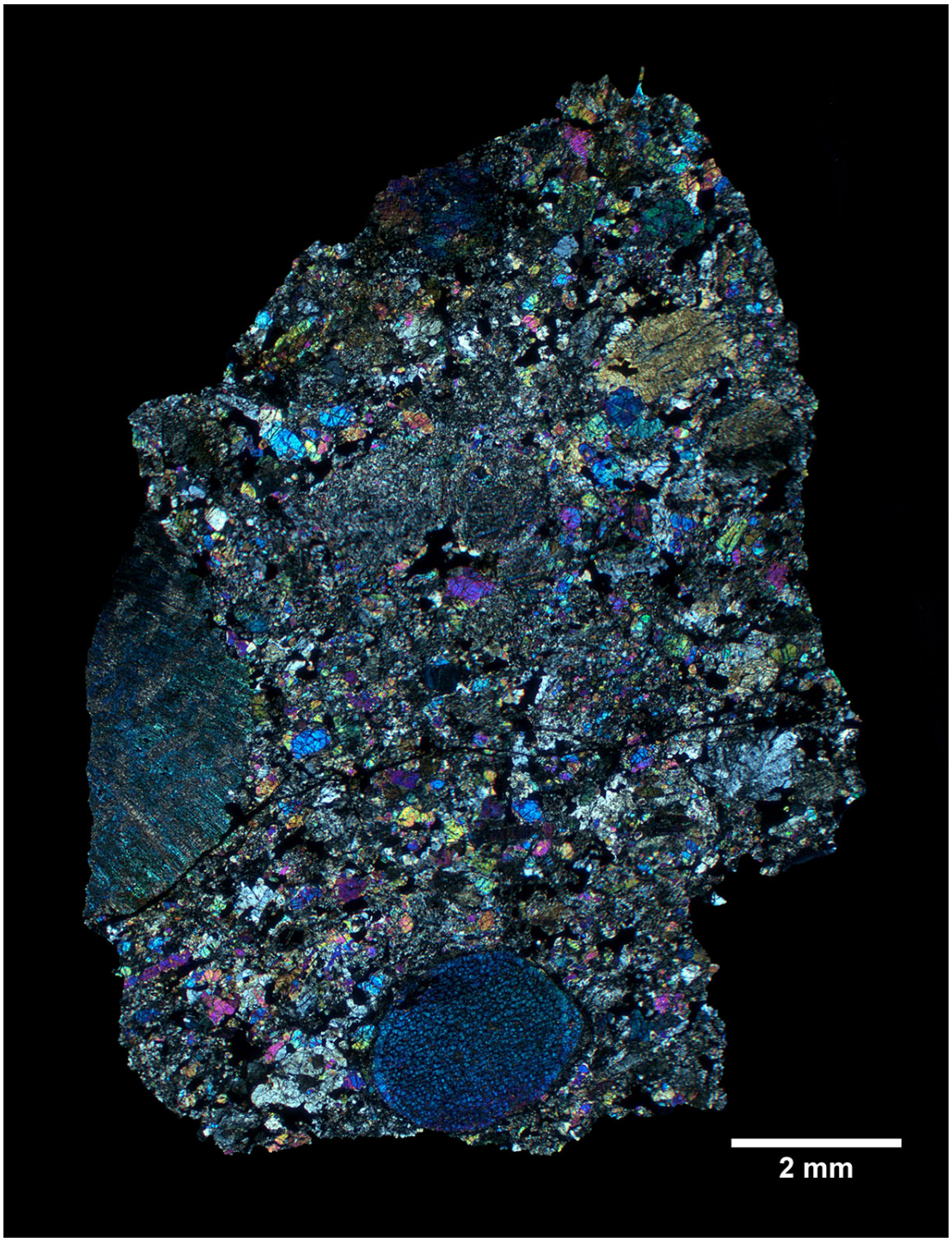

Figure 2.35: Photomicrograph of the polished thin section Beni M'Hira,01 (transmitted light, crossed-polarized light, TL-CPL).

Figure 2.36: Photomicrograph of the polished thin section Beni M'Hira,01 (reflected light, RL).

2.1.13 L6 Ordinary Chondrite: Dar al Gani 528

Find: Libya, 1997
Shock Stage: S6 Weathering Grade: W4
Section Label: DaG 528,01
Type Specimen: Museo Nazionale dell'Antartide (Siena)
HD Images: TL-PPL / TL-CPL / RL

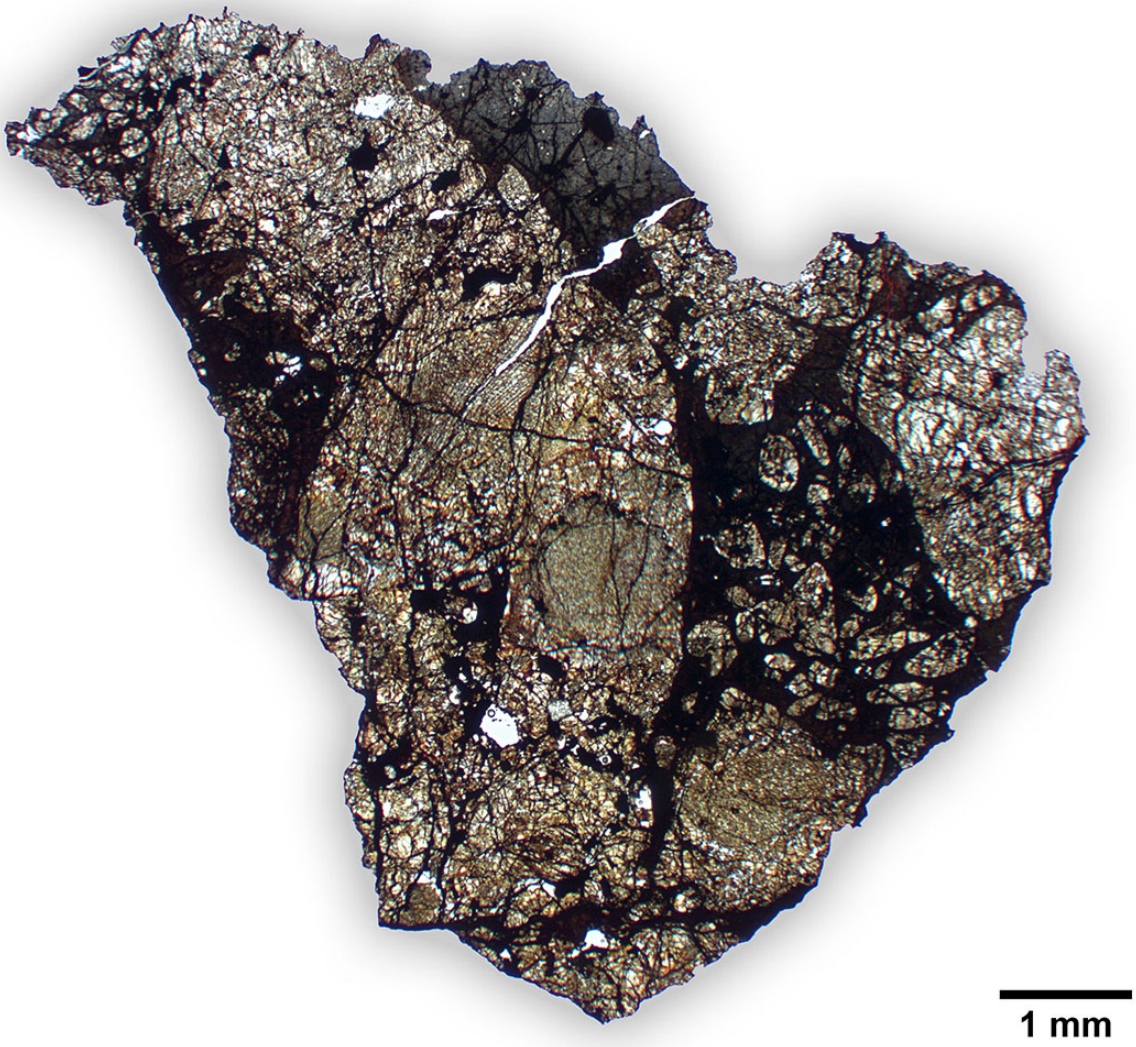

Figure 2.37: Photomicrograph of the polished thin section DaG 528,01 (transmitted light, plane-polarized light, TL-PPL).

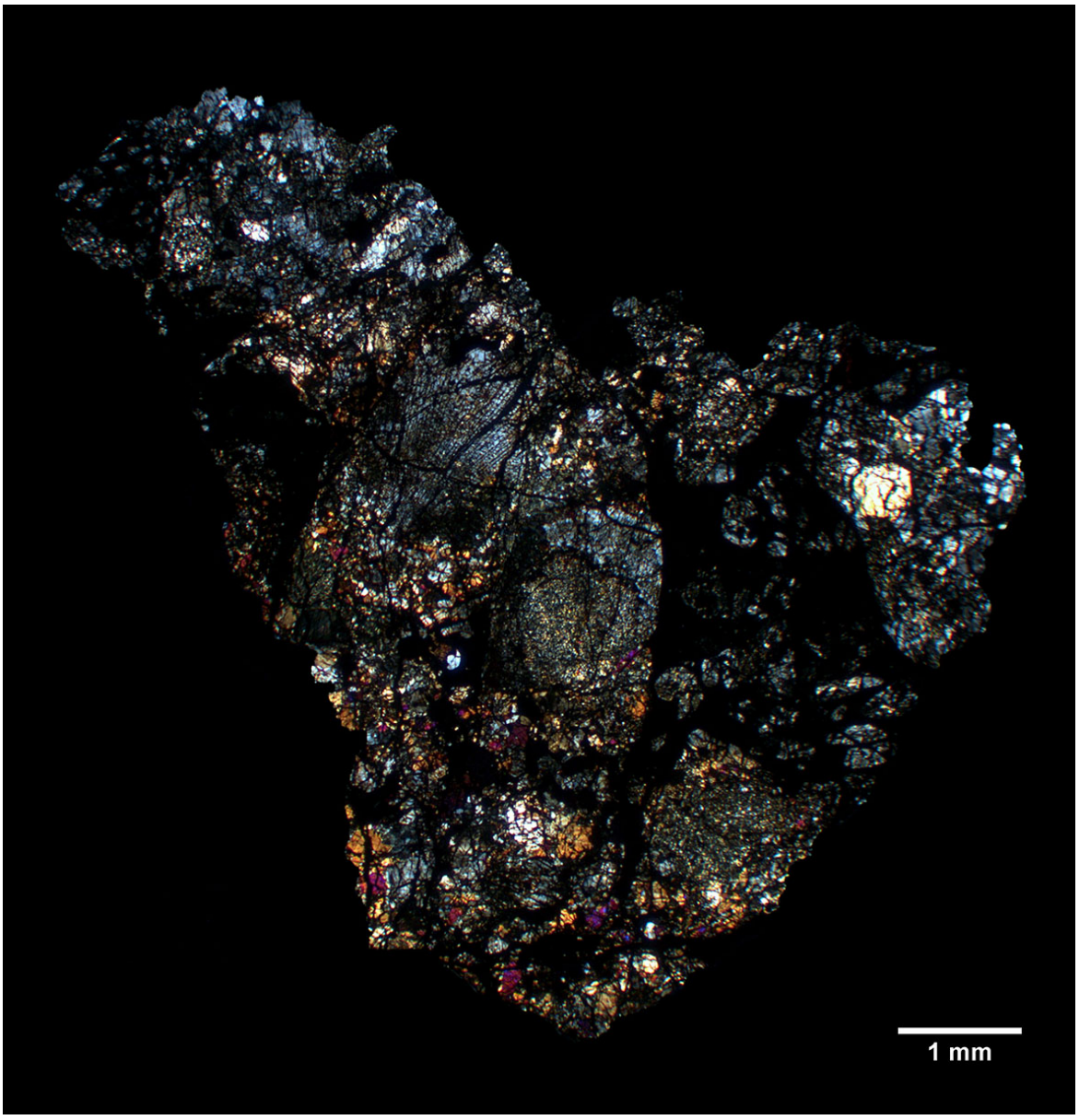

Figure 2.38: Photomicrograph of the polished thin section DaG 528,01 (transmitted light, crossed-polarized light, TL-CPL).

Figure 2.39: Photomicrograph of the polished thin section DaG 528,01 (reflected light, RL).

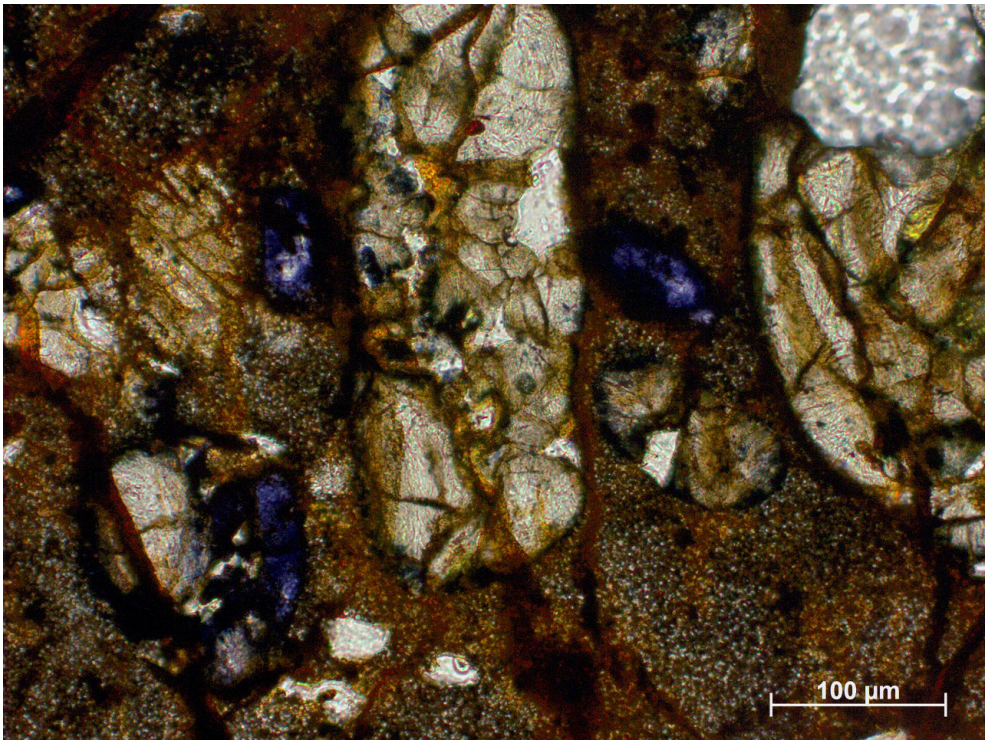

Figure 2.40: Photomicrograph of the polished thin section DaG 528,01 showing a detail of a clastic shock vein with ringwoodite microporphyroblasts (purple) set in a fine-grained matrix dominated by majorite (transmitted light, plane-polarized light, TL-PPL).

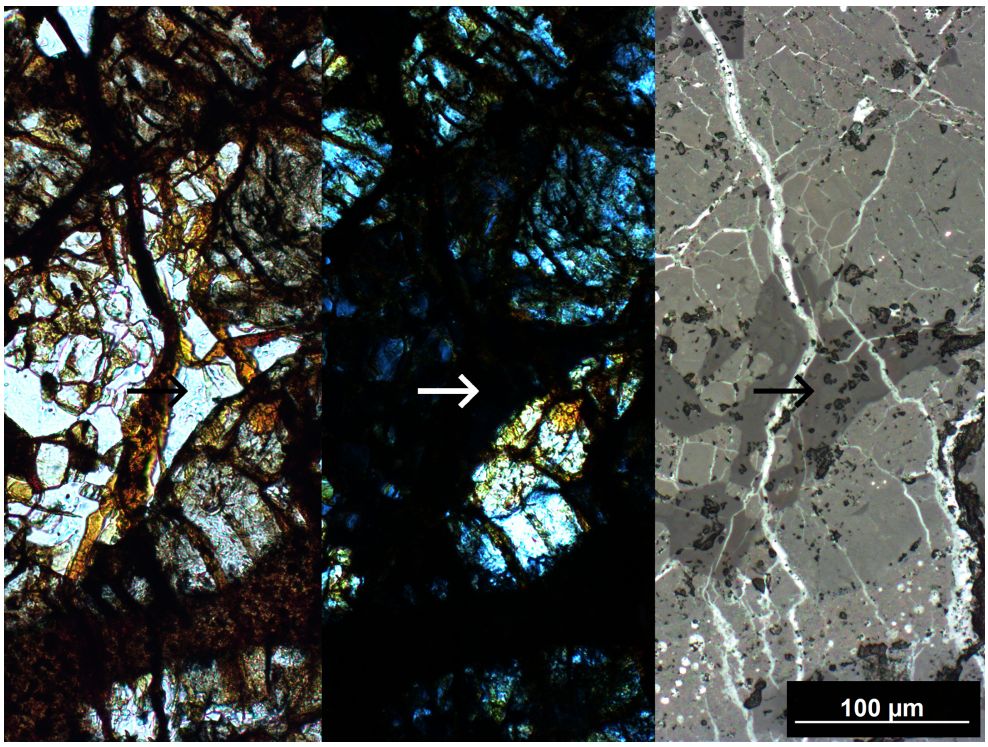

Figure 2.41: Photomicrograph of the polished thin section DaG 528,01 showing maskelynite (indicated by the arrows) in TL-PPL (left), TL-CPL (center), RL (right).

2.1.14 L6 Ordinary Chondrite: Dar al Gani 546

Find: Libya, 1997
Shock Stage: S6 Weathering Grade: W5
Section Label: DaG 546,01
Type Specimen: Museo Nazionale dell'Antartide (Siena)
HD Images: TL-PPL / TL-CPL

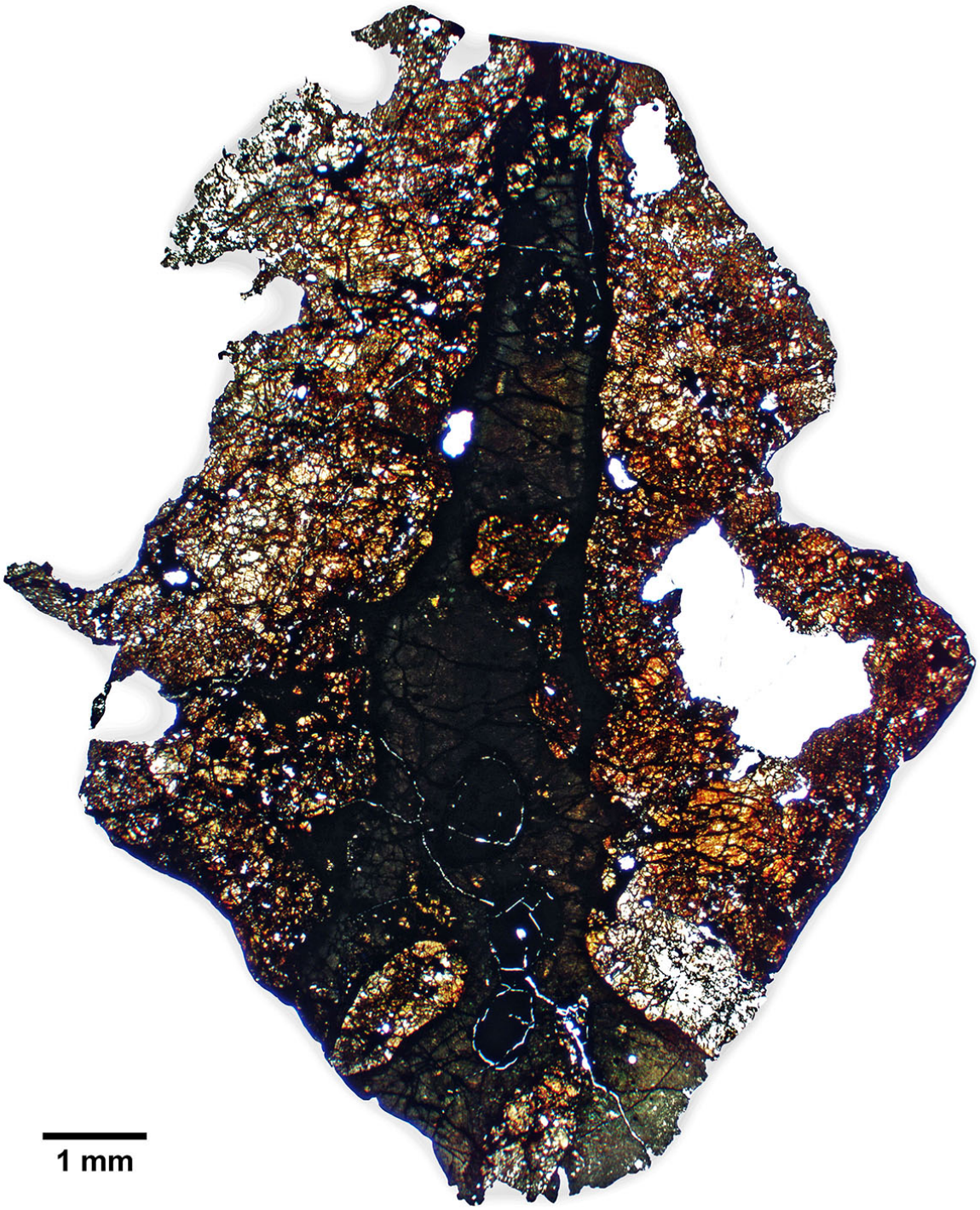

Figure 2.42: Photomicrograph of the polished thin section DaG 546,01 (transmitted light, plane-polarized light, TL-PPL).

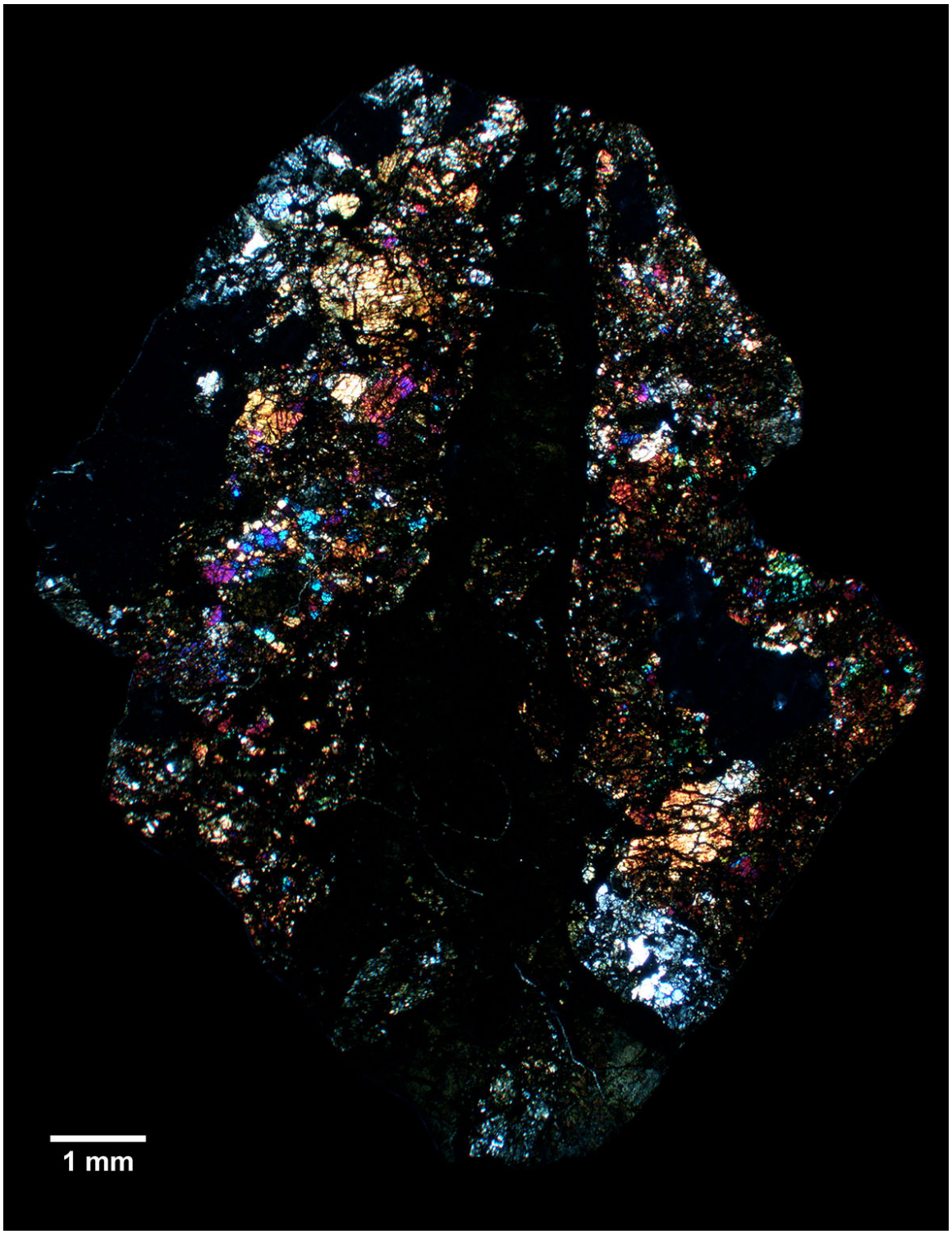

Figure 2.43: Photomicrograph of the polished thin section DaG 546,01 (transmitted light, crossed-polarized light, TL-CPL).

2.1.15 L6 Ordinary Chondrite: Frontier Mountain 03050

Find: Antarctica, 2003
Shock Stage: S4 Weathering Grade: W0
Section Label: FRO 03050,01
Type Specimen: Museo Nazionale dell'Antartide (Siena), PNRA
HD Images: TL-PPL / TL-CPL / RL

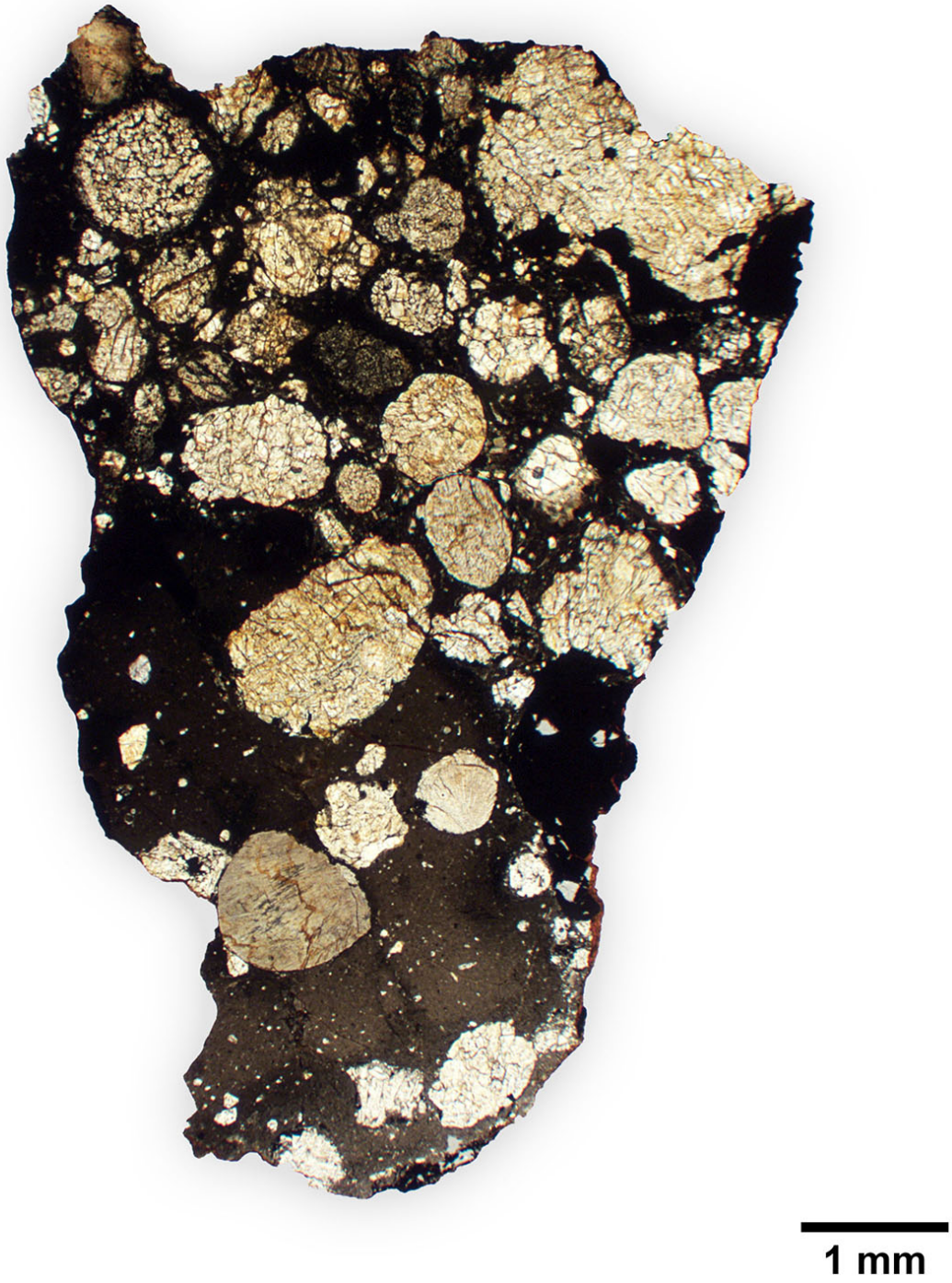

Figure 2.44: Photomicrograph of the polished thin section FRO 03050,01 (transmitted light, plane-polarized light, TL-PPL).

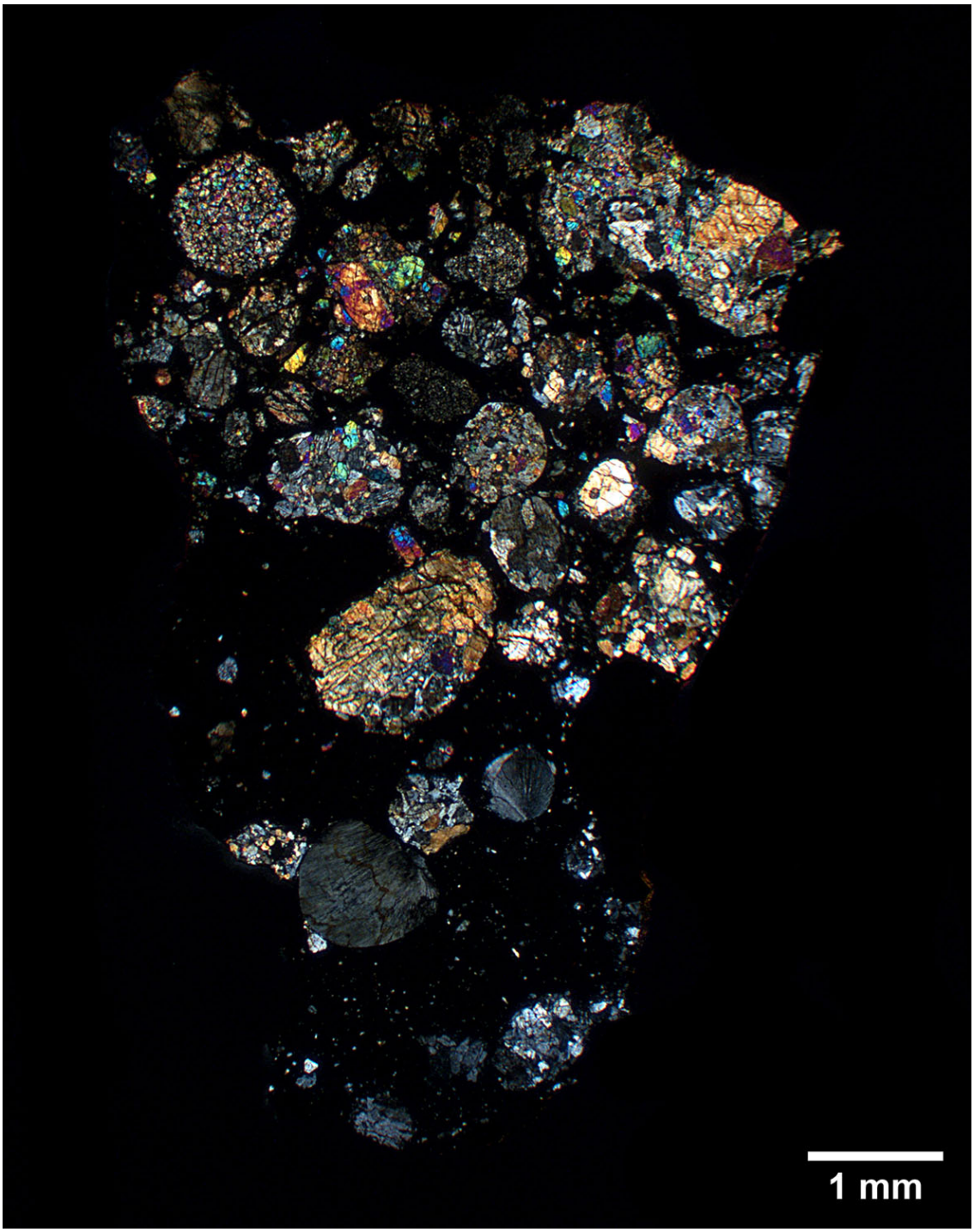

Figure 2.45: Photomicrograph of the polished thin section FRO 03050,01 (transmitted light, crossed-polarized light, TL-CPL).

Figure 2.46: Photomicrograph of the polished thin section FRO 03050,01 (reflected light, RL).

2.1.16 H3-4 Ordinary Chondrite Breccia: Frontier Mountain 90225

Find: Antarctica, 1990
Shock Stage: S2 Weathering Grade: W2
Section Label: FRO 90225,02
Type Specimen: Museo Nazionale dell'Antartide (Siena), PNRA
HD Images: TL-PPL / TL-CPL / RL

Figure 2.47: Photomicrograph of the polished thin section FRO 90225,02 (transmitted light, plane-polarized light, TL-PPL).

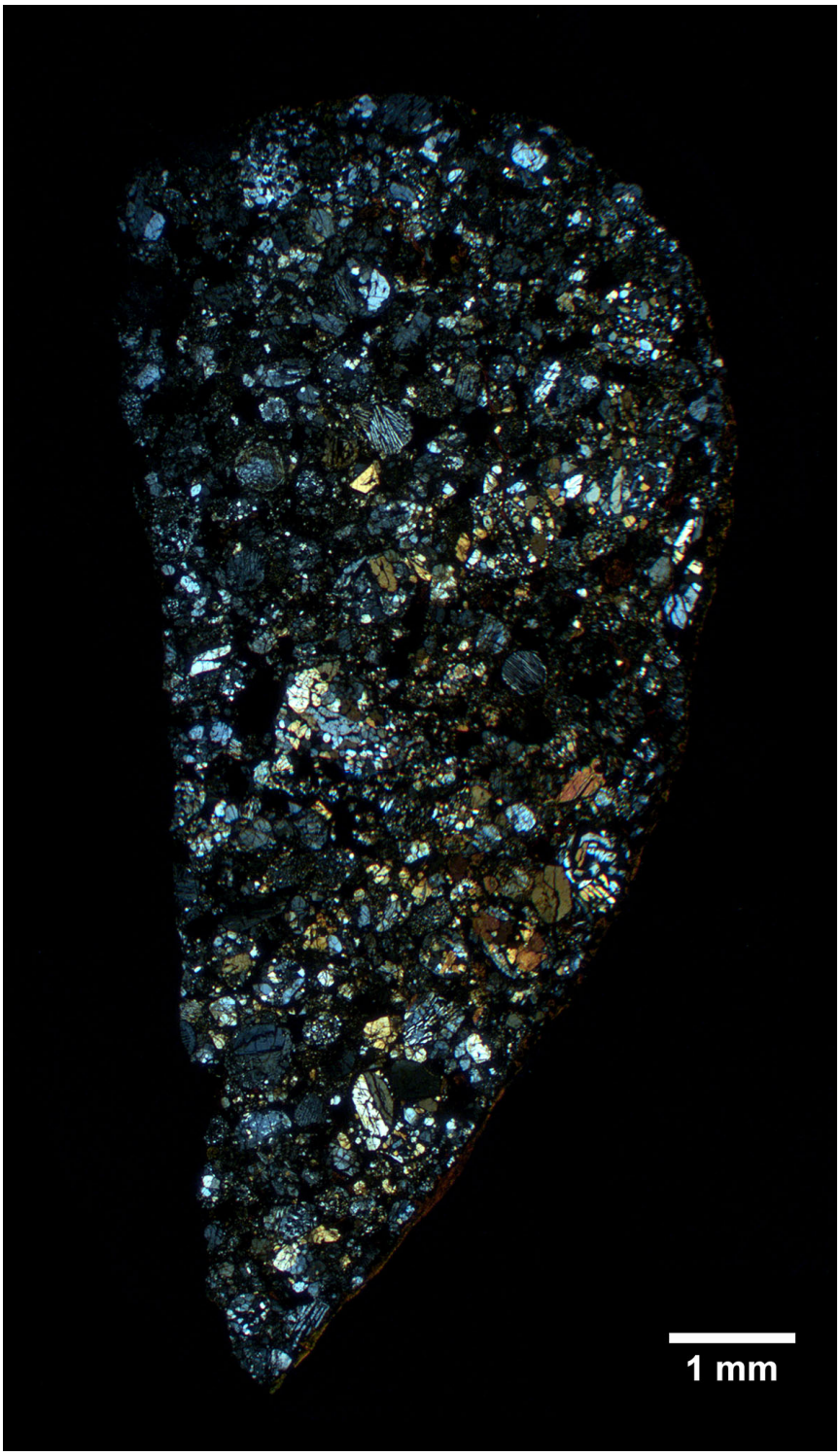

Figure 2.48: Photomicrograph of the polished thin section FRO 90225,02 (transmitted light, crossed-polarized light, TL-CPL).

Figure 2.49: Photomicrograph of the polished thin section FRO 90225,02 (reflected light, RL).

2.1.17 H4-5 Ordinary Chondrite Breccia: Frontier Mountain 90171

Find: Antarctica, 1990
Shock Stage: S2 Weathering Grade: W2
Section Label: FRO 90171,02
Type Specimen: Museo Nazionale dell'Antartide (Siena), PNRA
HD Images: TL-PPL / TL-CPL / RL

Figure 2.50: Photomicrograph of the polished thin section FRO 90171,02 (transmitted light, plane-polarized light, TL-PPL).

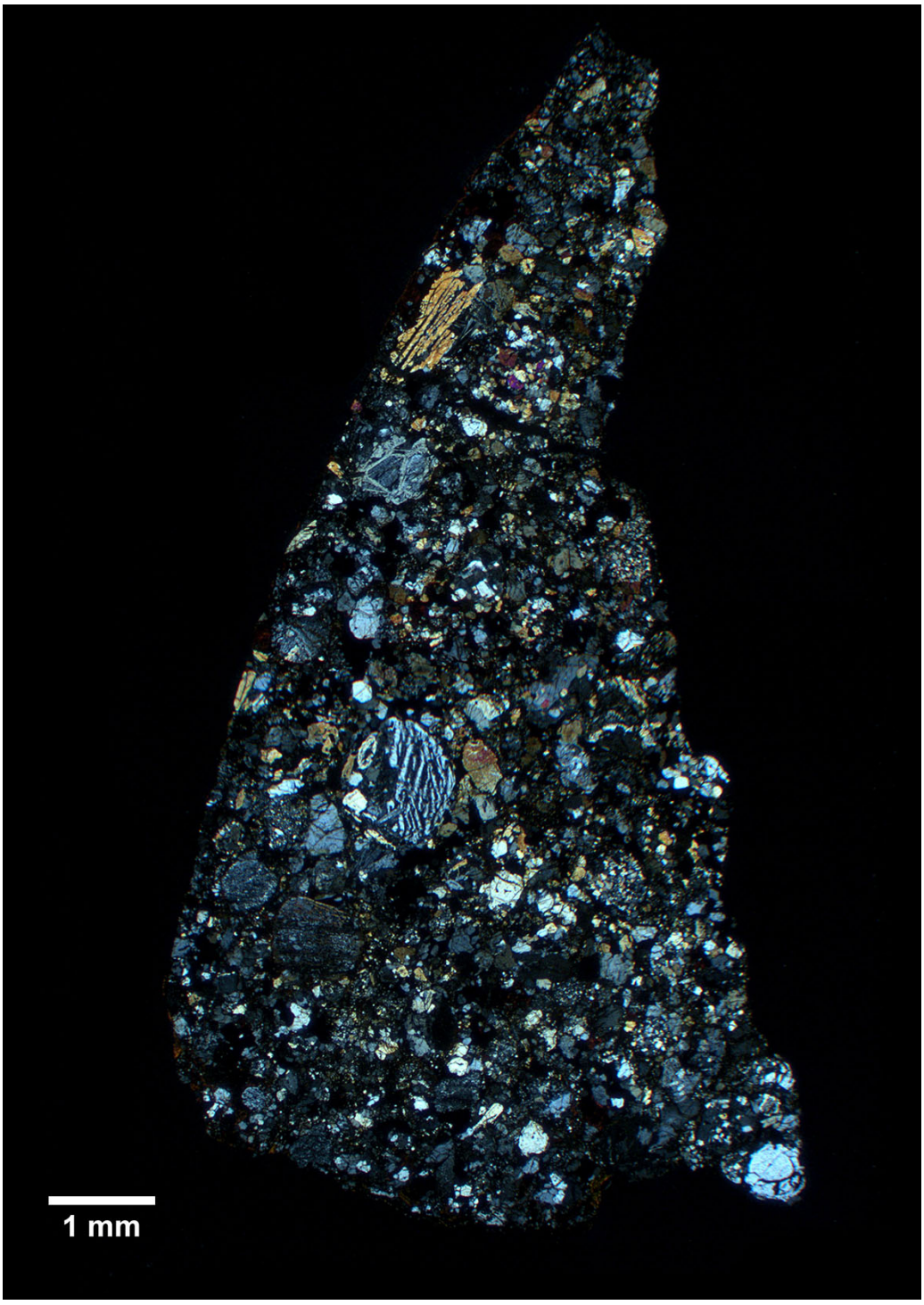

Figure 2.51: Photomicrograph of the polished thin section FRO 90171,02 (transmitted light, crossed-polarized light, TL-CPL).

Figure 2.52: Photomicrograph of the polished thin section FRO 90171,02 (reflected light, RL).

2.1.18 H5 Ordinary Chondrite: Allan Hills 14007

Find: Antarctica, 2014
Shock Stage: S2 Weathering Grade: W1
Section Label: ALH 14007,01
Type Specimen: Museo Nazionale dell'Antartide (Siena), PNRA
HD Images: TL-PPL / TL-CPL / RL

Figure 2.53: Photomicrograph of the polished thin section ALH 14007,01 (transmitted light, plane-polarized light, TL-PPL).

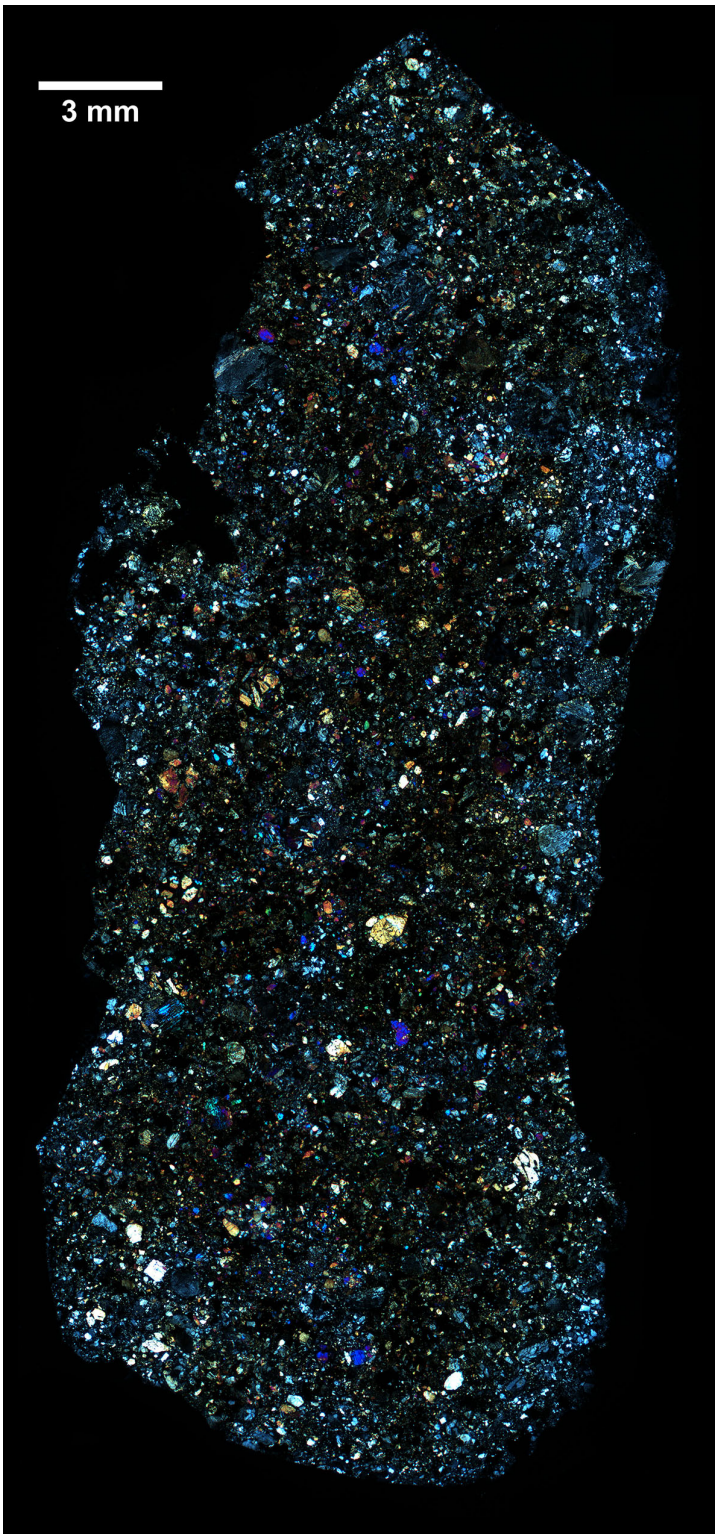

Figure 2.54: Photomicrograph of the polished thin section ALH 14007,01 (transmitted light, crossed-polarized light, TL-CPL).

Figure 2.55: Photomicrograph of the polished thin section ALH 14007,01 (reflected light, RL).

2.1.19 H5 Ordinary Chondrite: Johannessen Nunataks 01001

Find: Antarctica, 2001
Shock Stage: S1 Weathering Grade: W1
Section Label: JOH 01001,01
Type Specimen: Museo Nazionale dell'Antartide (Siena), PNRA
HD Images: TL-PPL / TL-CPL / RL

Figure 2.56: Photomicrograph of the polished thin section JOH 01001,01 (transmitted light, plane-polarized light, TL-PPL).

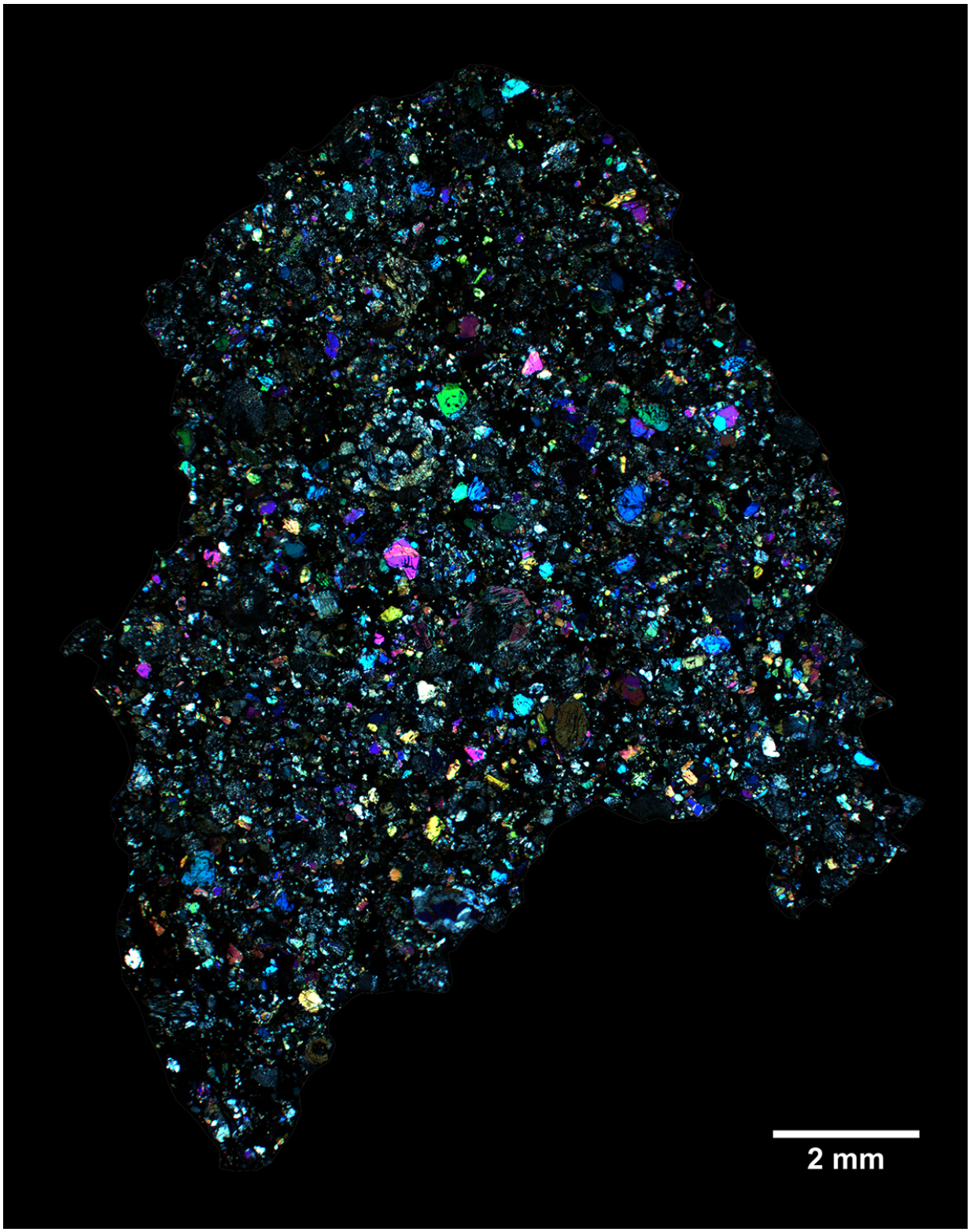

Figure 2.57: Photomicrograph of the polished thin section JOH 01001,01 (transmitted light, crossed-polarized light, TL-CPL).

Figure 2.58: Photomicrograph of the polished thin section JOH 01001,01 (reflected light, RL).

2.1.20 H6 Ordinary Chondrite Breccia: Frontier Mountain 03019

Find: Antarctica, 2003
Shock Stage: S3 Weathering Grade: W1
Section Label: FRO 03019,01
Type Specimen: Museo Nazionale dell'Antartide (Siena), PNRA
HD Images: TL-PPL / TL-CPL / RL

Figure 2.59: Photomicrograph of the polished thin section FRO 03019,01 (transmitted light, plane-polarized light, TL-PPL).

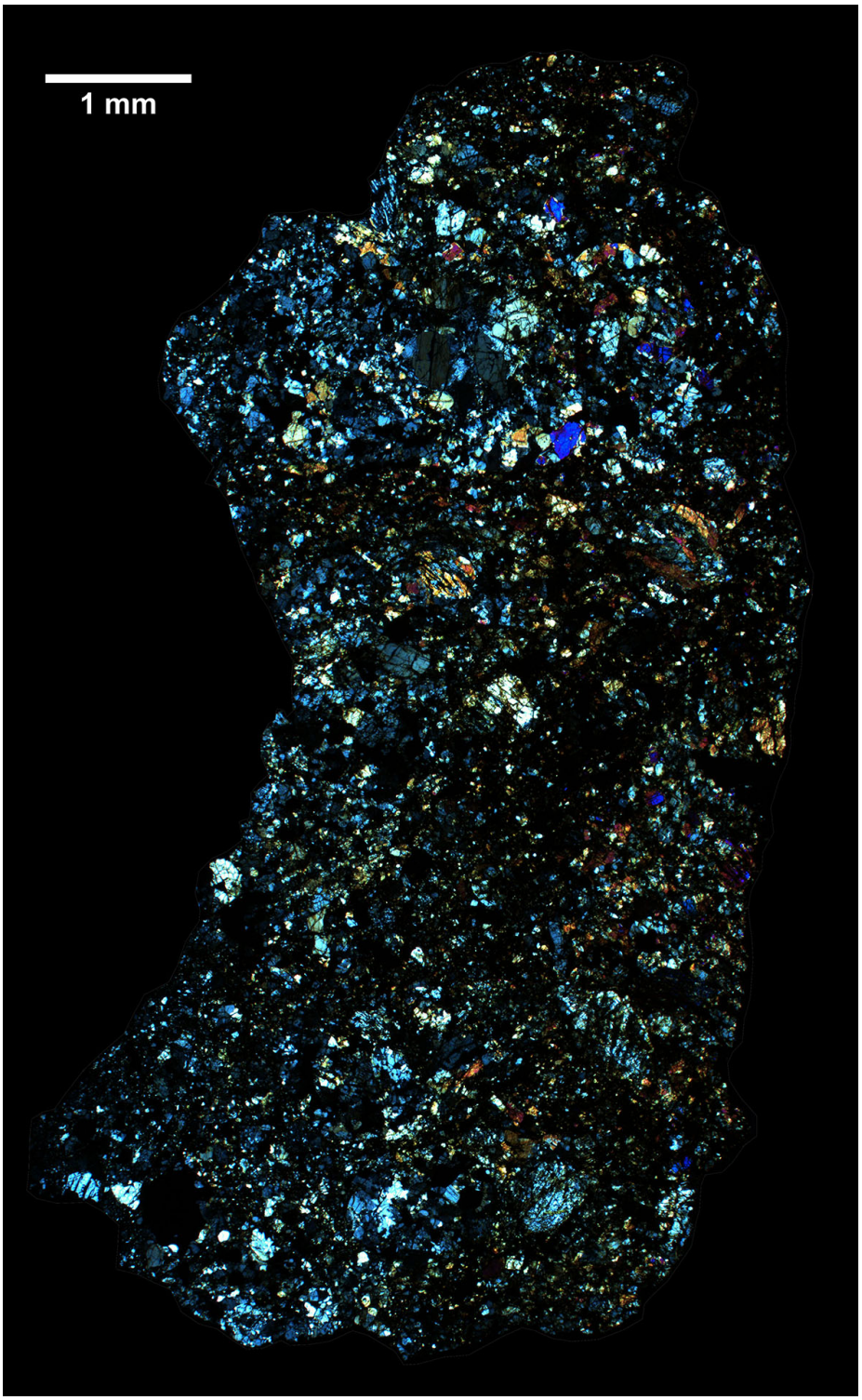

Figure 2.60: Photomicrograph of the polished thin section FRO 03019,01 (transmitted light, crossed-polarized light, TL-CPL).

Figure 2.61: Photomicrograph of the polished thin section FRO 03019,01 (reflected light, RL).

2.1.21 H6 Ordinary Chondrite: Frontier Mountain 03073

Find: Antarctica, 2004
Shock Stage: S1 Weathering Grade: W0
Section Label: FRO 03073,01
Type Specimen: Museo Nazionale dell'Antartide (Siena), PNRA
HD Images: TL-PPL / TL-CPL / RL

Figure 2.62: Photomicrograph of the polished thin section FRO 03073,01, a complete individual with thin fusion crust (transmitted light, plane-polarized light, TL-PPL).

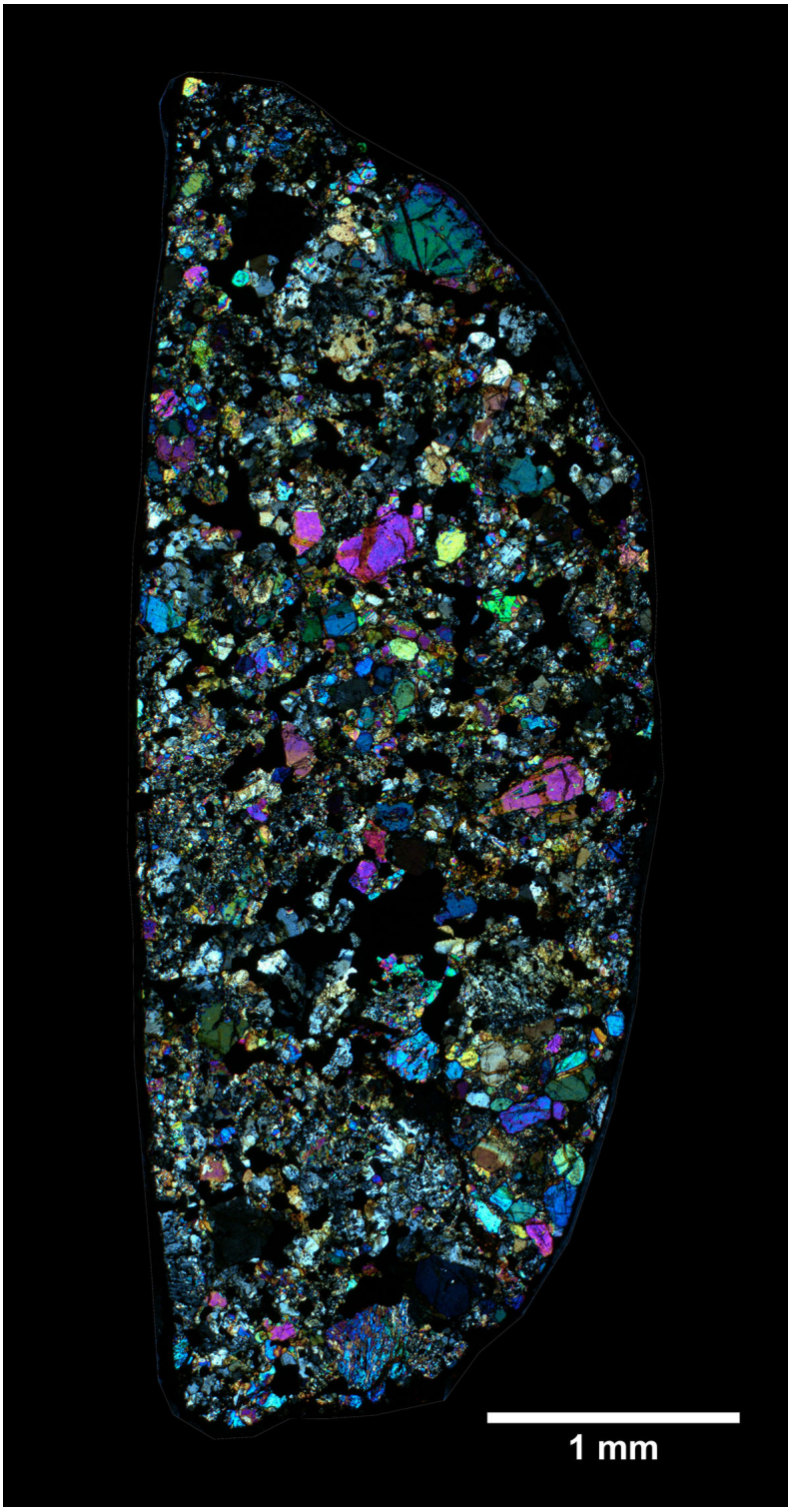

Figure 2.63: Photomicrograph of the polished thin section FRO 03073,01 (transmitted light, crossed-polarized light, TL-CPL).

Figure 2.64: Photomicrograph of the polished thin section FRO 03073,01 (reflected light, RL).

2.1.22 H Ordinary Chondrite impact melt: Dar al Gani 896

Find: Libya, 2000
Shock Stage: melted Weathering Grade: W1
Section Label: DaG 896
Type Specimen: Museo Nazionale dell'Antartide (Siena)
HD Images: TL-PPL / TL-CPL / RL

Figure 2.65: Photomicrograph of the polished thin section DaG 896 (transmitted light, plane-polarized light, TL-PPL).

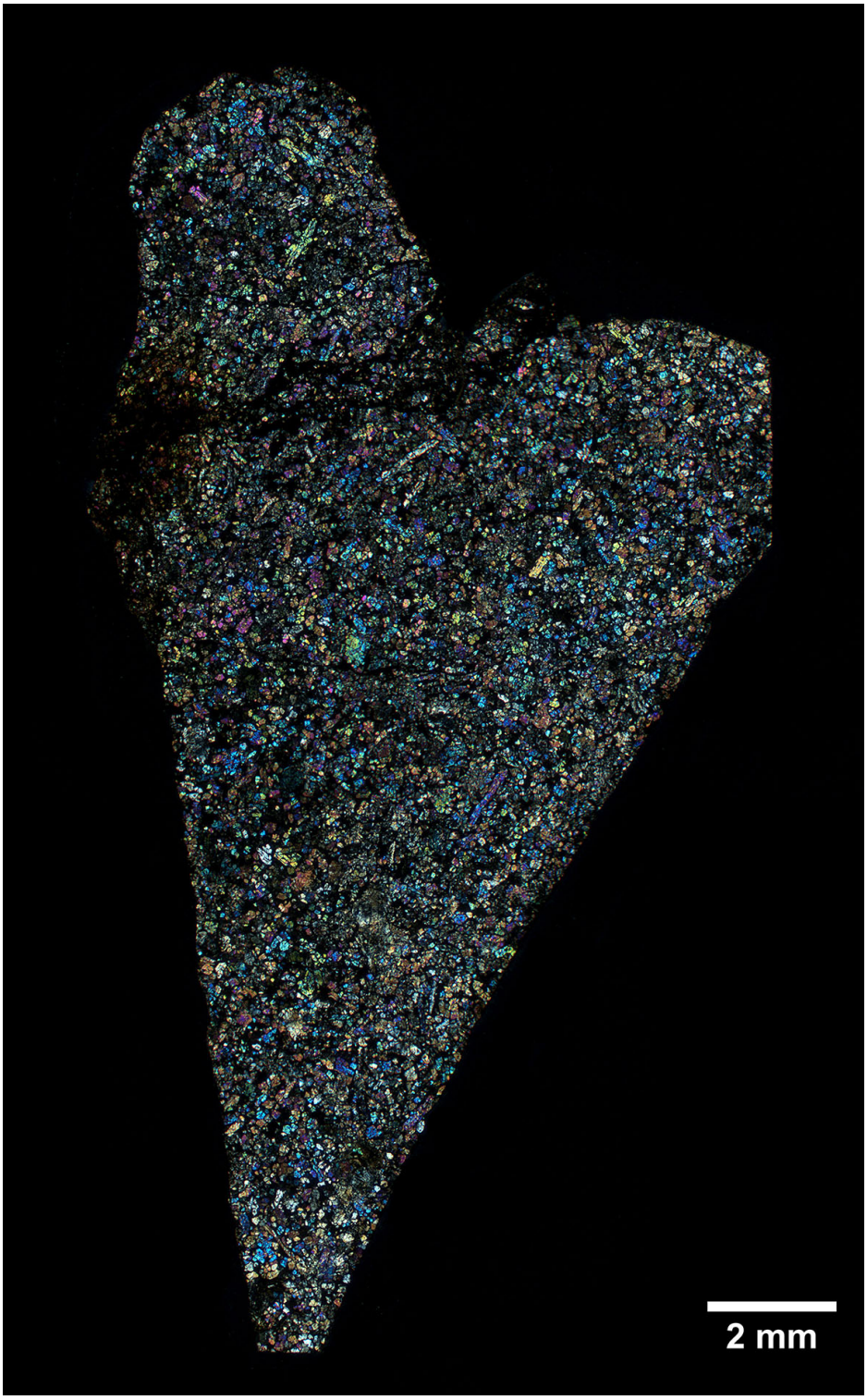

Figure 2.66: Photomicrograph of the polished thin section DaG 896 (transmitted light, crossed-polarized light, TL-CPL).

Figure 2.67: Photomicrograph of the polished thin section DaG 896 (reflected light, RL).

2.2 Carbonaceous Chondrites

2.2.1 CM Carbonaceous Chondrite: Mount DeWitt 12005

Find: Antarctica, 2013
Shock Stage: S2 Weathering Grade: W1
Section Label: DEW 12005,02
Type Specimen: Museo Nazionale dell'Antartide (Siena), PNRA
HD Images: TL-PPL / TL-CPL / RL

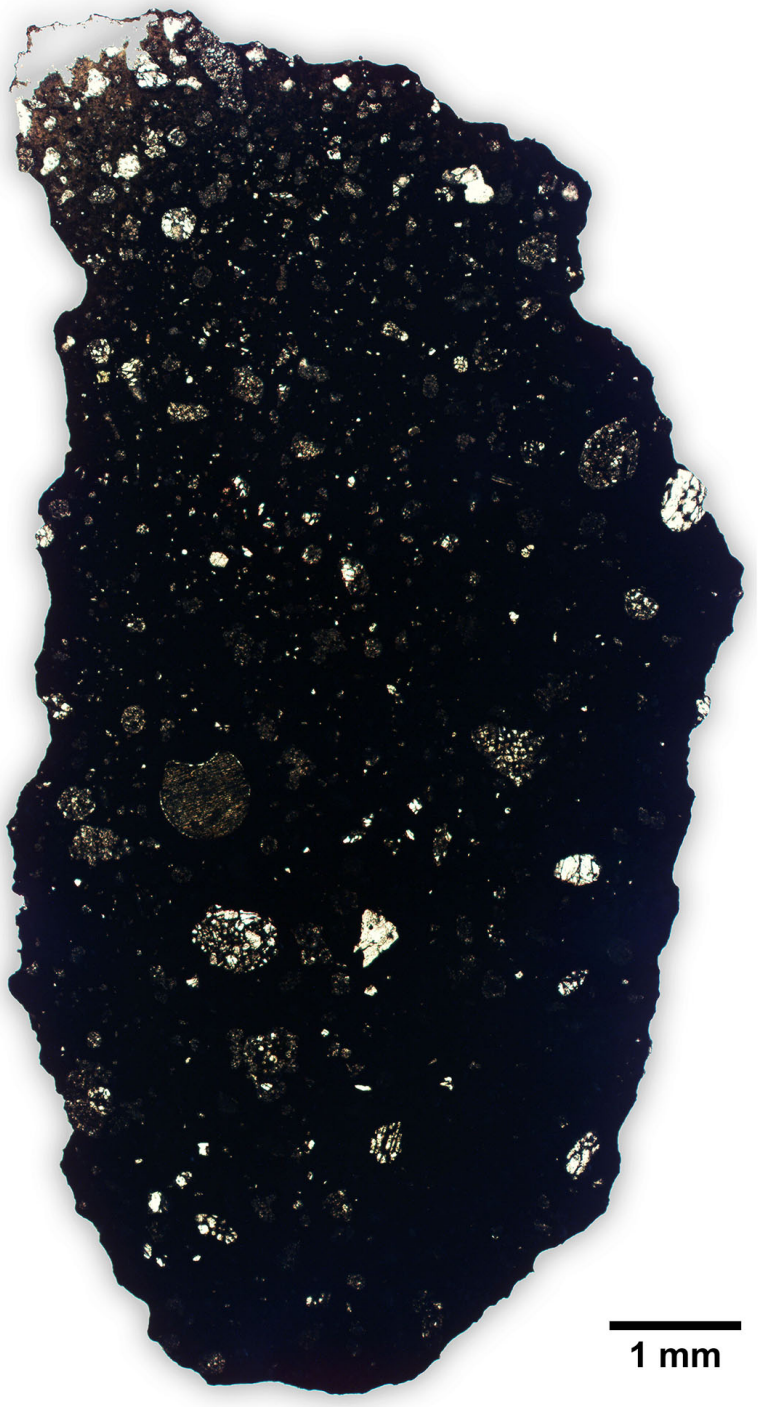

Figure 2.68: Photomicrograph of the polished thin section DEW 12005,02 (transmitted light, plane-polarized light, TL-PPL).

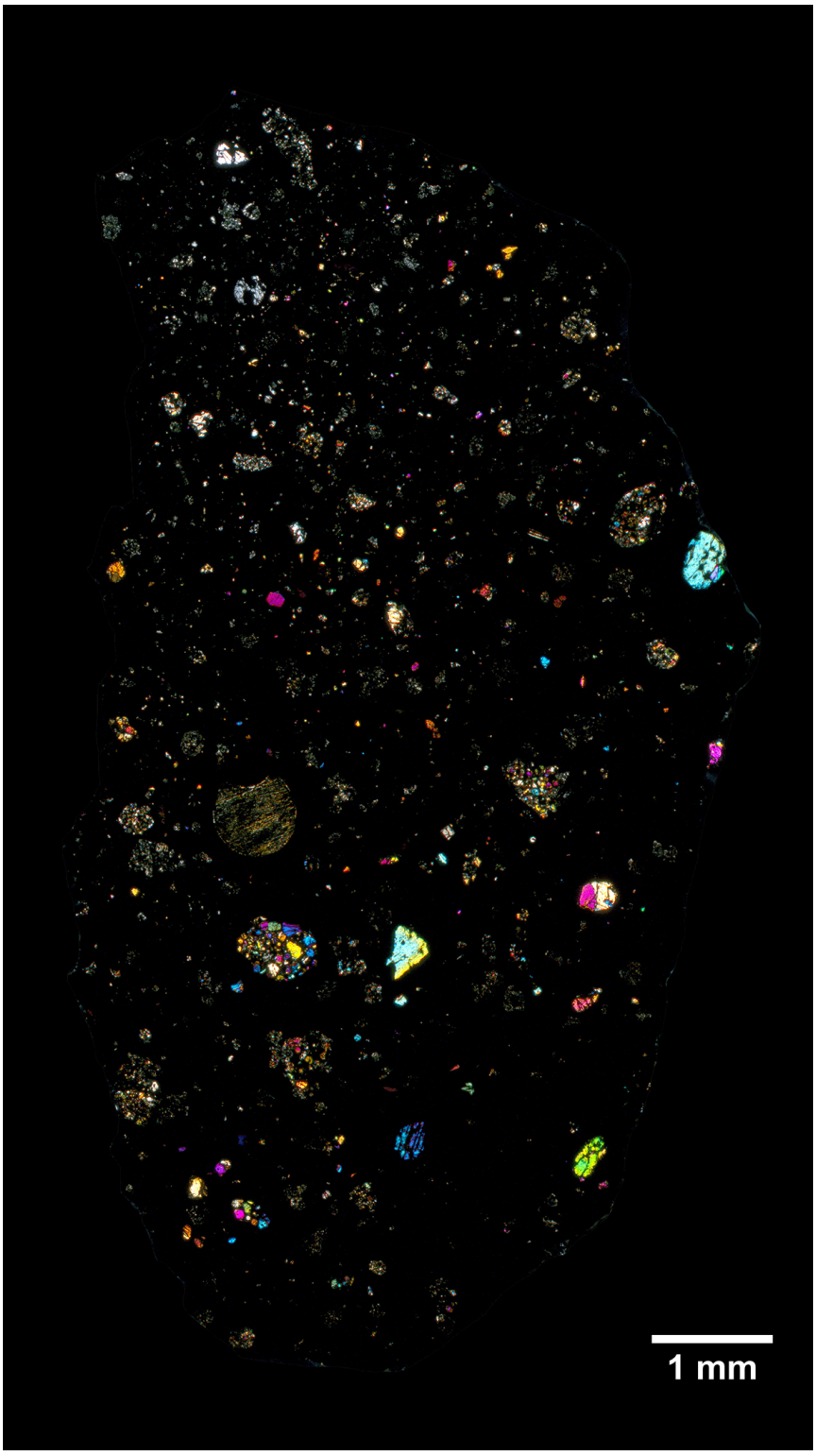

Figure 2.69: Photomicrograph of the polished thin section DEW 12005,02 (transmitted light, crossed-polarized light, TL-CPL).

2.2.2 CO3 Carbonaceous Chondrite: Dar al Gani 667

Find: Libya, 1999
Shock Stage: S1 Weathering Grade: W1
Section Label: DaG 667,01
Type Specimen: Museo Nazionale dell'Antartide (Siena)
HD Images: TL-PPL / TL-CPL / RL

Figure 2.70: Photomicrograph of the polished thin section DaG 667,01 (transmitted light, plane-polarized light, TL-PPL).

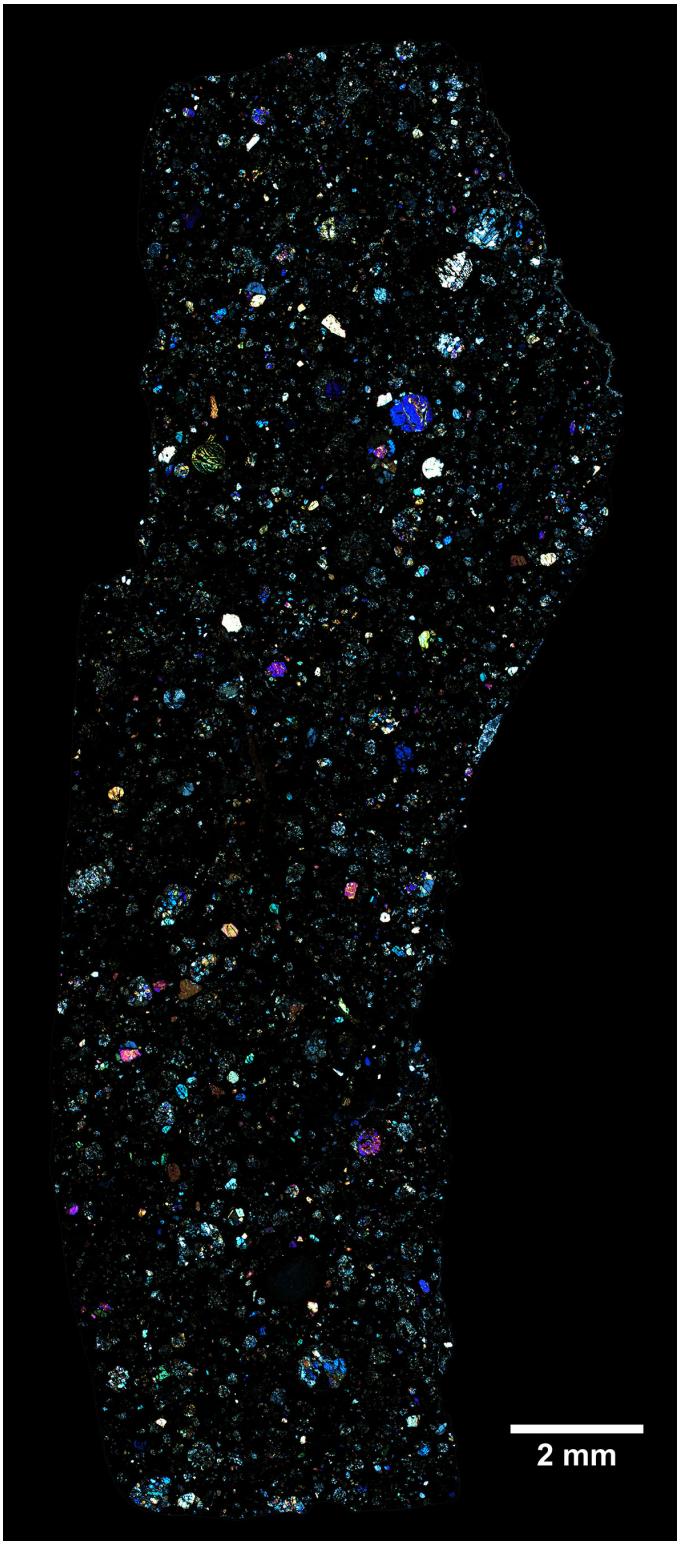

Figure 2.71: Photomicrograph of the polished thin section DaG 667,01 (transmitted light, crossed-polarized light, TL-CPL).

Figure 2.72: Photomicrograph of the polished thin section DaG 667,01 (reflected light, RL).

2.2.3 CO3 Carbonaceous Chondrite: Dar al Gani 668

Find: Libya, 1999
Shock Stage: S1 Weathering Grade: W1
Section Label: DaG 668,01
Type Specimen: Museo Nazionale dell'Antartide (Siena)
HD Images: TL-PPL / TL-CPL / RL

Figure 2.73: Photomicrograph of the polished thin section DaG 668,01 (transmitted light, plane-polarized light, TL-PPL).

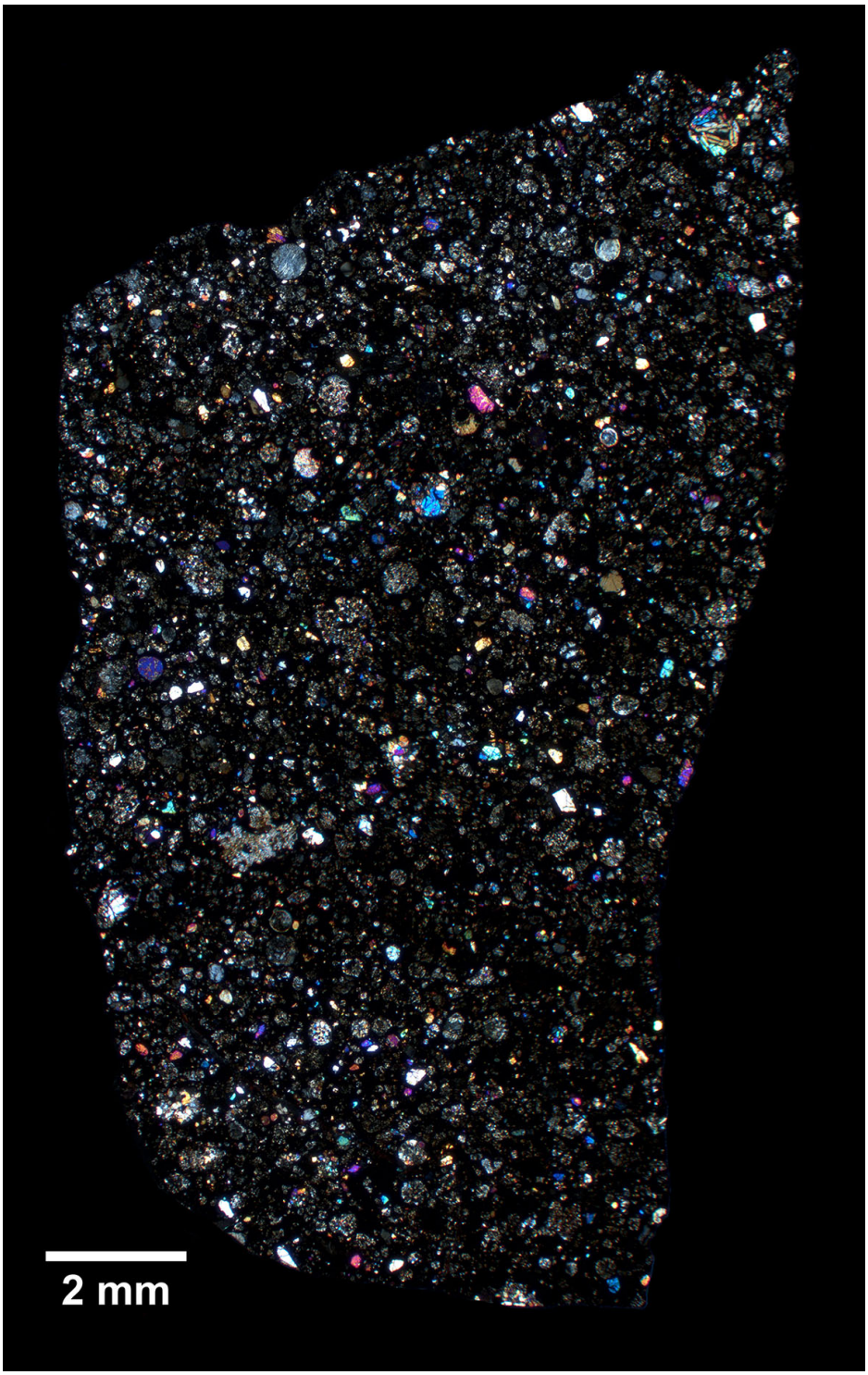

Figure 2.74: Photomicrograph of the polished thin section DaG 668,01 (transmitted light, crossed-polarized light, TL-CPL).

Figure 2.75: Photomicrograph of the polished thin section DaG 668,01 (reflected light, RL).

2.2.4 CV3 Carbonaceous Chondrite: Frontier Mountain 97002

Find: Antarctica, 1997
Shock Stage: S1 Weathering Grade: W0
Section Label: FRO 97002,01
Type Specimen: Museo Nazionale dell'Antartide (Siena), PNRA
HD Images: TL-PPL / TL-CPL / RL

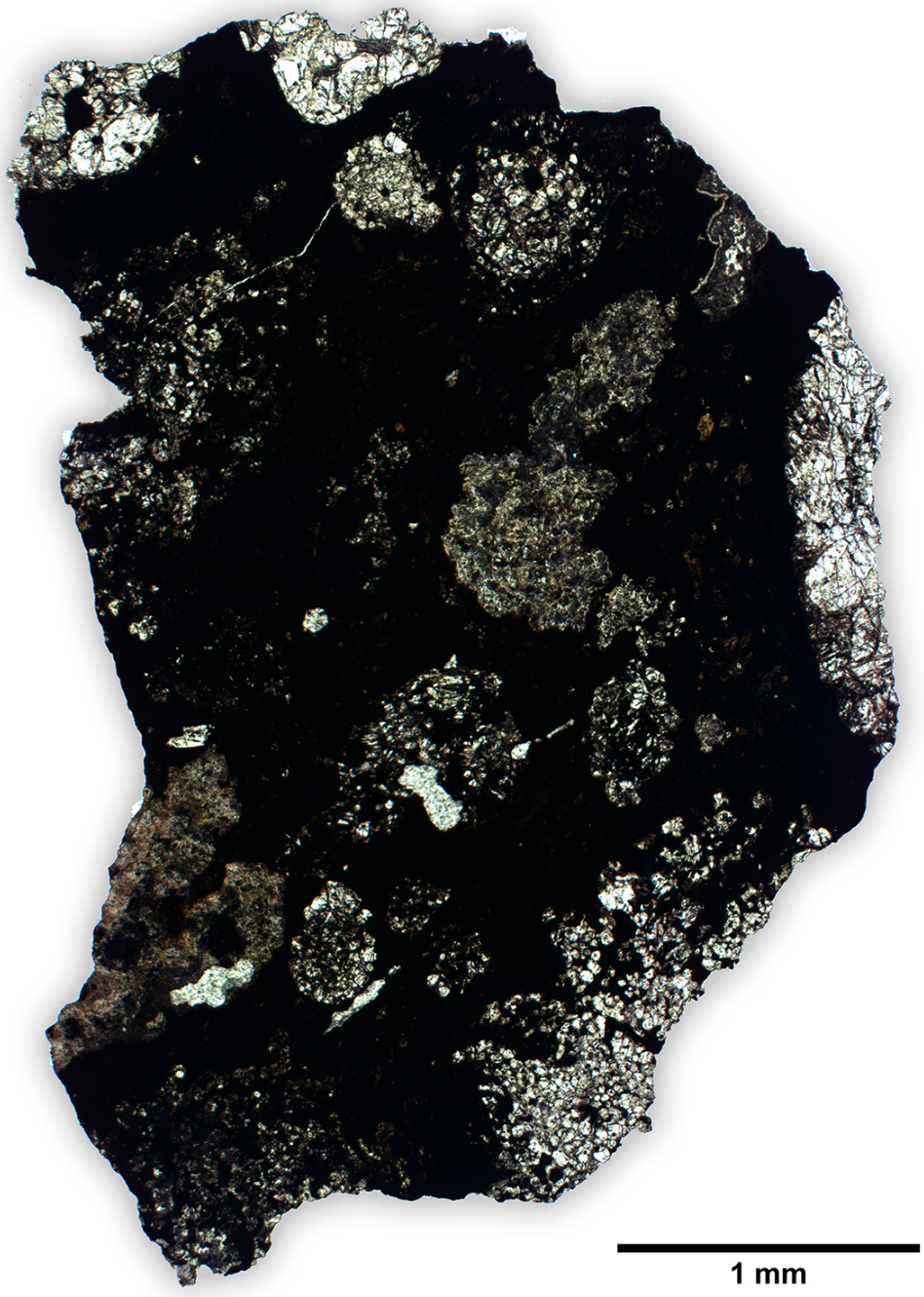

Figure 2.76: Photomicrograph of the polished thin section FRO 97002,01 (transmitted light, plane-polarized light, TL-PPL).

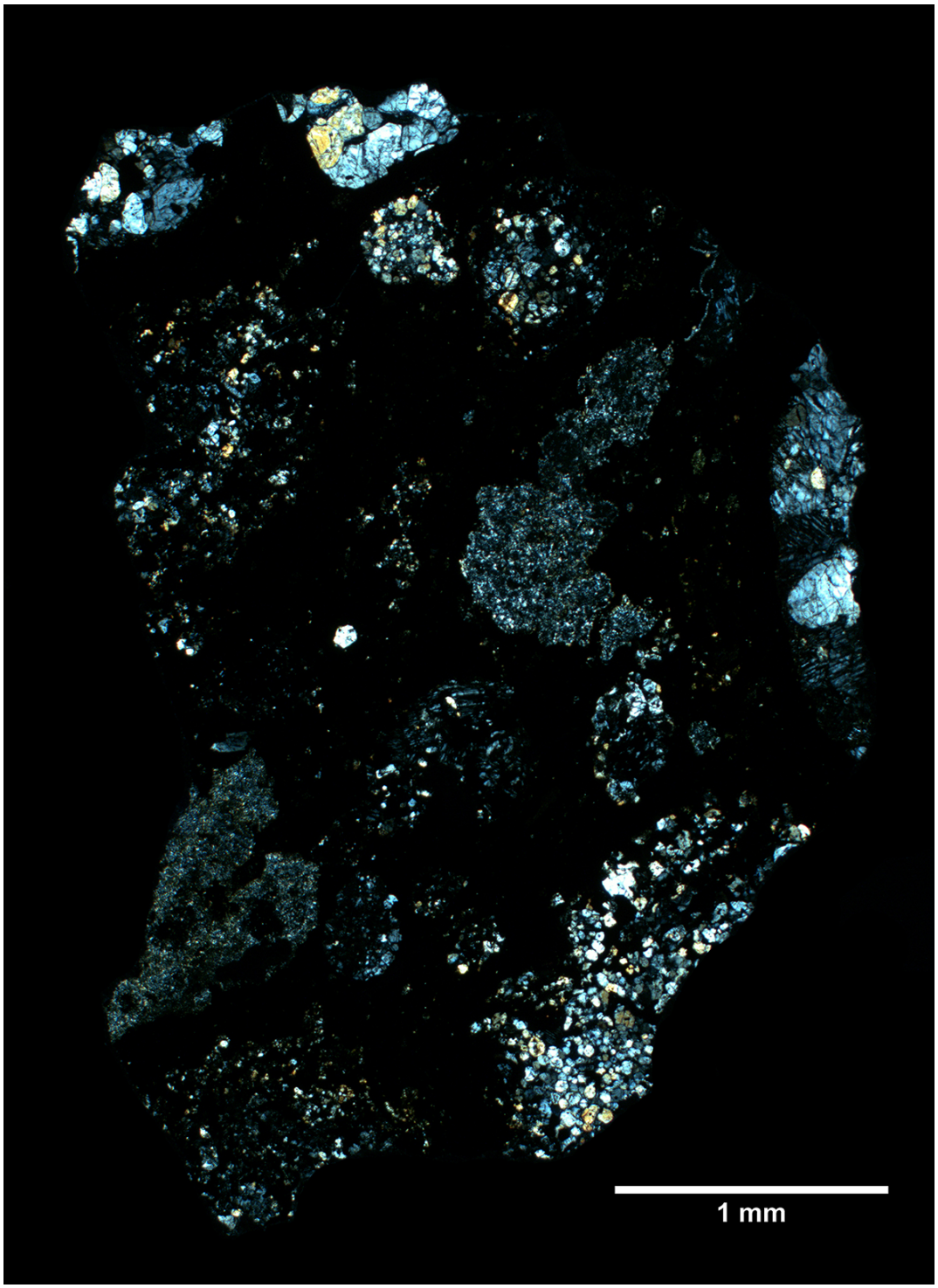

Figure 2.77: Photomicrograph of the polished thin section FRO 97002,01 (transmitted light, crossed-polarized light, TL-CPL).

Figure 2.78: Photomicrograph of the polished thin section FRO 97002,01 (reflected light, RL).

2.2.5 CC Carbonaceous Chondrite: Allan Hills 12034

Find: Antarctica, 2013
Shock Stage: S2 Weathering Grade: W0
Section Label: ALH 12034,01
Type Specimen: Museo Nazionale dell'Antartide (Siena), PNRA
HD Images: TL-PPL / TL-CPL / RL

Figure 2.79: Photomicrograph of the polished thin section ALH 12034,01 (transmitted light, plane-polarized light, TL-PPL).

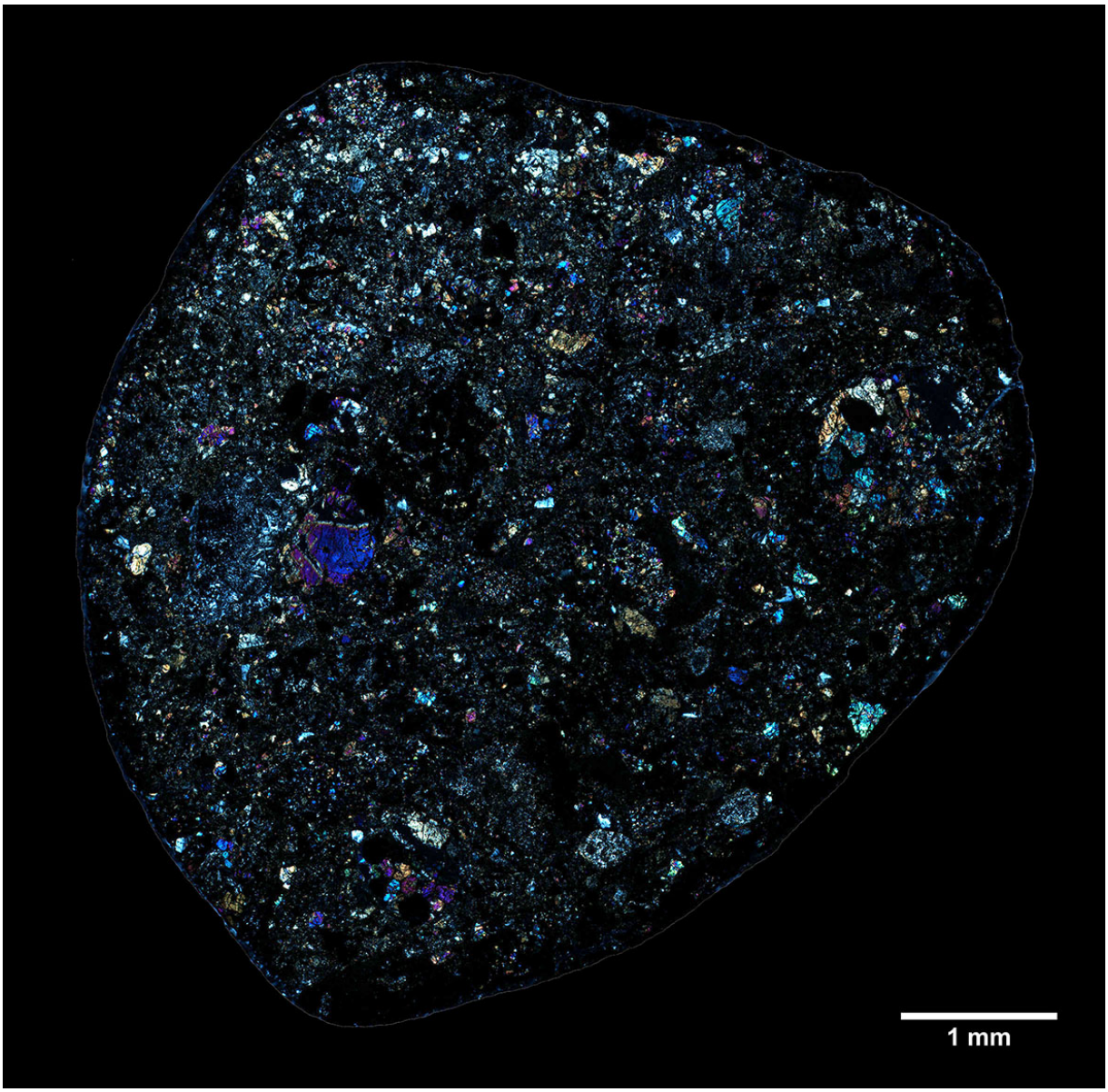

Figure 2.80: Photomicrograph of the polished thin section ALH 12034,01 (transmitted light, crossed-polarized light, TL-CPL). White rim is due to photo editing.

Figure 2.81: Photomicrograph of the polished thin section ALH 12034,01 (reflected light, RL).

2.2.6 CC Carbonaceous Chondrite: Elephant Moraine 14079

Find: Antarctica, 2014
Shock Stage: S2 Weathering Grade: W2
Section Label: EET 14079,01
Type Specimen: Museo Nazionale dell'Antartide (Siena), PNRA
HD Images: TL-PPL / TL-CPL / RL

Figure 2.82: Photomicrograph of the polished thin section EET 14079,01 (transmitted light, plane-polarized light, TL-PPL).

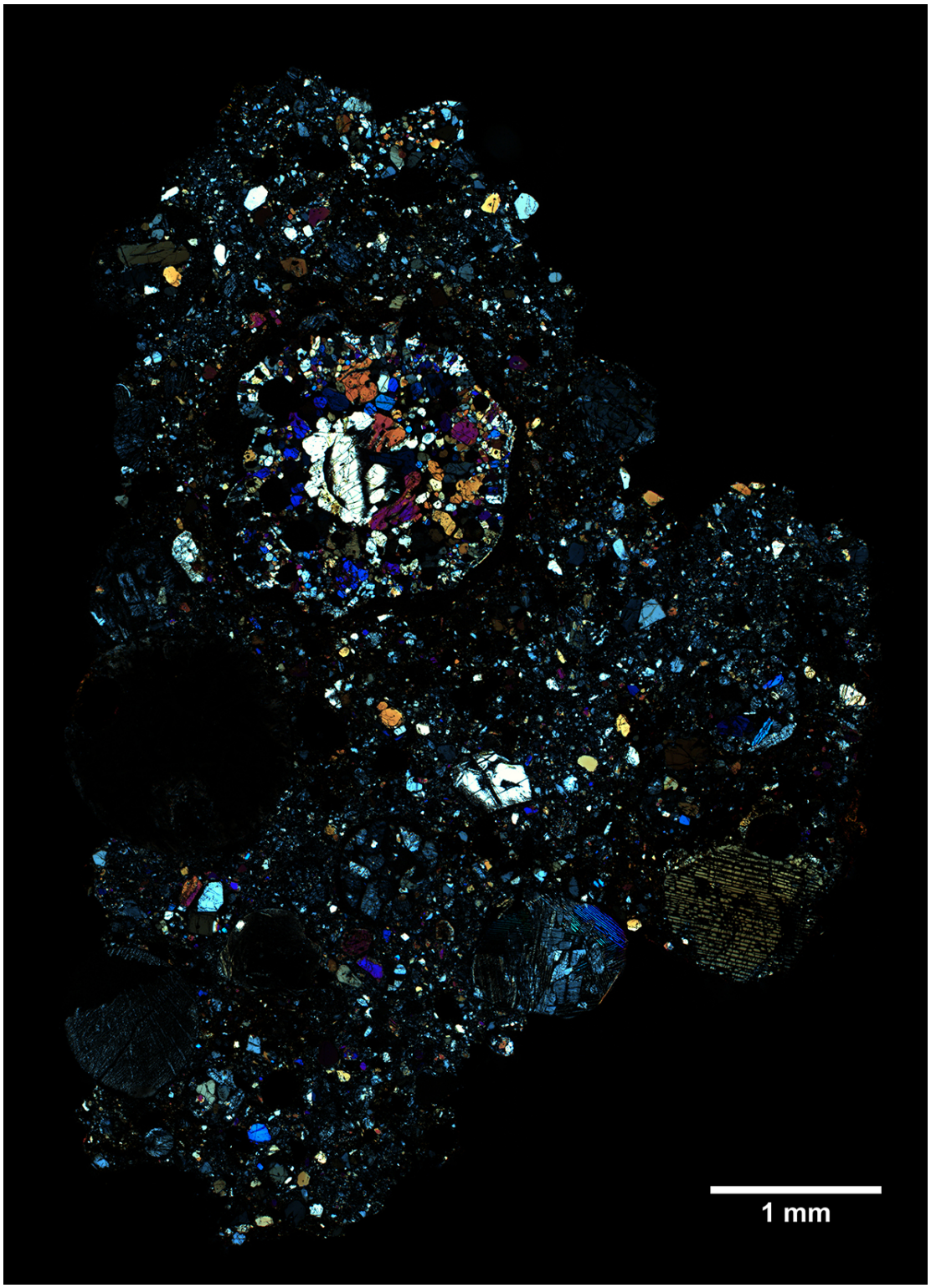

Figure 2.83: Photomicrograph of the polished thin section EET 14079,01 (transmitted light, crossed-polarized light, TL-CPL).

Figure 2.84: Photomicrograph of the polished thin section EET 14079,01 (reflected light, RL).

2.3 Enstatite Chondrites

2.3.1 EL4 Enstatite Chondrite: Frontier Mountain 03005

Find: Antarctica, 2004
Shock Stage: S1 Weathering Grade: W1
Section Label: FRO 03005,01
Type Specimen: Museo Nazionale dell'Antartide (Siena), PNRA
HD Images: TL-PPL / TL-CPL / RL

Figure 2.85: Photomicrograph of the polished thin section FRO 03005,01 (transmitted light, plane-polarized light, TL-PPL).

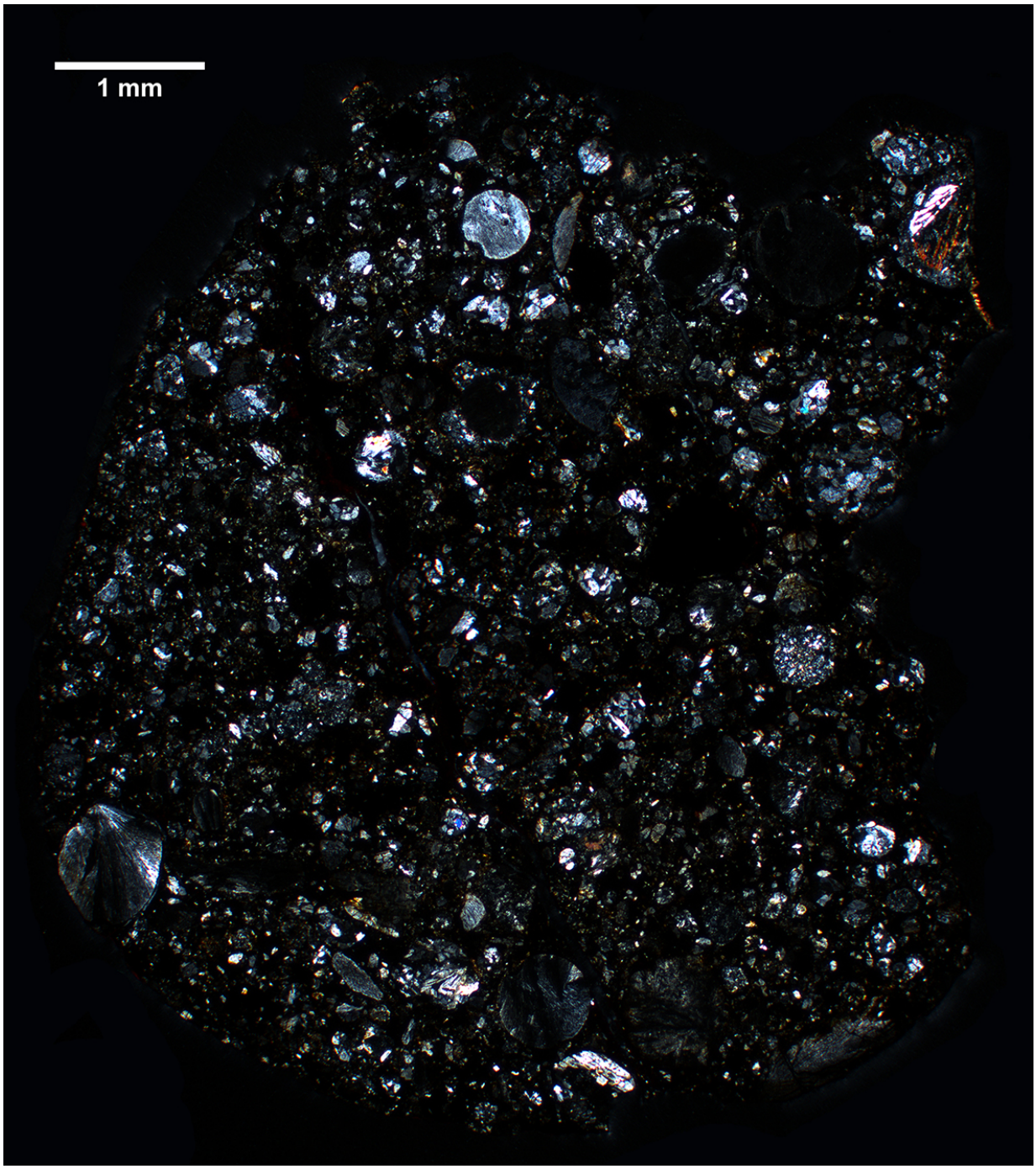

Figure 2.86: Photomicrograph of the polished thin section FRO 03005,01 (transmitted light, crossed-polarized light, TL-CPL).

Figure 2.87: Photomicrograph of the polished thin section FRO 03005,01 (reflected light, RL).

2.3.2 EL6 Enstatite Chondrite: Eagle 01

Fall: United States, 1946/1947
Shock Stage: S2 Weathering Grade: W0
Section Label: EAGLE 01
Type Specimen: Museo Nazionale dell'Antartide (Siena)
HD Images: TL-PPL / TL-CPL / RL

Figure 2.88: Photomicrograph of the polished thin section EAGLE 01 (transmitted light, plane-polarized light, TL-PPL).

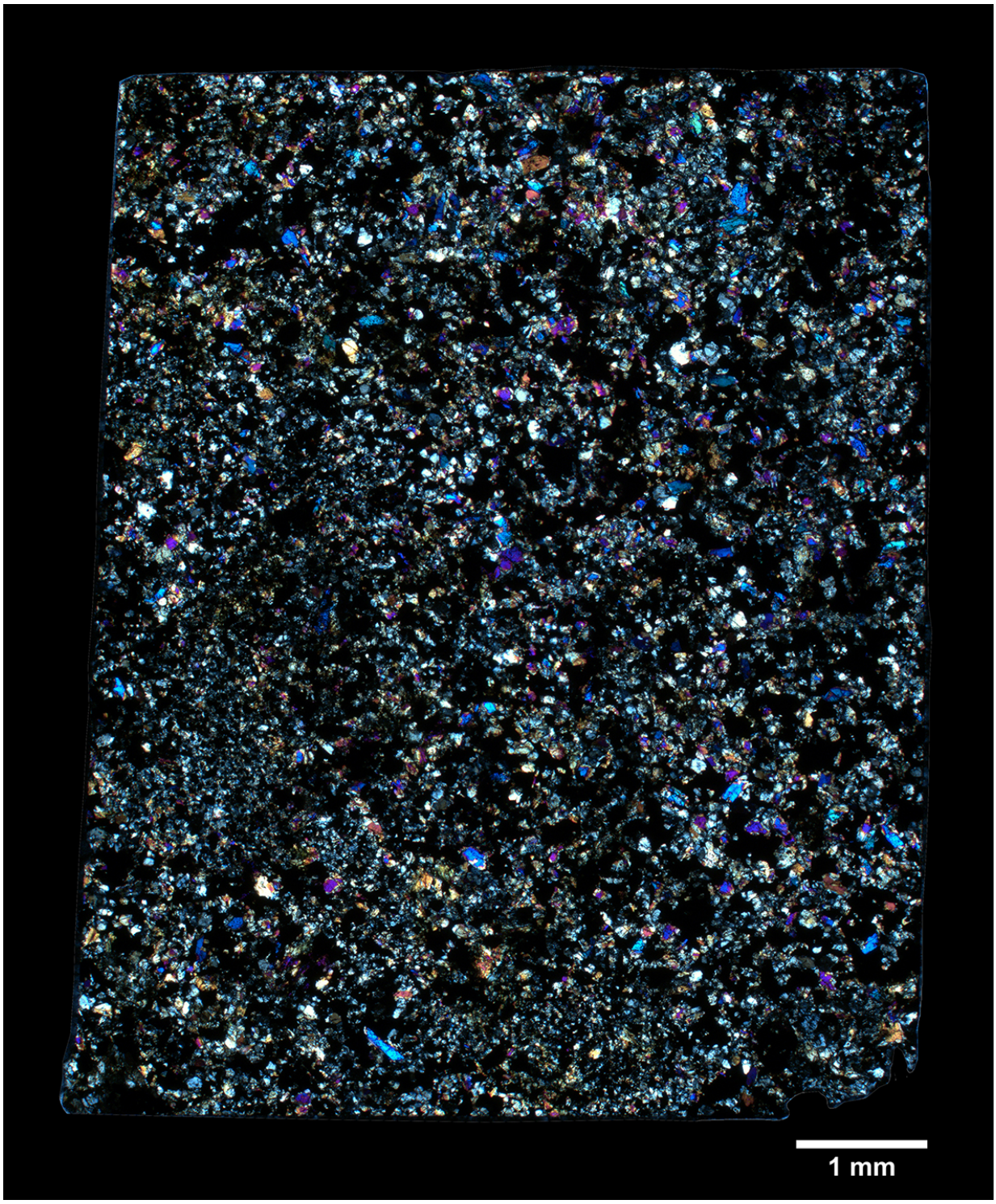

Figure 2.89: Photomicrograph of the polished thin section EAGLE 01 (transmitted light, crossed-polarized light, TL-CPL).

Figure 2.90: Photomicrograph of the polished thin section EAGLE 01 (reflected light, RL).

2.3.3 EL Enstatite Chondrite impact melt: Al Haggounia 001

Fall: Saguia el Hamra (Western Sahara), 2006
Shock Stage: melted Weathering Grade: W1
Section Label: ALHAGGOUNIA 001
Type Specimen: Museo Nazionale dell'Antartide (Siena)
HD Images: TL-PPL / TL-CPL / RL

Figure 2.91: Photomicrograph of the polished thin section ALHAGGOUNIA 001 (transmitted light, plane-polarized light, TL-PPL).

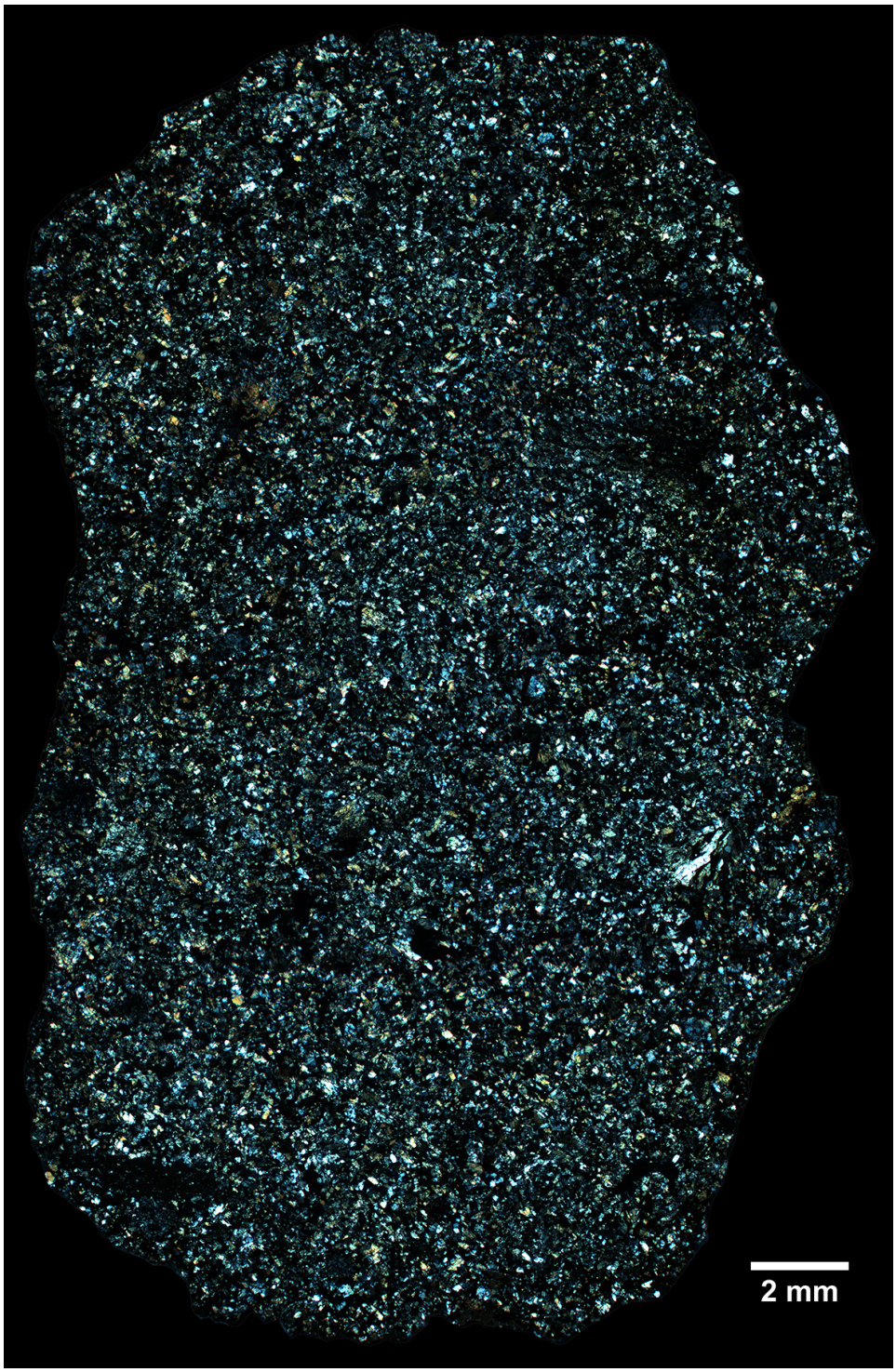

Figure 2.92: Photomicrograph of the polished thin section ALHAGGOUNIA 001 (transmitted light, crossed-polarized light, TL-CPL).

Figure 2.93: Photomicrograph of the polished thin section ALHAGGOUNIA 001 (reflected light, RL).

Chapter 3

Non-Chondritic Meteorites

Non-chondritic meteorites comprise primitive and differentiated achondrites, irons and stony-irons, and planetary meteorites (Tab. 2.1). Thin sections from all these meteorite groups but irons and stony-irons are featured in this atlas.
Achondrites are stony meteorites formed through metamorphic and igneous processes. As their name suggests, their textures are characterized by the absence of chondrules (in contrast to chondrites), and they can be subdivided in (1) Primitive achondrites and (2) Differentiated achondrites. Primitive achondrites have achondritic texture but nearly chondritic mineral and bulk composition. Relic chondrules are still visible in some primitive achondrites, indicating a chondritic origin. They are comprised of the groups of Acapulcoites, Lodranites, and Winonaites, and the clans of acapulcoite-lodranite and winonaites/IAB irons.

Acapulcoites and *lodranites* share similar mineralogy and textures: crystals of olivine, pyroxene, metals, and sulfides in a granoblastic texture. Veins of metals and sulfides mark the thermal event that caused the mobilization or fractionation of the minimum melt composition in the metal-sulfide system first, and then in lodranites in the silicate system. Indeed lodranites, differently from acapulcoites, are depleted of incompatible elements, plagioclase, and high Ca-pyroxenes, and have a slightly coarser grained texture.

Winonaites have chondritic mineralogy and a granoblastic texture, such as the other primitive achondrites, but they have a different O-isotopic composition. Silicate inclusions of winonaites have been identified inside IAB-iron meteorites, questioning what could have been the origin of these meteorites and the history that brought to their association with such a diverse material.

Differentiated achondrites are originated in asteroids that experienced temperature high enough to cause partial melting. Igneous rocks with highly fractionated bulk compositions (compared to chondrites) are formed. Differentiated achondrites are: Angrites, Brachinites, Aubrites, Ureilites, and Howardite Eucrite Diogenite meteorites (or HEDs). In this atlas the Mesosiderite silicate fractions are also considered as part of the differentiated achondrites.
Even if the distinction between primitive and differentiated achondrites is clear, the choice to place one group to one category or the other is not obvious: some achondrites, such as the ureilites, show characteristics typical to both primitive and differentiated meteorites. Uncertainty is often due to the low number of samples present for a certain group.

Angrites are basaltic rocks characterized by Ca-rich mineralogy: fassaite (Ca-Al-Ti pyroxene), Ca-rich olivine, and anorthite (Ca-rich plagioclase). Their O-isotopic composition overlaps with that of HED's, but different mineralogy defines them as their own group. Based on radiometric datings they are considered the oldest basalts of the solar system.

Aubrites are brecciated pyroxenites, particularly interesting for their unique, reduced min-

eralogy: FeO-free enstatite is the main component, and it is associated with several minerals unknown on Earth.

Brachinites are almost exclusively composed of olivine. Few samples of brachinites have been discovered, some with nearly chondritic bulk compositions and others more fractionated. For this reason, they were once considered to be primitive achondrites and their origin is still debated.

Ureilites are the second major group of differentiated achondrites, after HEDs. They are ultramafic rocks mainly made of olivine, pyroxene (mainly pigeonite) and characterized by the presence of interstitial carbon phases. There seems to be a close relationship between ureilites and CCs, namely their O-isotopic composition plots on the carbonaceous chondrite mixing line (CCAM), and they are thought to have been originated from a CC-parent body.

Howardite, Eucrite, and *Diogenite meteorites* (HEDs) form the largest group of achondrites and the only group with a possible parent body candidate: the asteroid 4 Vesta. Most of the HEDs are brecciated rocks. Eucrites occur as basaltic and cumulate rocks: basaltic eucrites have (sub)-ophitic textures, with anorthite and low-Ca pyroxenes as major components (typical are the exsolution lamellae of augite on pigeonite crystals), and cumulate eucrites are coarse-grained gabbros with similar compositions of their basaltic counterpart. Diogenites are coarse-grained orthopyroxenites and howardites are polymict breccias made up of eucrites and diogenites clasts.

Mesosiderites are breccias characteristically comprising nearly equal proportions of silicates and Fe,Ni-metal plus troilite. The silicate fraction typically consists of lithic and mineral clasts in a fine-grained clastic or igneous matrix (e.g., Mittlefehldt et al., 1998 [15]). Lithic clasts include basalts, gabbros, and pyroxenites with minor amounts of dunite and rare anorthosite (Scott et al., 2001 [19]). Mineral clasts consist of coarse-grained orthopyroxene, olivine, and Ca-plagioclase and tridymite. Fe,Ni-metal typically occurs as millimeter or submillimeter grains, intimately mixed with silicate grains of similar size.

Planetary meteorites comprise lunar meteorites, and the martian Shergottite Nakhilite Chassignite meteorites (or SNCs).

Lunar meteorites are a group of meteorites for which we have a direct comparison between meteorites and samples collected from their parent body surface. Nevertheless, the importance of studying lunar meteorites resides in the fact that they provide an unbiased sampling of the lunar surface. The majority of them are brecciated meteorites, and can be subdivided in: (1) Highland rocks, that comprise the groups of ferroan anorthosite, alkali anorthosite, and the magnesian suite; (2) Mare basalts, mainly composed of pigeonite and anorthite, and characterized by high concentrations of TiO_2; (3) Lunar regolith breccias, that are lithified soils, where several different clasts with various origins can be found embedded in the lunar soil.

Shergottite, Nakhlite, and *Chassignite meteorites* (SNCs) have come from Mars. This fact has been proved in the 1990's by the match between noble gas abundances trapped in impact melt glass in a shergottite and those detected in the martian atmosphere by the Viking missions in the 1970s. SNCs are the product of the long history of volcanic activity on Mars: from about 4.5 Ga to 180 Ma. Shergottites exist as basalts and ultramafic cumulates: basaltic shergottites with clinopyroxenes (augite and pigeonite) and intermediate plagioclase, sometimes with mm-sized olivine crystals and in this case called olivine-phyric shergottites; lherzolitic shergottites are ultramafic cumulates, mainly made of olivine and pyroxene. Shergottites have been subjected to high pressure shock events, as testified by the widespread presence of maskelynite, a diaplectic glass formed from plagioclase. Nakhlites and chassignites are both coarse-grained ultramafic cumulates, the former with pyroxene (augite) and olivine, the latter mostly made up of olivine.

Finally, another single membered group of meteorites should be considered within SNCs, that would comprise ALH 84001, the unique orthopyroxenite from Mars.

This atlas presents a wide and remarkable spectrum of achondrites: two samples of primitive achondrites, representative of the acapulcoite-lodranite clan; three samples of ureilites; four HEDs (howardites and eucrites); two lunar meteorites, both regolith breccias; one martian olivine phyric basaltic shergottite.

3.1 Primitive Achondrites

3.1.1 Acapulcoite: Frontier Mountain 95029

Find: Antarctica, 1995
Shock Stage: S1 Weathering Grade: W1
Section Label: FRO 95029,01
Type Specimen: Museo Nazionale dell'Antartide (Siena), PNRA
HD Images: TL-PPL / TL-CPL / RL

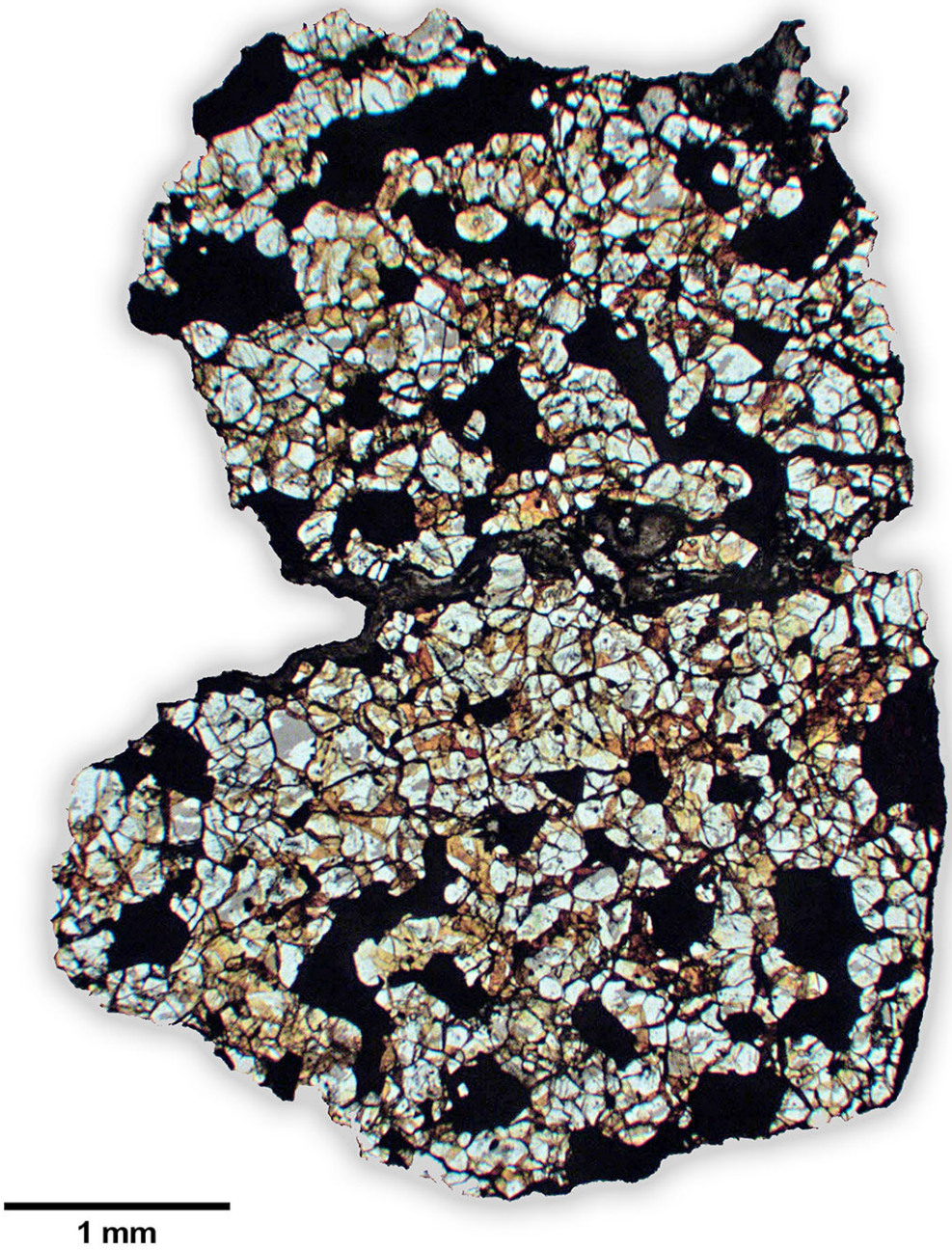

Figure 3.1: Photomicrograph of the polished thin section FRO 95029,01 (transmitted light, plane-polarized light, TL-PPL).

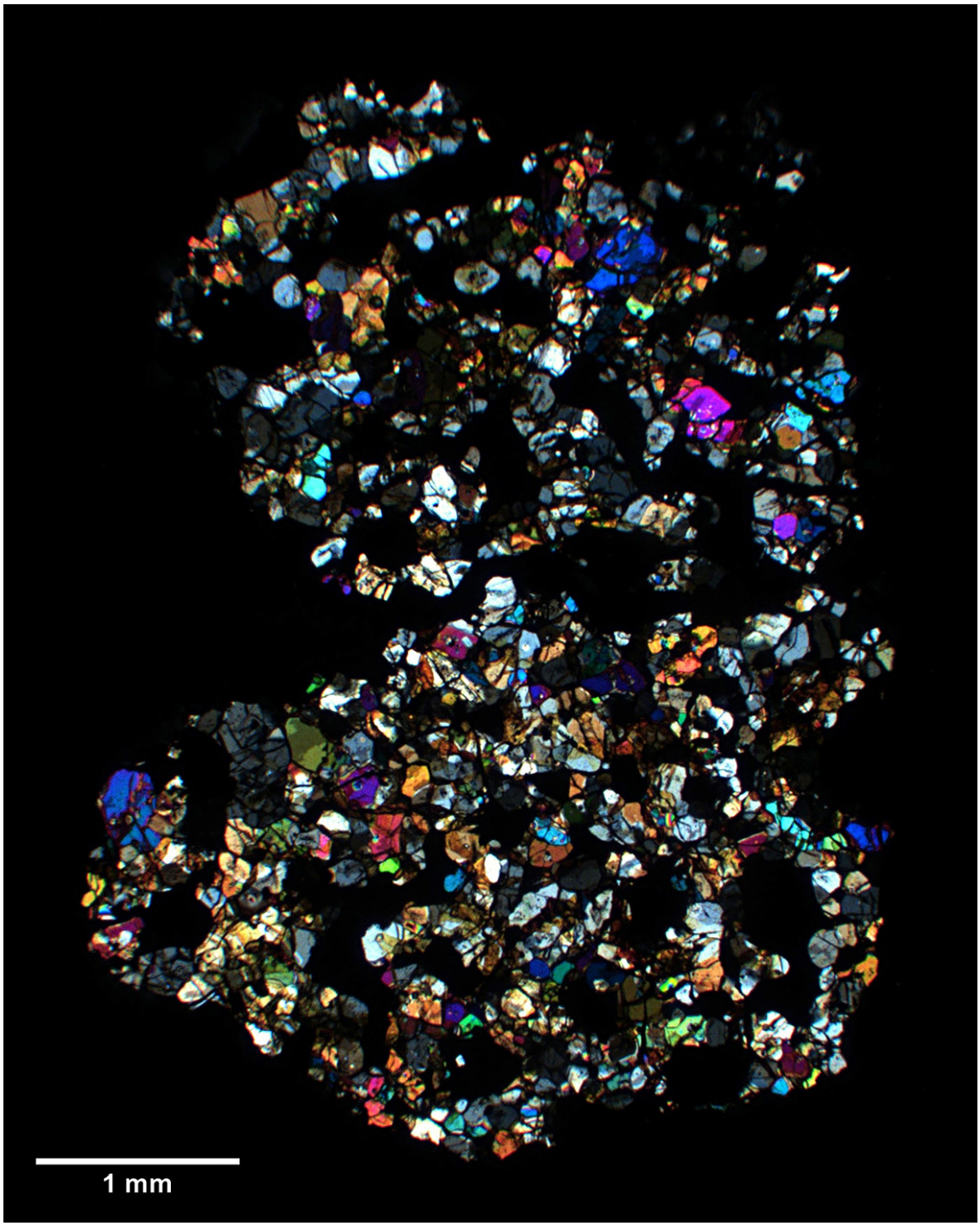

Figure 3.2: Photomicrograph of the polished thin section FRO 95029,01 (transmitted light, crossed-polarized light, TL-CPL).

Figure 3.3: Photomicrograph of the polished thin section FRO 95029,01 (reflected light, RL).

3.1.2 Lodranite: Frontier Mountain 03001

Find: Antarctica, 2003
Shock Stage: S1 Weathering Grade: W0
Section Label: FRO 03001,01
Type Specimen: Museo Nazionale dell'Antartide (Siena), PNRA
HD Images: TL-PPL / TL-CPL / RL

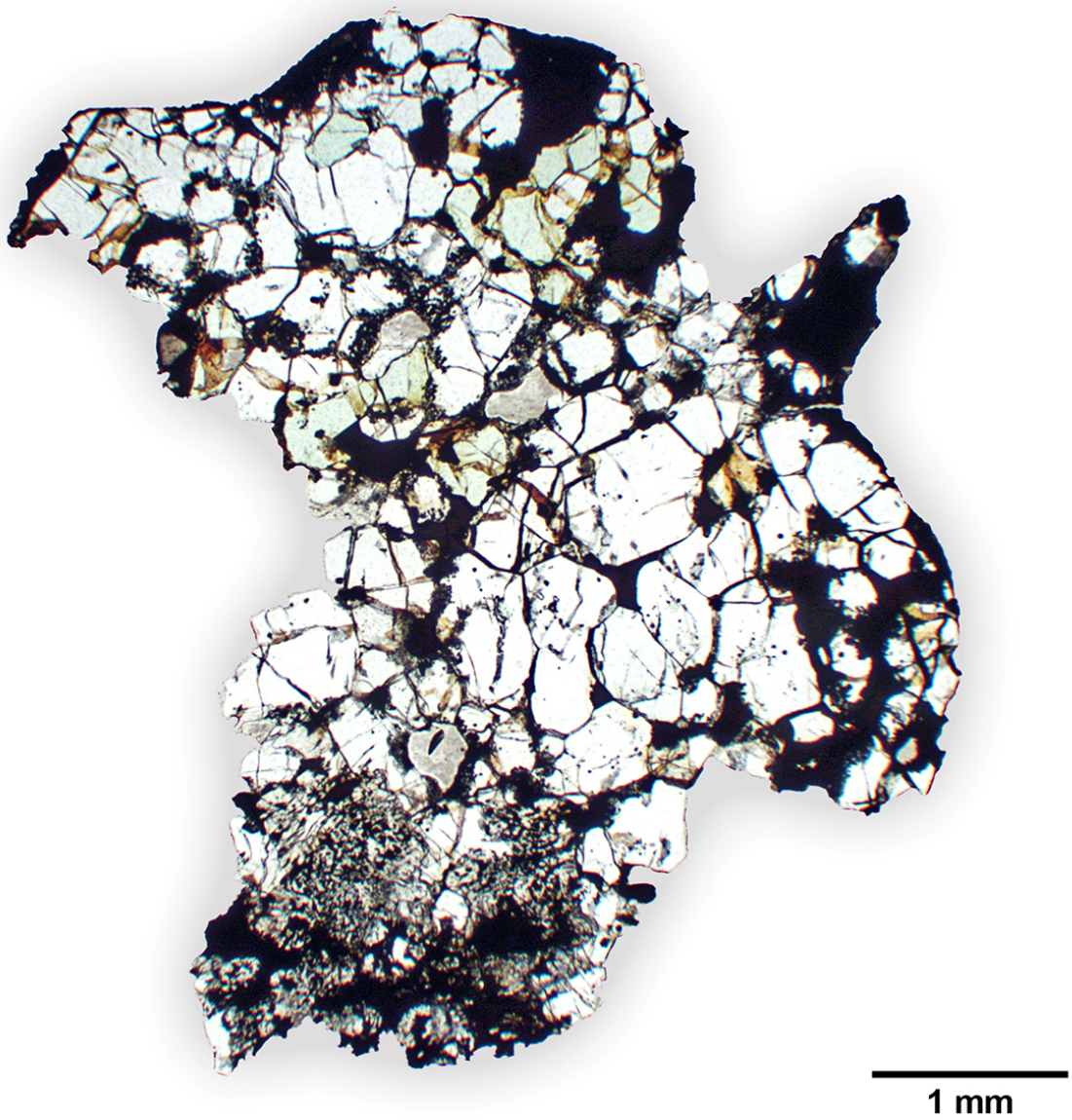

Figure 3.4: Photomicrograph of the polished thin section FRO 03001,01 (transmitted light, plane-polarized light, TL-PPL).

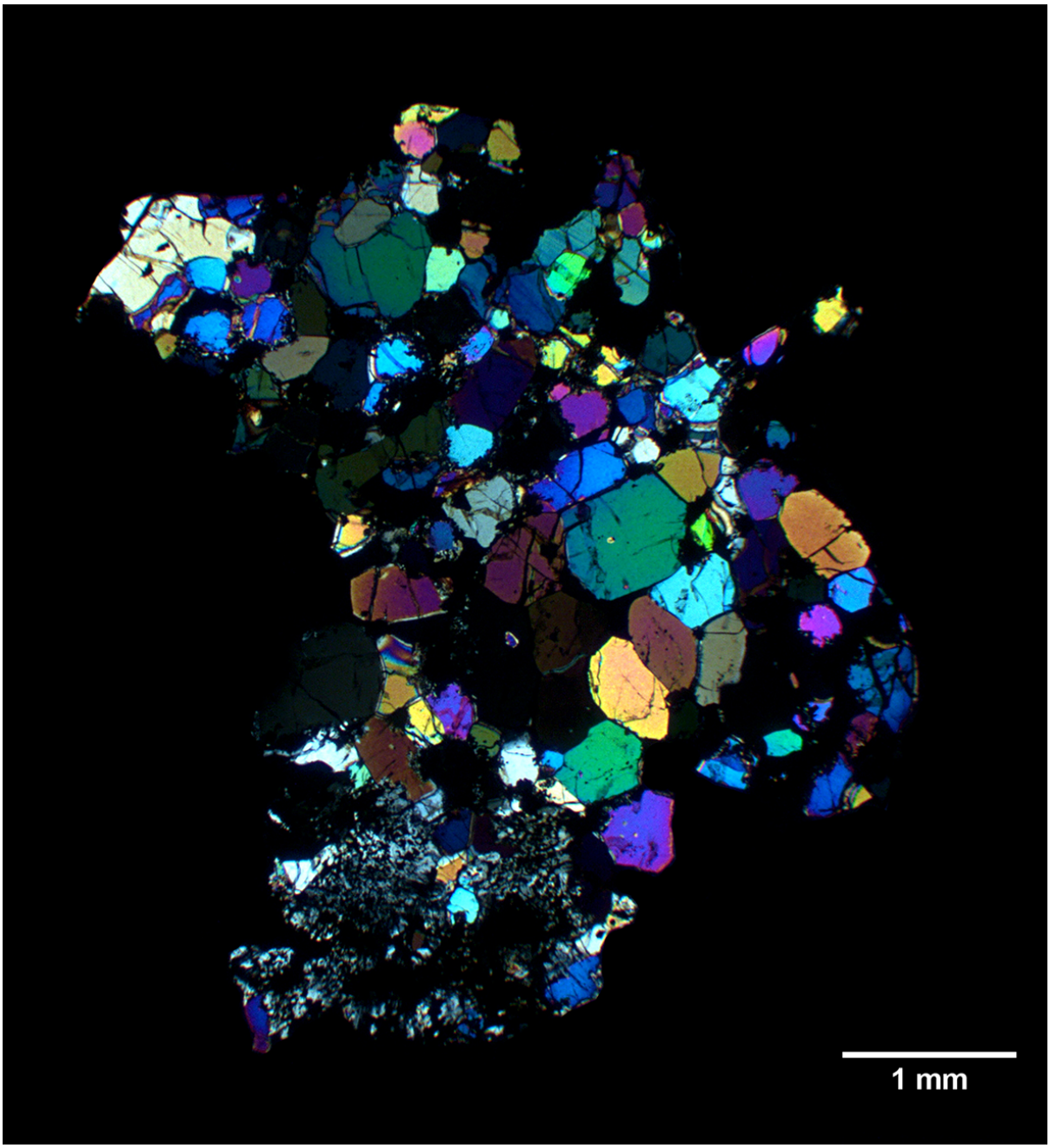

Figure 3.5: Photomicrograph of the polished thin section FRO 03001,01 (transmitted light, crossed-polarized light, TL-CPL). High interference colours are due to the thickness of the section ($> 30\ \mu m$).

Figure 3.6: Photomicrograph of the polished thin section FRO 03001,01 (reflected light, RL).

3.2 Differentiated Achondrites

3.2.1 Ureilite: Dar al Gani 179

Find: Libya, -
Shock Stage: S4 Weathering Grade: little weathered
Section Label: BAB 179,01
Type Specimen: Museo Nazionale dell'Antartide (Siena)
HD Images: TL-PPL / TL-CPL / RL

Figure 3.7: Photomicrograph of the polished thin section BAB 179,01 (transmitted light, plane-polarized light, TL-PPL).

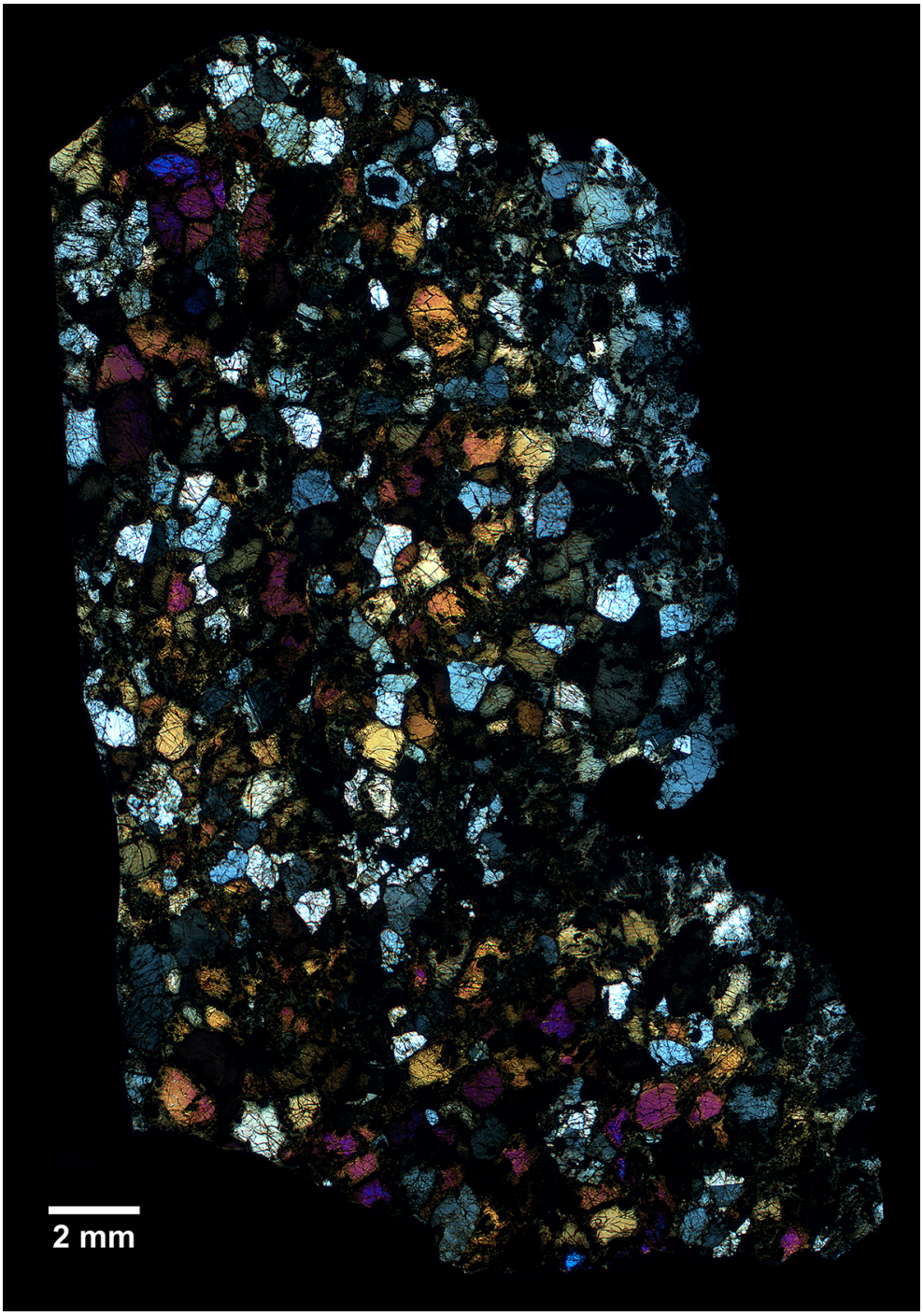

Figure 3.8: Photomicrograph of the polished thin section BAB 179,01 (transmitted light, crossed-polarized light, TL-CPL).

3.2.2 Ureilite: Dar al Gani 660

Find: Libya, 1999
Shock Stage: S3 Weathering Grade: moderately weathered
Section Label: DaG 660,01
Type Specimen: Museo Nazionale dell'Antartide (Siena)
HD Images: TL-PPL / TL-CPL / RL

Figure 3.9: Photomicrograph of the polished thin section DaG 660,01 (transmitted light, plane-polarized light, TL-PPL).

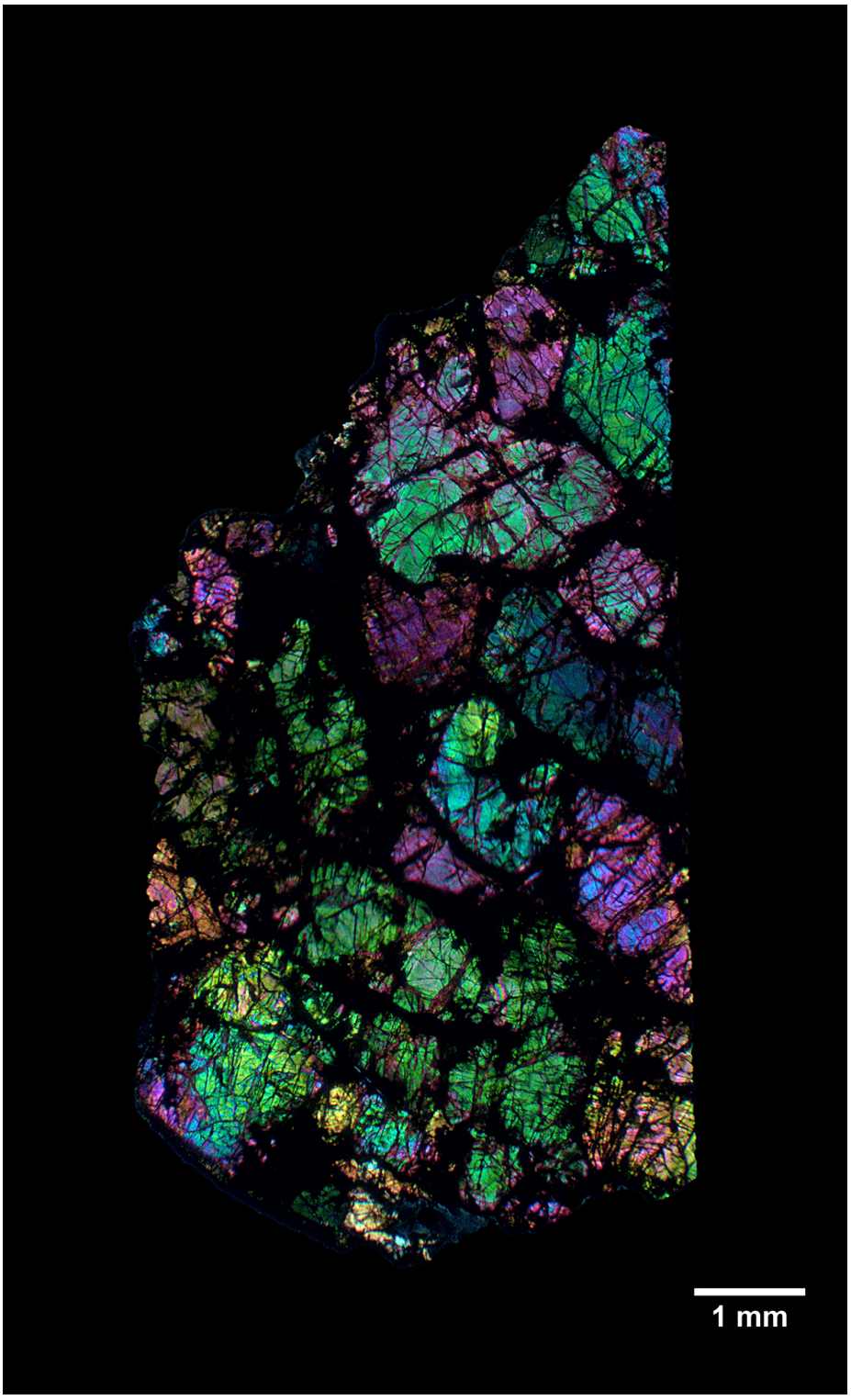

Figure 3.10: Photomicrograph of the polished thin section DaG 660,01 (transmitted light, crossed-polarized light, TL-CPL). High interference colours are due to the thickness of the section (> 30 μm).

3.2.3 Ureilite: Frontier Mountain 97013

Find: Antarctica, 1997
Shock Stage: S3 Weathering Grade: little weathered
Section Label: FRO 97013,02
Type Specimen: Museo Nazionale dell'Antartide (Siena), PNRA
HD Images: TL-PPL / TL-CPL / RL

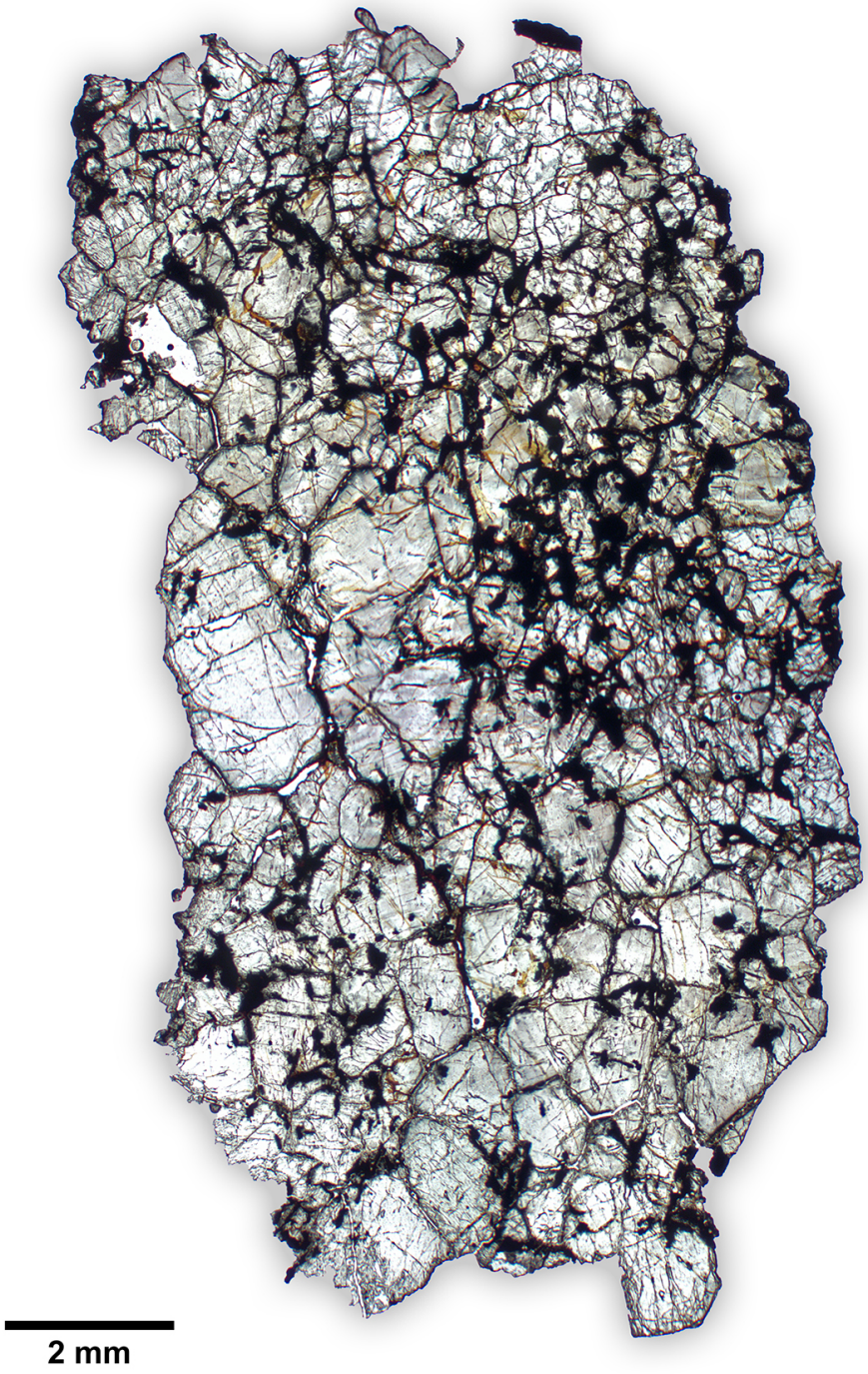

Figure 3.11: Photomicrograph of the polished thin section FRO 97013,02 (transmitted light, plane-polarized light, TL-PPL).

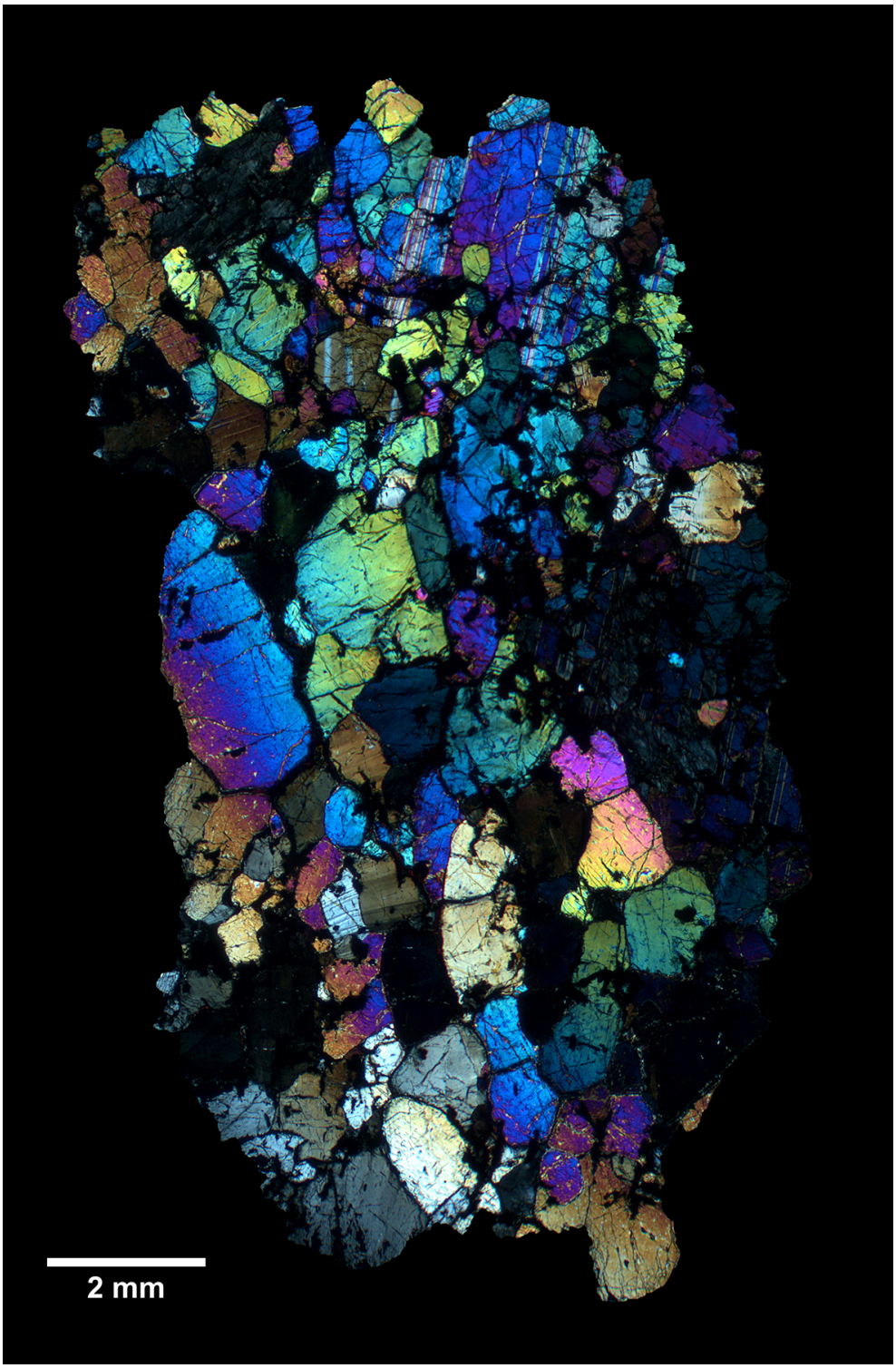

Figure 3.12: Photomicrograph of the polished thin section FRO 97013,02 (transmitted light, crossed-polarized light, TL-CPL).

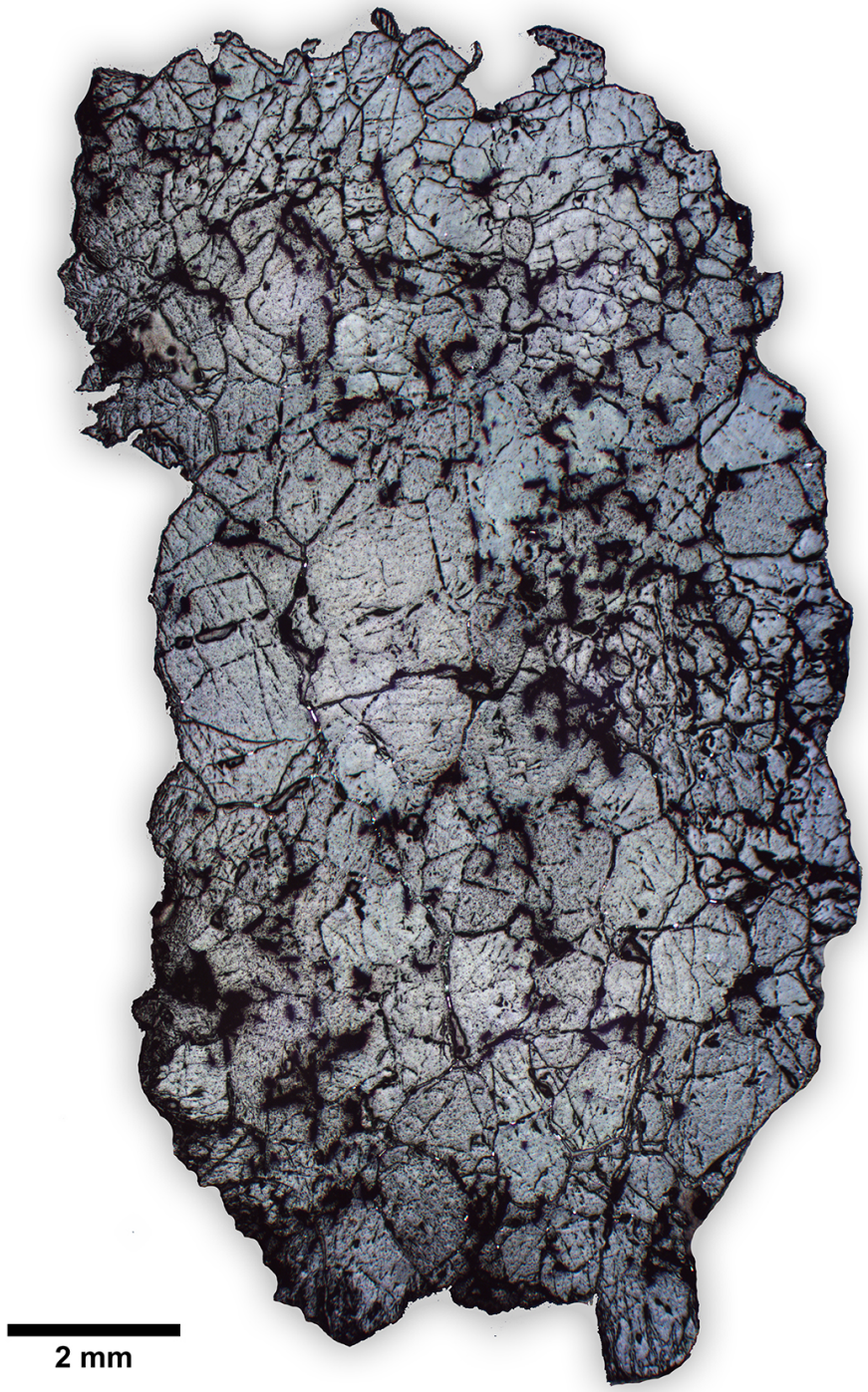

Figure 3.13: Photomicrograph of the polished thin section FRO 97013,02 (reflected light, RL).

3.2.4 Brachinite: AIT 04

Find/Fall: Morocco, -
Shock Stage: S4 Weathering Grade: highly weathered
Section Label: AIT 04
Type Specimen: Museo Nazionale dell'Antartide (Siena)
HD Images: TL-PPL / TL-CPL / RL

Figure 3.14: Photomicrograph of the polished thin section AIT 04 (transmitted light, plane-polarized light, TL-PPL).

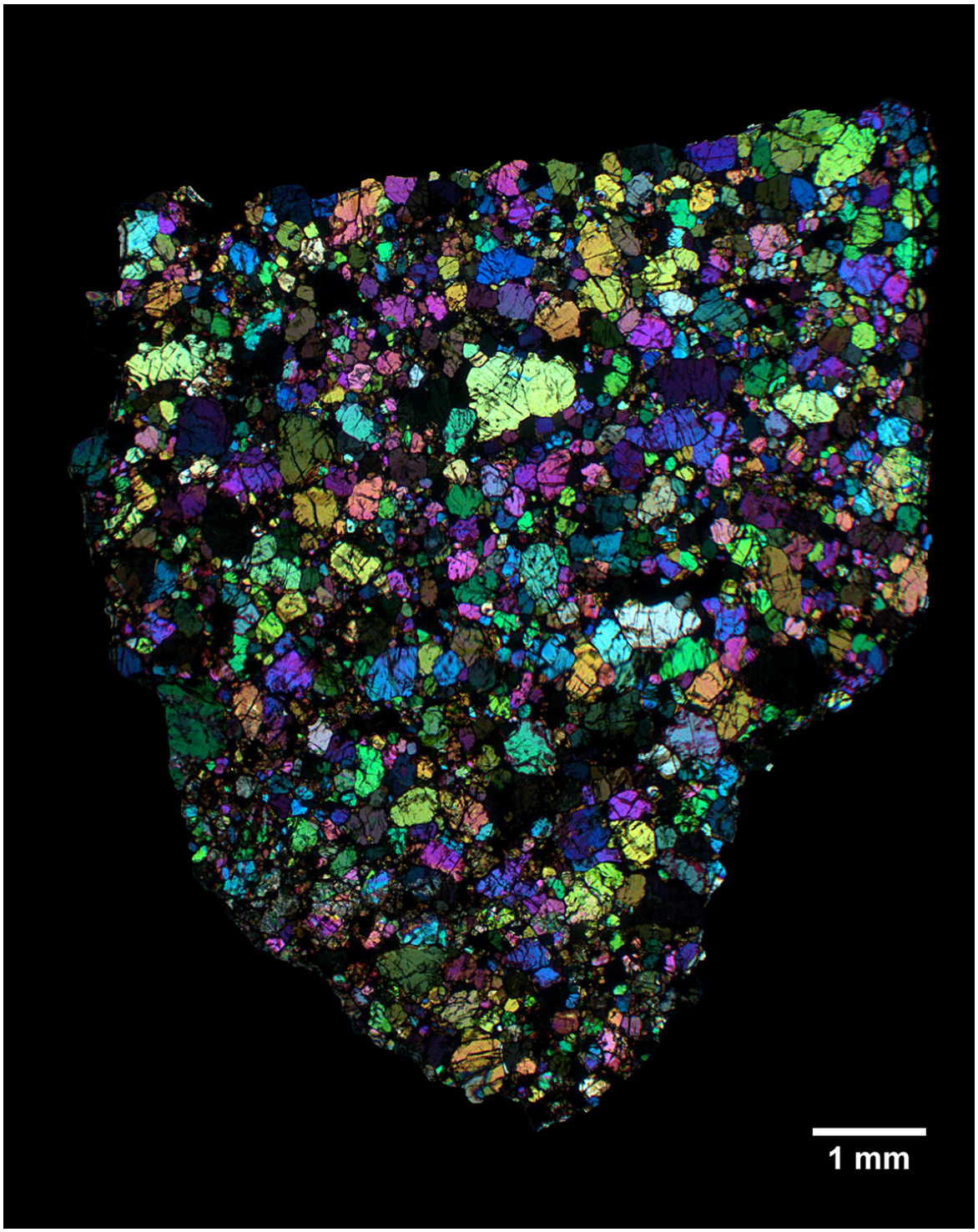

Figure 3.15: Photomicrograph of the polished thin section AIT 04 (transmitted light, crossed-polarized light, TL-CPL).

Figure 3.16: Photomicrograph of the polished thin section AIT 04 (reflected light, RL).

3.2.5 Basaltic Eucrite: Dar al Gani 684

Find: Libya, 1999
Shock Stage: moderately shocked Weathering Grade: little weathered
Section Label: DaG 684,01
Type Specimen: Museo Nazionale dell'Antartide (Siena)
HD Images: TL-PPL / TL-CPL / RL

Figure 3.17: Photomicrograph of the polished thin section DaG 684,01 (transmitted light, plane-polarized light, TL-PPL).

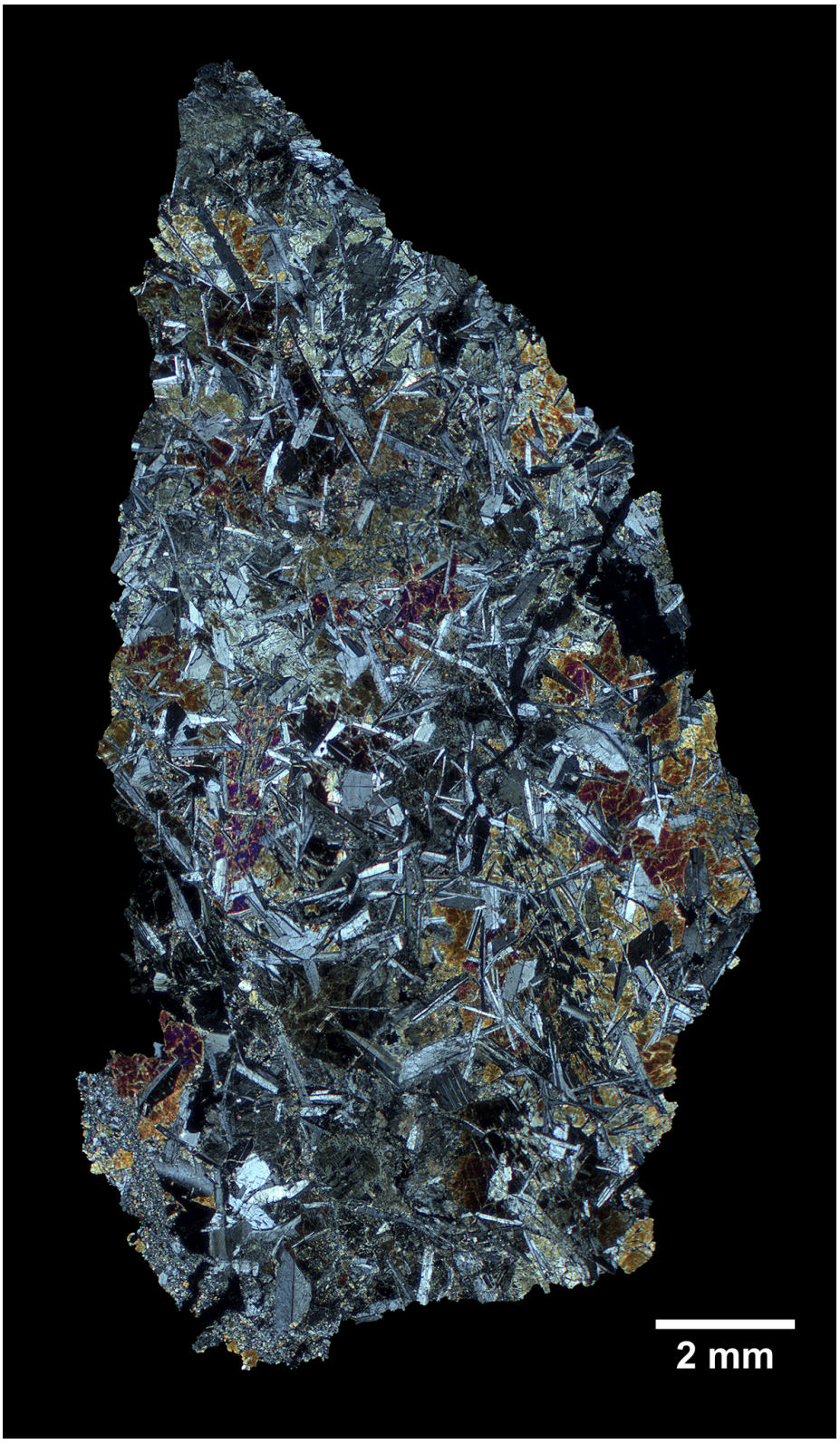

Figure 3.18: Photomicrograph of the polished thin section DaG 684,01 (transmitted light, crossed-polarized light, TL-CPL).

3.2.6 Howardite: Dar al Gani 669

Find: Libya, 1999
Shock Stage: moderately shocked Weathering Grade: little weathered
Section Label: DaG 669,01
Type Specimen: Museo Nazionale dell'Antartide (Siena)
HD Images: TL-PPL / TL-CPL / RL

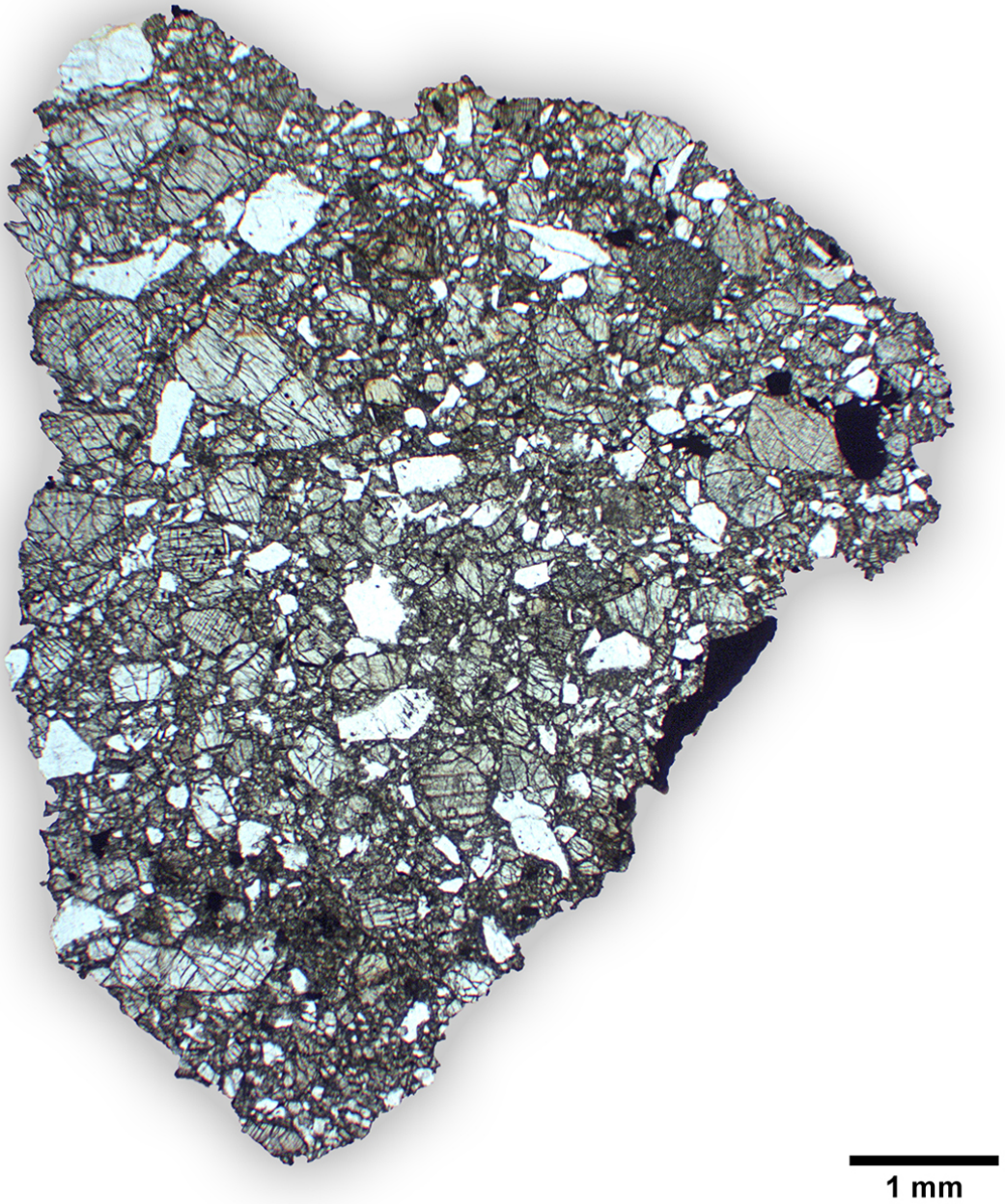

Figure 3.19: Photomicrograph of the polished thin section DaG 669,01 (transmitted light, plane-polarized light, TL-PPL).

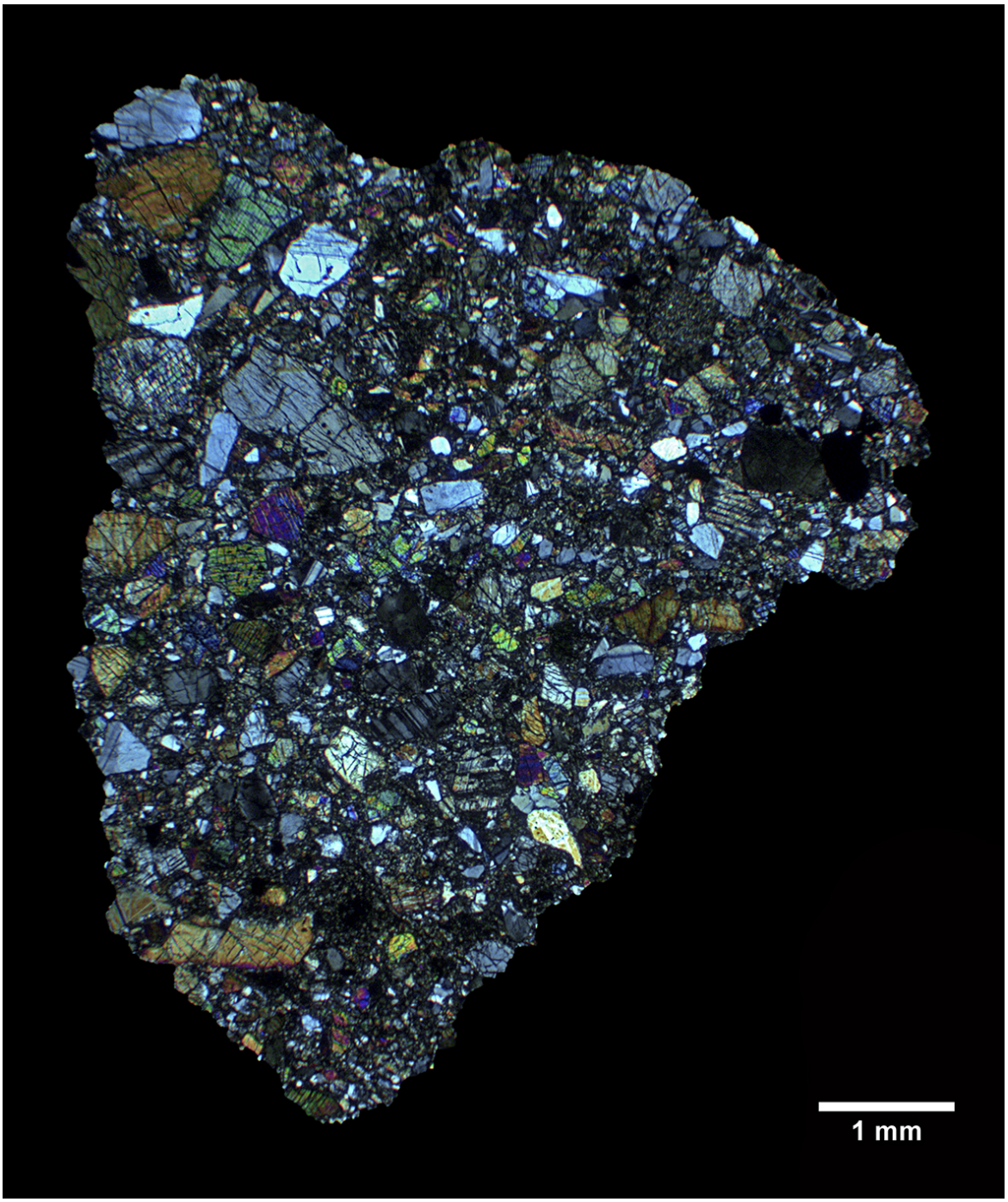

Figure 3.20: Photomicrograph of the polished thin section DaG 669,01 (transmitted light, crossed-polarized light, TL-CPL).

3.2.7 Howardite: Dar al Gani 671

Find: Libya, 1999
Shock Stage: weakly shocked Weathering Grade: little weathered
Section Label: DaG 671,01
Type Specimen: Museo Nazionale dell'Antartide (Siena)
HD Images: TL-PPL / TL-CPL

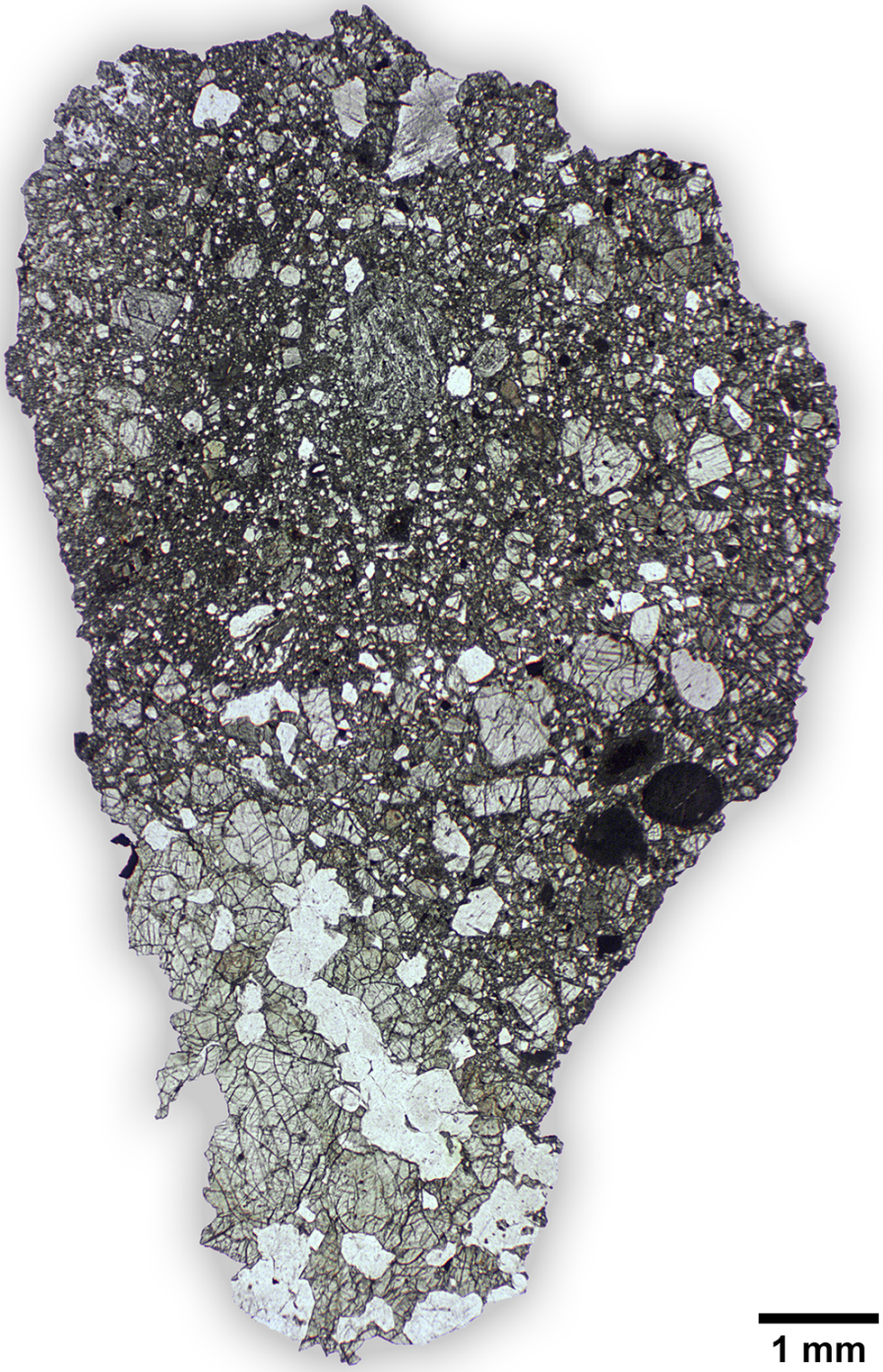

Figure 3.21: Photomicrograph of the polished thin section DaG 671,01 (transmitted light, plane-polarized light, TL-PPL).

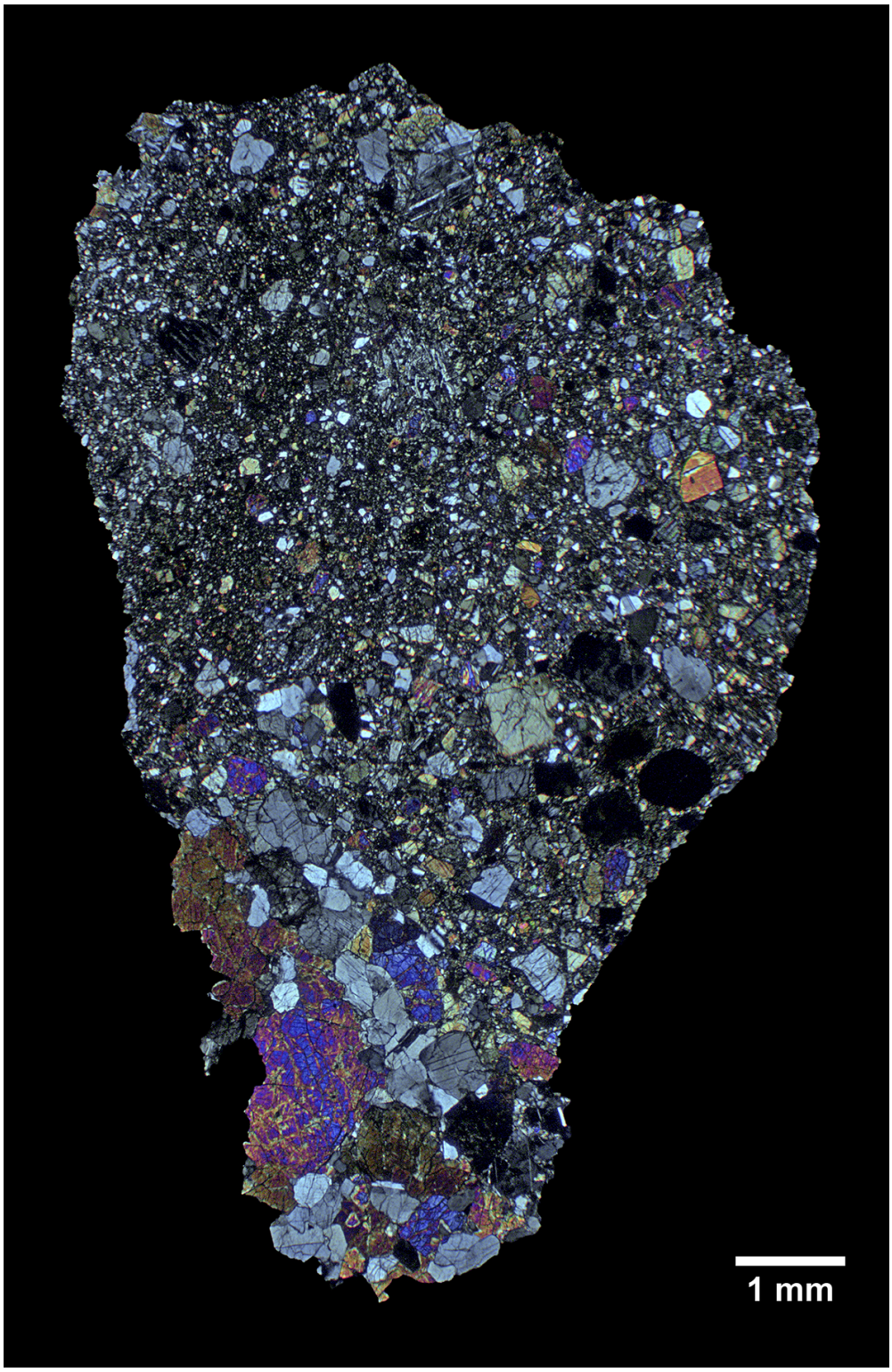

Figure 3.22: Photomicrograph of the polished thin section DaG 671,01 (transmitted light, crossed-polarized light, TL-CPL).

3.2.8 Howardite: Reckling Peak 17029

Find: Antarctica, 2017
Shock Stage: moderately shocked Weathering Grade: little weathered
Section Label: RKP 17029,01
Type Specimen: Museo Nazionale dell'Antartide (Siena), PNRA
HD Images: TL-PPL / TL-CPL

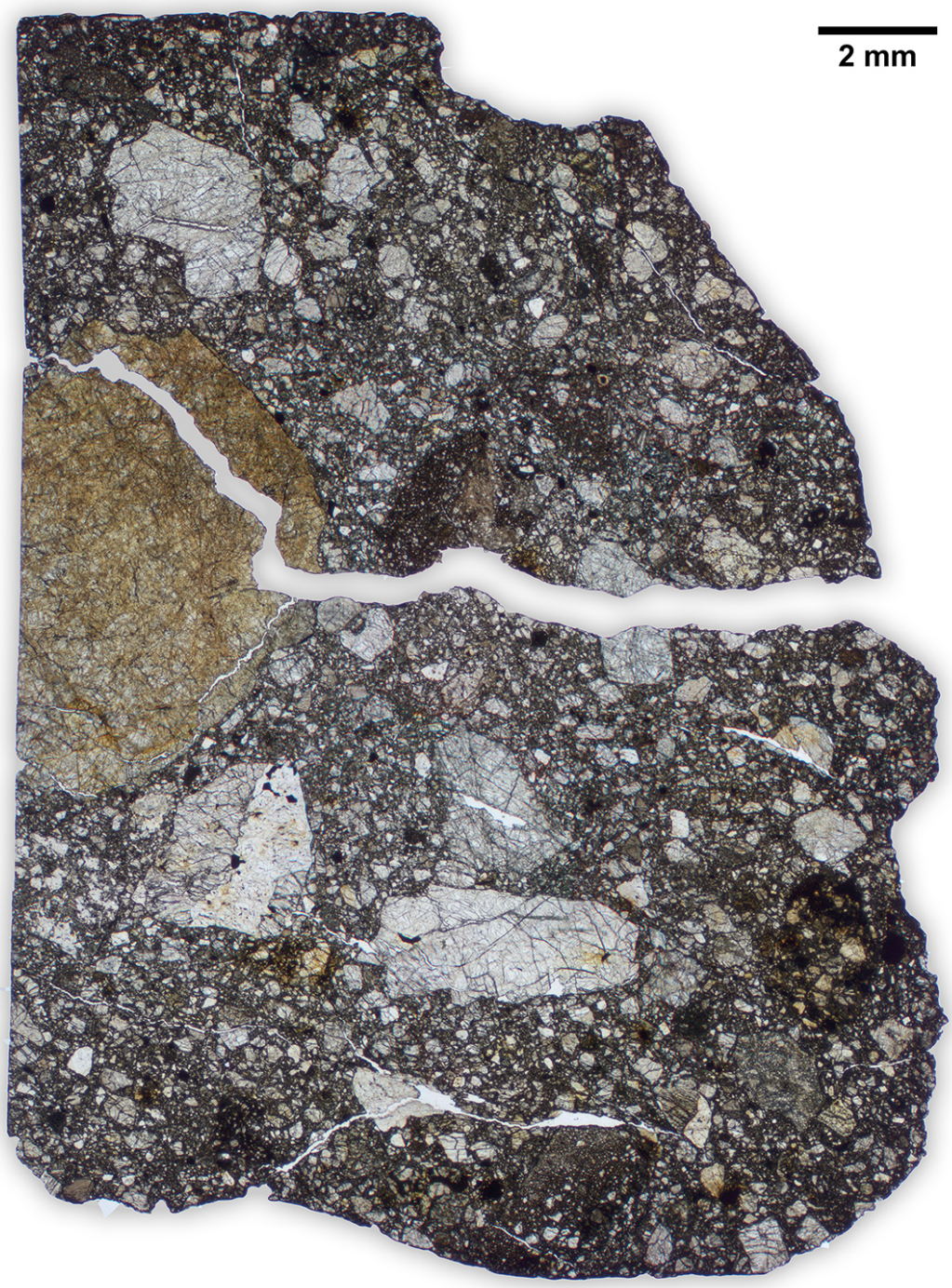

Figure 3.23: Photomicrograph of the polished thin section RKP 17029,01 (transmitted light, plane-polarized light, TL-PPL).

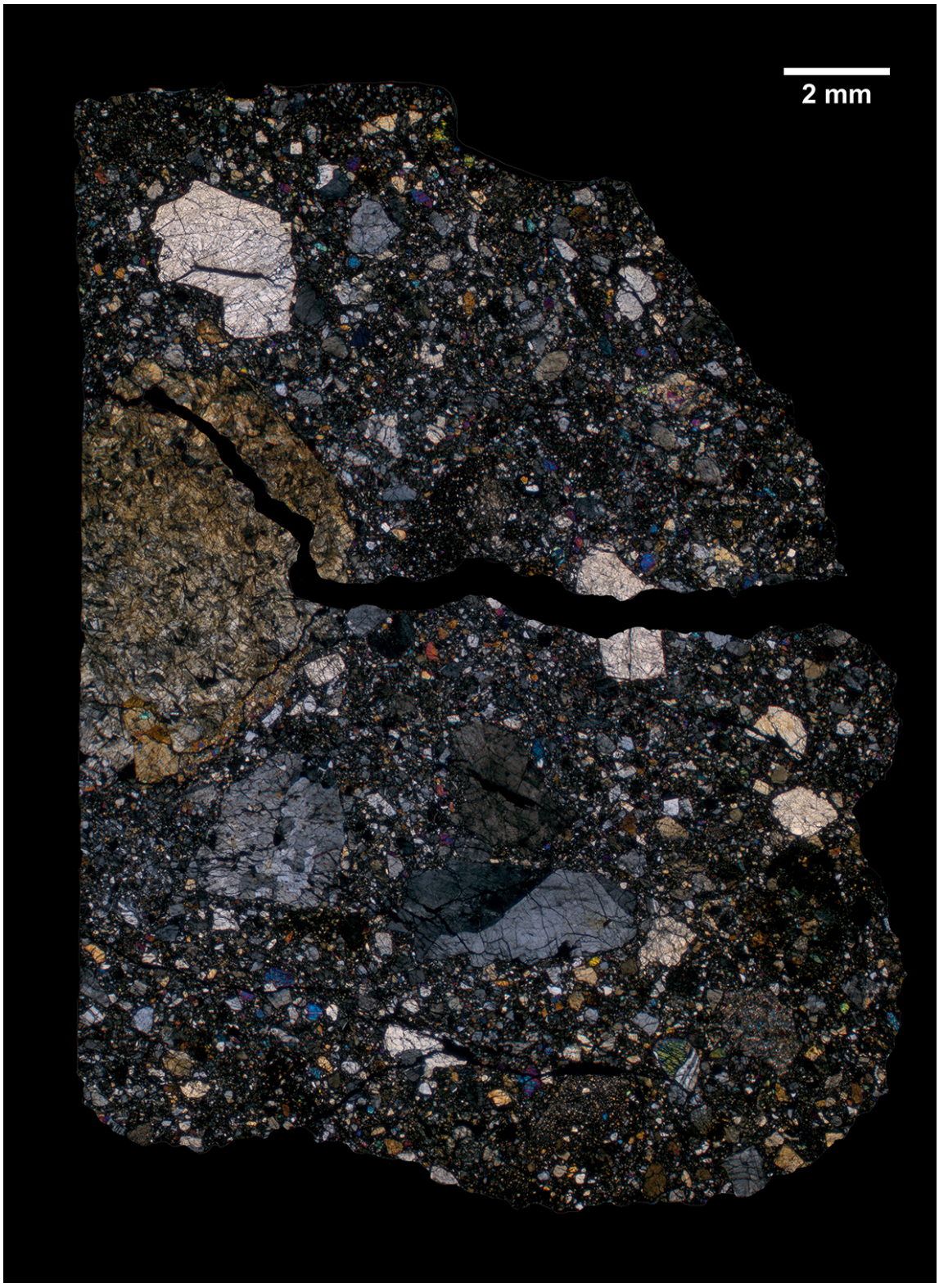

Figure 3.24: Photomicrograph of the polished thin section RKP 17029,01 (transmitted light, crossed-polarized light, TL-CPL).

3.2.9 Mesosiderite silicate fraction: Allan Hills 12073

Find: Antarctica, 2012
Shock Stage: - Weathering Grade: moderately weathered
Section Label: ALH 12073
Type Specimen: Museo Nazionale dell'Antartide (Siena), PNRA
HD Images: TL-PPL / TL-CPL / RL

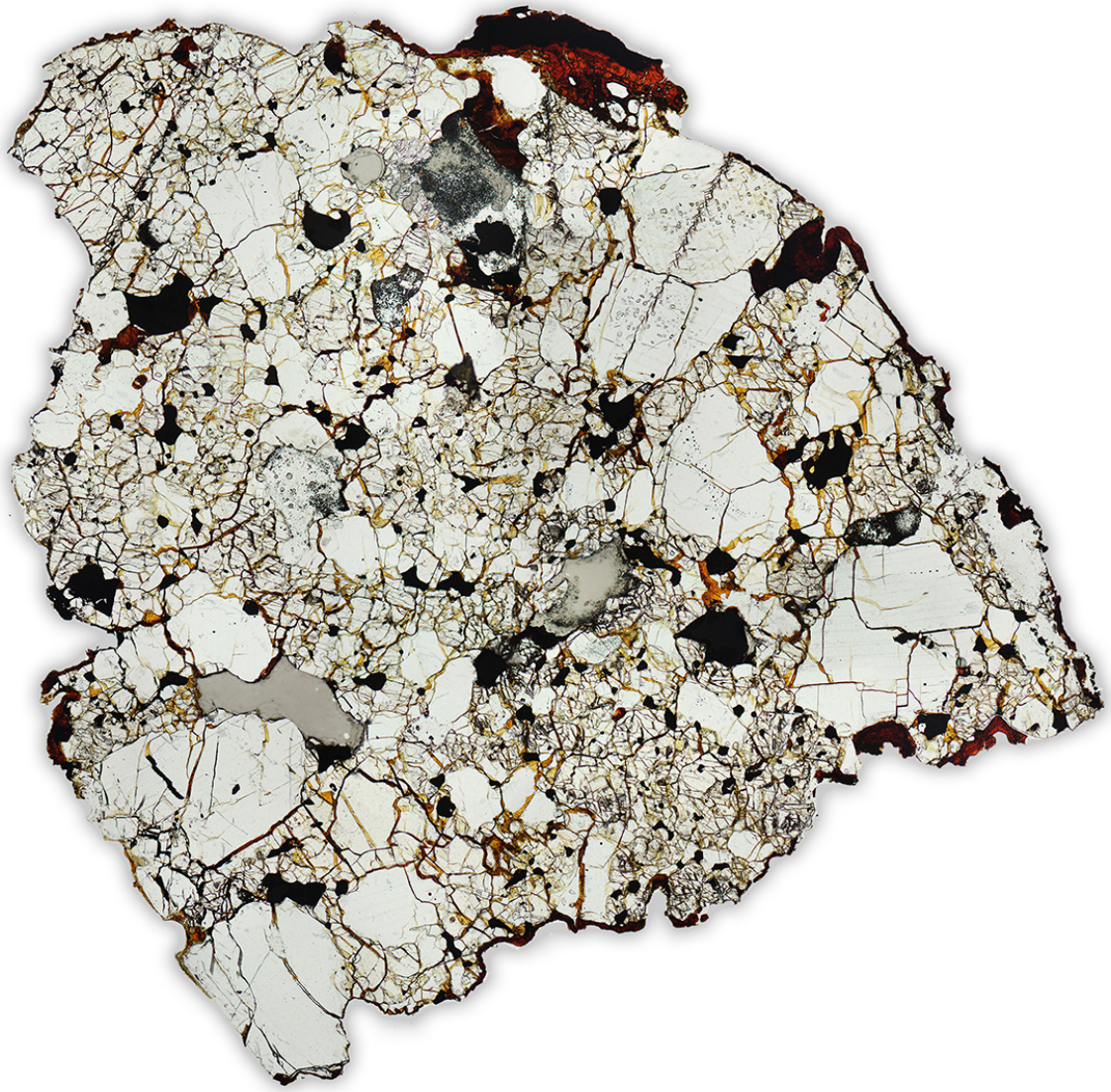

Figure 3.25: Photomicrograph of the polished thin section ALH 12073 (transmitted light, plane-polarized light, TL-PPL).

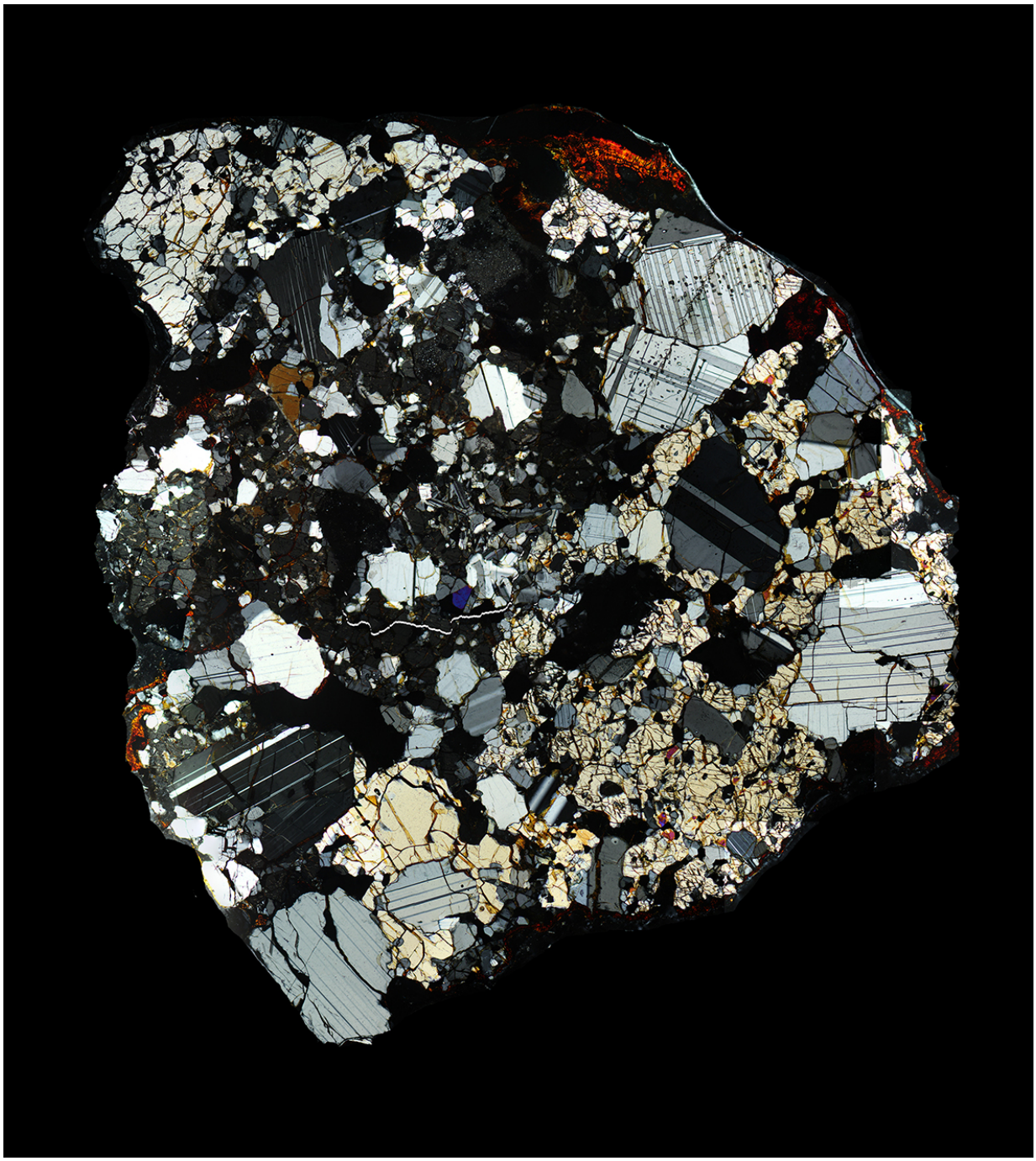

Figure 3.26: Photomicrograph of the polished thin section ALH 12073 (transmitted light, crossed-polarized light, TL-CPL).

Figure 3.27: Photomicrograph of the polished thin section ALH 12073 (reflected light, RL).

3.3 Planetary Meteorites

3.3.1 Lunar Regolith Breccia: Mount DeWitt 12007

Find: Antarctica, 2013
Shock Stage: moderately shocked Weathering Grade: little weathered
Section Label: DEW 12007,01
Type Specimen: Museo Nazionale dell'Antartide (Siena), PNRA
HD Images: TL-PPL / TL-CPL / RL

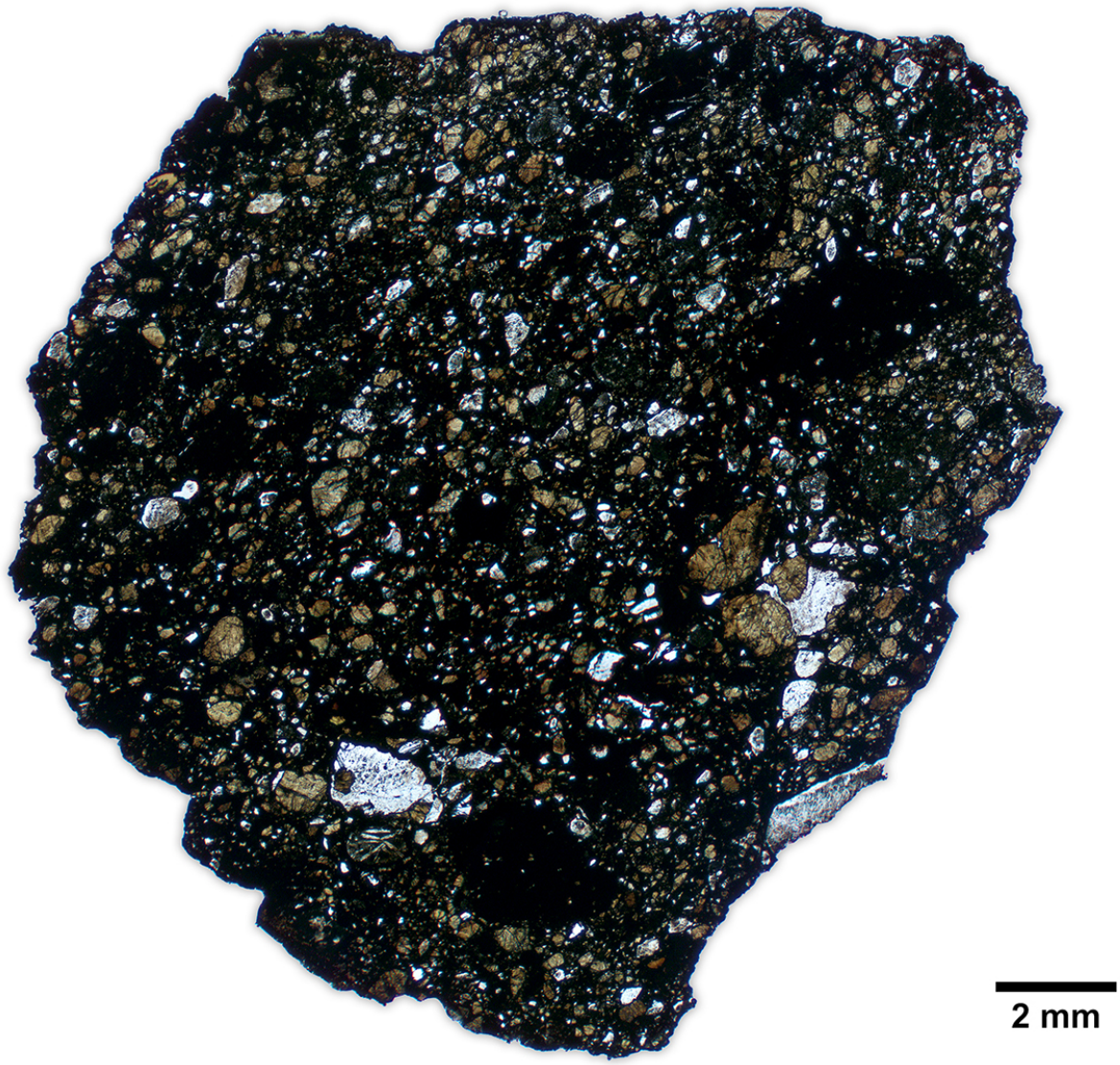

Figure 3.28: Photomicrograph of the polished thin section DEW 12007,01 (transmitted light, plane-polarized light, TL-PPL).

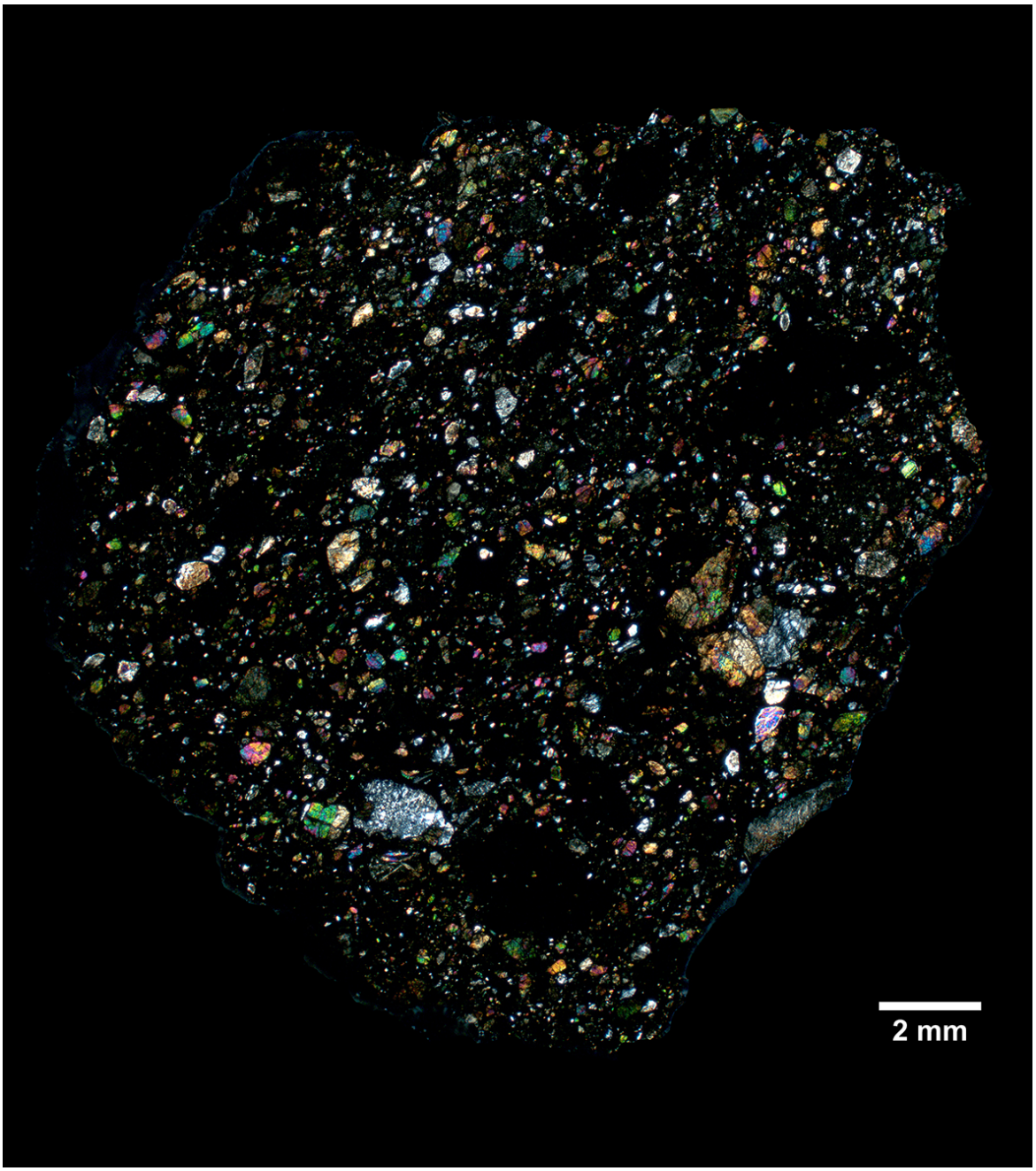

Figure 3.29: Photomicrograph of the polished thin section DEW 12007,01 (transmitted light, crossed-polarized light, TL-CPL).

3.3.2 Lunar Regolith Breccia: Reckling Peak 17064

Find: Antarctica, 2017
Shock Stage: weakly shocked Weathering Grade: little weathered
Section Label: RKP 17064,01
Type Specimen: Museo Nazionale dell'Antartide (Siena), PNRA
HD Images: TL-PPL / TL-CPL

Figure 3.30: Photomicrograph of the polished thin section RKP 17064,01 (transmitted light, plane-polarized light, TL-PPL).

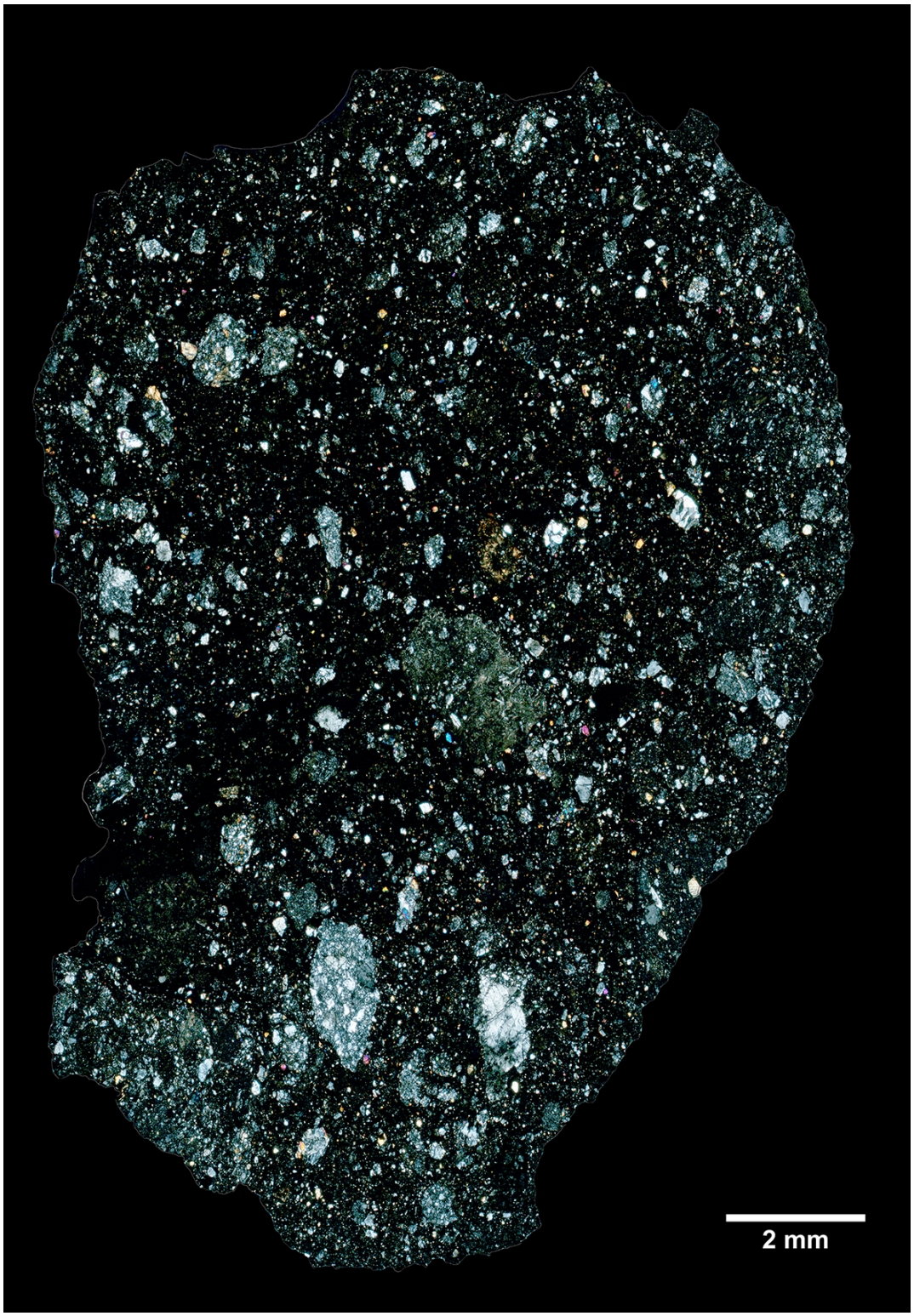

Figure 3.31: Photomicrograph of the polished thin section RKP 17064,01 (transmitted light, crossed-polarized light, TL-CPL).

3.3.3 Basaltic Shergottite: Dar al Gani 670

Find: Libya, 1999
Shock Stage: S5 Weathering Grade: highly weathered
Section Label: DaG 670,07
Type Specimen: Museo Nazionale dell'Antartide (Siena)
HD Images: TL-PPL / TL-CPL / RL

Figure 3.32: Photomicrograph of the polished thin section DaG 670,07 (transmitted light, plane-polarized light, TL-PPL).

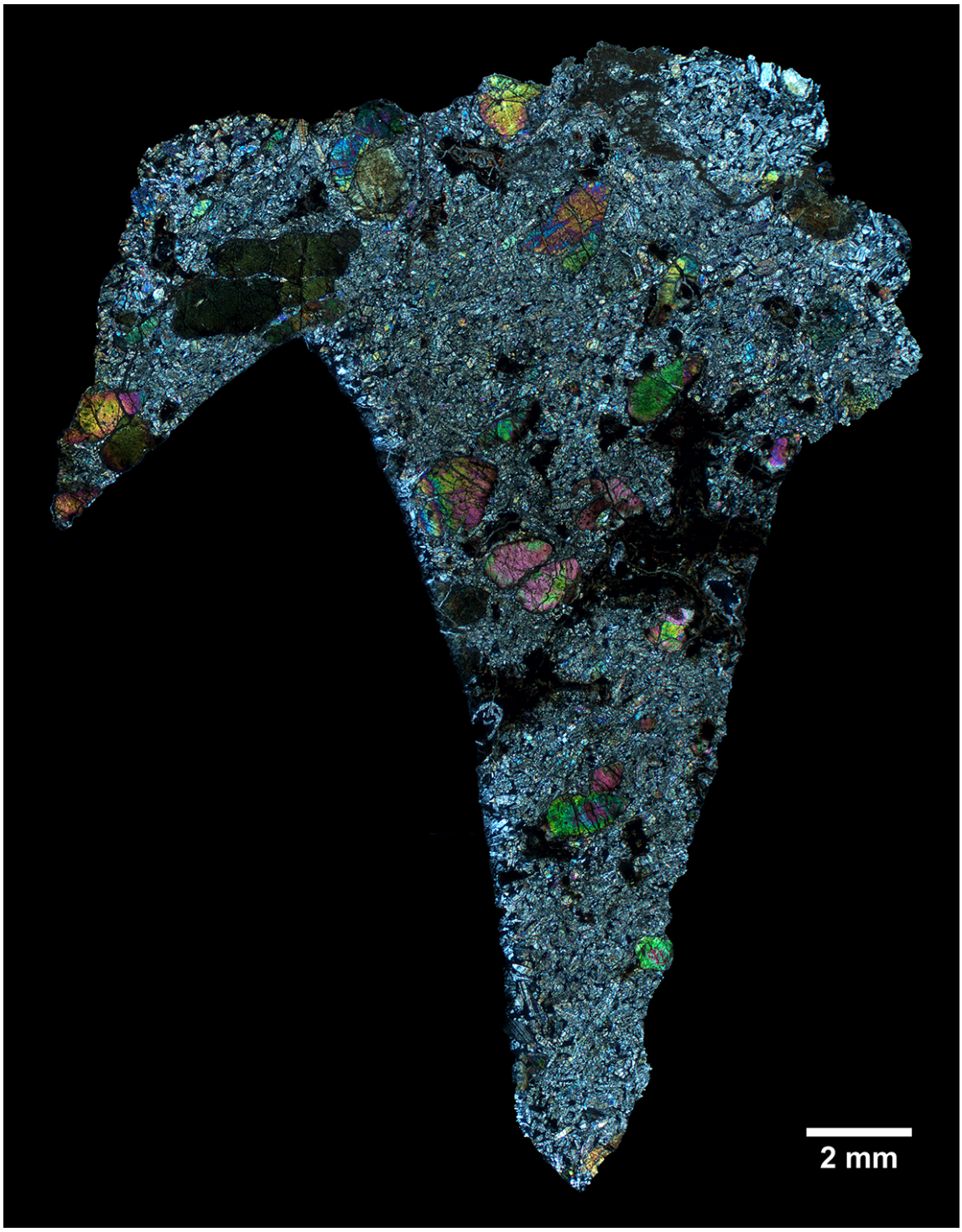

Figure 3.33: Photomicrograph of the polished thin section DaG 670,07 (transmitted light, crossed-polarized light, TL-CPL).

Appendix

Table 3.1: Petrologic types classification scheme after Krot et al., 2014 [8]. Classification reported in two tables: the first one is for petrologic types 1 to 3; the second one for petrologic types 4 to 6.

Criterion	**Petrologic type**		
	1	*2*	*3*
Homogeneity of olivine and low-Ca pyroxene compositions	——— >5% mean deviations ———		
Structural state of low-Ca pyroxene	——— Predominantly monoclinic ———		
Feldspar	——— Minor primary grains only ———		
Chondrule glass		Altered, mostly absent	Clear, isotropic, variable abundance
Maximum Ni in metal		<20 wt%; taenite minor or absent	>20 wt% kamacite and taenite in exsolution relationship
Mean Ni in sulfides		>0.5 wt%	<0.5 wt%
Matrix	All fine-grained, opaque	Mostly fine, opaque	Clastic, minor opaque
Chondrule-matrix integration	No chondrules	Chondrules very sharply defined	
Carbon (wt%)	3 - 5	0.8 - 2.6	<1.5
Water (wt%)	18 - 22	2 - 16	0.3 - 3

Criterion	**Petrologic type**		
	4	*5*	*6*
Homogeneity of olivine and low-Ca pyroxene compositions	<5%	——— Homogeneous ———	
Structural state of low-Ca pyroxene	>20% monoclinic	<20% monoclinic	Orthorombic
Feldspar	Secondary, <2 μm grains	Secondary, 2-50 μm grains	Secondary, >50 μm grains
Chondrule glass	——— Devitrified absent ———		
Maximum Ni in metal	>20 wt% kamacite and taenite in exsolution relationship		
Mean Ni in sulfides	<0.5 wt%	<0.5 wt%	<0.5 wt%
Matrix	Transparent, recrystallized coarsening from 4 to 6		
Chondrule-matrix integration	Chondrules well defined	Chondrules readily delineated	Chondrules poorly defined
Carbon (wt%)	<1.5	<1.5	<1.5
Water (wt%)			<1.5

Table 3.2: Shock stages (SS) classification scheme (after Krot et al., 2014 [8]).

SS	**Description**	**Effect resulting from equilibration peak shock pressure**			**Shock P (GPa)**
		Olivine	*Plagioclase*	*Orthopyroxene*	
S1	Unshocked	Sharp optical extinction, irregular fractures.	Sharp optical extinction, irregular fractures.	Sharp optical extinction, irregular fractures.	<4 - 5
S2	Very weakly shocked	Undulatory extinction, irregular fractures.	Undulatory extinction, irregular fractures.	Undulatory extinction, irregular and some planar fractures.	5 - 10
S3	Weakly shocked	Planar fractures, undulatory extinction, irregular fractures.	Undulatory extinction.	Clinoenstatite lamellae on (100), undulatory extinction, planar and irregular fractures.	15 - 20
S4	Moderately shocked	Weak mosaicism, planar fractures.	Undulatory extinction, partially isotropic, planar deformation features.		30 - 35
S5	Strongly shocked	Strong mosaicism, planar fractures, planar deformation fractures.	Maskelynite.		45 - 55
S6	Very strongly shocked	Solid-state recrystallization and staining, ringwoodite, melting.	Shock melted (normal glass).	Majorite, melting.	75 - 90
	Shock melted	Whole-rock melting (impact-melt rocks and melt breccias).			

Table 3.3: Weathering Grade (WG) classification scheme (after Wlotzka et al., 1993 [23]).

Weathering Grade	**Description**
W0	No visible oxidation of metal or sulfide; a limonitic staining may be visible in TL
W1	Minor oxide rims around metal and troilite; minor oxide veins
W2	Moderate oxidation of metal, about 20-60% being affected
W3	Heavy oxidation of metal and troilite, 60-95% being replaced
W4	Complete (>95%) oxidation of metal and troilite; no alteration of silicates
W5	Alteration of mafic silicates, mainly along cracks
W6	Massive replacement of silicates by clay minerals and oxides

Bibliography

[1] Bland P. A. (2004) *The Desert Fireball Network*. Astronomy and Geophysics 45, Issue 5, 5.20-5.23.

[2] Brearley A. J. and Jones R. H. (1998) *Chondritic Meteorites*. In Planetary Materials, Reviews in Mineralogy & Geochemistry (Papike J. J., ed.). De Gruyter 36, 3-1 - 3-398.

[3] Bridges J. C., Catling D. C., Saxton J. M., Swindle T. D., Lyon I. C., Grady M. M. (2001) *Alteration Assemblages in Martian Meteorites: Implications for Near-Surface Processes*. Space Science Reviews 96, 365–392.

[4] Chambers J. (2006) *Meteoritic Diversity and Planetesimal Formation*. In Meteorites and the Early Solar System II (Lauretta D. S. and McSween H. Y. Jr., eds.). Amsterdam University Press, 487-497.

[5] Chennaoui Aoudjehane H., Avice G., Barrat J. A., Boudouma O., Chen G., Duke M. J. M., Franchi I. A., Gattacceca J., Grady M. M., Greenwood R. C., Herd C. D. K., Hewins R., Jambon A., Marty B., Rochette P., Smith C. L., Sautter V., Verchovsky A., Weber P., Zanda B. (2012) *Tissint Martian Meteorite: A Fresh Look at the Interior, Surface and Atmosphere of Mars*. Science 338, 785–788.

[6] D'Orazio M. (2007) *Meteorite records in the ancient Greek and Latin literature: Between history and myth*. In Myth and Geology (Piccardi L. and Masse W. B., eds.). Geological Society London Special Publications 273, 215–225.

[7] Halliday I., Blackwell A. T., Griffin A. A. (1978) *The Innisfree meteorite and the Canadian camera network*. Journal of the Royal Astronomical Society of Canada 72, 15–39.

[8] Krot A. N., Keil K., Scott E. R. D., Goodrich C. A., Weisberg M. K. (2014) *Classification of Meteorites and Their Genetic Relationships*. In Meteorites and Cosmochemical Processes, Volume 1 of Treatise on Geochemistry, Second Edition (Davis A. M., ed.). Elsevier Science, 1–63.

[9] Lauretta D. S. and Killgore M. (2004) *A Color Atlas of Meteorites in Thin Section*. Golden Retriever Publications and Southwest Meteorite Press.

[10] McCoy T. J., Mittlefehldt D. W., Wilson L. (2006) *Asteroid Differentiation*. In Meteorites and the Early Solar System II (Lauretta D. S. and McSween H. Y. Jr., eds.). Amsterdam University Press, 733–745.

[11] McCrosky R. E., Posen A., Schwartz G., Shao C. Y. (1971) *Lost City meteorite — Its recovery and a comparison with other fireballs*. Journal of Geophysical Research 76, 4090–4108.

[12] McSween H. Y, McLennan S. M. (2014) *Mars*. In Planets, Asteroids, Comets and The Solar System, Volume 2 of Treatise on Geochemistry, Second Edition (Davis A. M., ed.). Elsevier Science, 251–300.

[13] McSween H. Y., Lauretta D. S., Lexhin L. A. (2006) *Recent advances in meteoritics and cosmochemistry*. In Meteorites and the Early Solar System II (Lauretta D. S. and McSween H. Y. Jr., eds.). Amsterdam University Press, 53–66.

[14] McSween H. Y. Jr. (1999) *Meteorites and Their Parent Planets*. Second edition. Cambridge University Press.

[15] Mittlefehldt D. W., McCoy T. J., Goodrich C. A., Kracher A. (1998) *Non-chondritic meteorites from asteroidal bodies*. In Planetary Materials, Reviews in Mineralogy & Geochemistry (Papike J. J., ed.). De Gruyter 36, 4-1 - 4-495.

[16] Oberst J., Molau S., Heinlein D., Gritzner C., Schindler M., Spurny P., Ceplecha Z., Rendtel J., Betlem H. (1998) *The "European Fireball Network": Current status and future prospects*. Meteoritics and Planetary Science 33, 49–56.

[17] Rubin A. E. and Grossman J. N. (2010) *Meteorite and meteoroid: New comprehensive definitions*. Meteoritics & Planetary Science 45, 114–122.

[18] Russell S. S., Hartman L., Cuzzi J., Krot A. N., Gounelle M., Weidenschilling S. (2006) *Timescales of the Solar Protoplanetary Disk*. In Meteorites and the Early Solar System II (Lauretta D. S. and McSween H. Y. Jr., eds.). Amsterdam University Press, 233–251.

[19] Scott E. R. D., Haack H., Stanley G. (2001) *Formation of mesosiderites by fragmentation and reaccretion of a large differentiated asteroid*. Meteoritics & Planetary Science 36, Issue 7, 869-881.

[20] Scott E. R. D. and Krot A. N. (2014) *Chondrites and Their Components*. In Meteorites and Cosmochemical Processes, Volume 1 of Treatise on Geochemistry, Second Edition (Davis A. M., ed.). Elsevier Science, 65–137.

[21] Stöffler D., Keil K., Scott E. R. D. (1991) *Shock metamorphism of ordinary chondrites*. Geochimica et Cosmochimica Acta 55, Issue 12, 3845-3867.

[22] Warren P. H. and Taylor G. J. (2014) *The Moon*. In Planets, Asteroids, Comets and The Solar System, Volume 2 of Treatise on Geochemistry, Second Edition (Davis A. M., ed.). Elsevier Science, 213–250.

[23] Wlotzka F. (1993) *A Weathering Scale for the Ordinary Chondrites*. Meteoritics 28, 460.